UNCOVERING THE UNDERLYING GENETIC MECHANISMS OF SEX DETERMINATION, GONAD DIFFERENTIATION, AND DOSAGE COMPENSATION IN THE BROWN ANOLE LIZARD, *ANOLIS SAGREI*

by

MEGAN K. MOTLEY

(Under the Direction of Douglas B. Menke)

ABSTRACT

The accurate and timely initiation of sex determination is fundamental to species survival and reproductive success. Despite its importance, genetic sex determination mechanisms have only been carefully studied in a few vertebrate species, and our understanding of reptilian genetic sex determination systems remains limited. With over 12,000 species, reptiles make up one of the largest vertebrate species groups and, unlike typical model systems such as mammals and birds, a highly diverse array of sex determination systems have been observed. Most of what we know about genetic sex determination comes from groups that have very little diversity in the underlying genetic mechanisms of sex determination, i.e., we know a lot about a little. By examining the molecular mechanisms underlying genetic sex determination in more diverse species groups, we can gain a broader and deeper understanding of genetic sex determination across the tree of life. Here, I explore the ancient, deeply conserved XX/XY genetic sex determination system of *Anolis*, with a particular

focus in uncovering the genetic signal cascade, clarifying the timing of embryonic gonad differentiation, tracing the evolution of the sex chromosomes, identifying the genetic basis of primary sex determination, and examining dosage compensation in the brown anole lizard, *Anolis sagrei*. Using genomic and transcriptomic methods, I propose *rpl6y* as a candidate determinant of primary sex determination in *A. sagrei*. Additionally, I demonstrate regional differences in dosage compensation across the *A. sagrei* X chromosome. This work reveals a novel mechanism for genetic sex determination in *Anolis* and the nuances of dosage compensation in neo-sex chromosome systems that have undergone fusion events. This work is the beginning of large-scale comparative work across pleurodonts, the order to which *Anolis* lizards belong.

INDEX WORDS: *Anolis*; Pleurodonts; Sex determination; Dosage compensation; Gonad differentiation; Brown anole; Sex chromosome evolution

UNCOVERING THE UNDERLYING GENETIC MECHANISMS OF SEX DETERMINATION, GONAD DIFFERENTIATION, AND DOSAGE COMPENSATION IN THE BROWN ANOLE LIZARD, *ANOLIS SAGREI*

by

MEGAN K. MOTLEY

B.S., University of California at Davis, 2017

A Dissertation Submitted to the Graduate Faculty of The University of Georgia in Partial Fulfillment of the Requirements for the Degree

DOCTOR OF PHILOSOPHY

ATHENS, GEORGIA

2025

UNCOVERING THE UNDERLYING GENETIC MECHANISMS OF SEX DETERMINATION, GONAD DIFFERENTIATION, AND DOSAGE COMPENSATION IN THE BROWN ANOLE LIZARD, *ANOLIS SAGREI*

by

MEGAN K. MOTLEY

Major Professor:	Douglas B. Menke
Committee:	Casey Bergman
	Kelly Dyer
	James D. Lauderdale
	Michael A. White

Electronic Version Approved:

Ron Walcott
Vice Provost for Graduate Education and Dean of the Graduate School
The University of Georgia
December 2025

DEDICATION

To all the women who came before me, and all the women who will come after me, your resilience, perseverance, and pursuit of knowledge made this possible.

To every first-generation student walking this path, I walk beside you.

You are worthy, you are needed, and you belong here.

And to my dad, I wish you were here to celebrate this moment with me. This is for you.

ACKNOWLEDGEMENTS

Getting a PhD truly takes a village. I will never have the words to fully express my gratitude for every single person who has been integral to my success, but I will try.

I want to start by thanking members of my excellent healthcare team: Dr. Finbar Woitalla; Minou Rysiew, MSW, LCSW; Angie Ruhlen, MFCS, RDN, LD; Peggy Peterson, DPT, ATC, WCS, Cert DN; Brandy Sims, LMT; Jan Nodine, PMHCNS-BC, APRN; the entire UHC Pharmacy Dept.; and the Piedmont hospital staff that saved my life in 2022. I would not be here without the care and support I have received from each one of you.

I want to thank my PhD advisor, Dr. Doug Menke, for letting me start a project from the ground up with very few guardrails. Your input, advice, and scientific guidance have been crucial for tackling a project this big and this bold. It was an honor to work alongside you, and I wouldn't be where I am today without your mentorship.

I must give a huge thank you to Dr. Sungdae Park for answering every question and helping me with this project. I will miss your curiosity, our long scientific discussions, and our teamwork deeply. I could not have done this without you.

To my committee members, Drs. Kelly Dyer, Jim Lauderdale, Mike White, and Casey Bergman, your support, ideas, and influence have been vital in shaping this project. Thank you for your investment in my graduate education and career development. To Kelly, Thanks for not letting me quit. I wouldn't be here without your unwavering faith in me.

To my former mentors, Dr. Turid Reid, Dr. Judy Wexler, and Dr. Brandon Cooper, thank you for giving me opportunities to grow, learn, make mistakes, and become a “real” scientist. I owe so much to you all.

To the UGA Genetics Dept., thank you for supporting and amplifying student voices, for deeply caring about our wellbeing, and for being a safe space. To Susan White, thank you for all you do. To current and former students and faculty, thank you for your feedback, advice, help, and chats. I am so thankful to be a part of such a vibrant community of scientists. Thank you for everything.

To past members of the Menke Lab: Dr. Aaron Alcala, Dr. Sukhada Samudra, Dr. Ashley Rasys, Dr. Sergio Minchey, and Dr. Christina Sabin; thank you for training me and supporting me throughout the years. I am the scientist I am today because of you all.

To my lab ladies, Dr. Rida Osman, Anna Iouchmanov, Makenna Burslie, and Sneha Mohan, thank you for always taking me as I am. Your scientific contributions have been integral to this research, and your camaraderie has gotten me through my worst days.

To my girl gang, Dr. Theresa Erlenbach, Dr. Mattie Usey, Dr. Audrey Ward, and Dr. Miranda Tolbert, thank you for believing in me, loving me, and supporting me through every day of the last six years. I owe so much to the friendships we formed in our 1st year. If nothing else, our friendship has made this journey worthwhile.

To my closest friends, thank you for supporting me from near and far. Many of you have hopped on planes and driven miles to share memories with me throughout this chapter in my life. I am lucky to have you all in my life.

To my family, your support is unwavering. To my mom, thank you for everything. I wouldn't be celebrating this achievement without the sacrifices you made to give me this life. Thank you for always encouraging me to chase my dreams. To my sister, thank you for all you've done to support me over the last six years, and for spending countless hours on the phone with me. Thank you for hopping on planes and always being there, no matter what. I love you both so much.

I'd also like to thank my in-laws, Bill and Susie, for their support over the years and genuine curiosity in my work. Thank you to my brother-in-law, Danny, for all the love, support, and witty jokes throughout the years. Thank you to my sister and brother-in-law, KimMai and Clinton, for checking in, sending love and support, and giving me a nephew. Wilder, you have changed everything I knew about my ability to love. Thank you for being my best bud. I love you.

To my partner in life and love, Billy. We did it. I owe so much to you for picking up your whole life to follow me on this journey. I will never have the words to thank you for all you have done for me. None of this would have been possible without you. This degree is as much mine as it is yours. Thank you for each and every day you show up for me, love me, and support me. I love you endlessly.

And lastly, to my cats, Patches and Ripley. Thank you for saving me whenever I need it most. The best thing I did in the last six years was adopting you both.

TABLE OF CONTENTS

Page

LIST OF TABLES

Page

LIST OF FIGURES

Page

CHAPTER 1

INTRODUCTION AND LITERATURE REVIEW

Genetic sex determination in vertebrates

Across much of Eukaryota, sexual reproduction has driven the evolution of two distinct sexes, typically males and females, that exhibit some degree of gamete and gonad dimorphism (Bachtrog et al., 2014; J. Bull, 1983; J. J. Bull, 1985; Charlesworth, 1991; Otto, 2009). Sexual reproduction ensures fitness advantages by offsetting mutational load and increasing genetic variation, enabling populations to adapt to changing environments. Within a species, the sexes commonly display sexual dimorphism, characterized by striking physical differences in color, size, structure, or form. Underlying these morphological traits is an organism's sex-determination system. This system, comprising sex-specific variation in downstream molecular pathways, determines which sex the developing embryo will become. In vertebrates, sex determination initiates the differentiation of the bipotential embryonic gonad into either a testis or an ovary that will produce sperm or eggs, respectively. The accurate and timely initiation of sex determination and gonad differentiation mechanisms is fundamental to species survival and reproductive success, and influences core evolutionary processes such as speciation, sex-specific adaptation, and genetic conflict (Bachtrog et al., 2014; Branco et al., 2017; Dufresnes & Crochet, 2022; Thomas Lenormand & Denis Roze, 2025; Zhou & Bachtrog, 2012).

Vertebrate sex determination can occur through two general mechanisms: environmental sex determination and genetic sex determination (J. Bull, 1983). Environmental sex determination is initiated by an environmental cue, while genetic sex determination is initiated by genetic differences in chromosomes, including gene expression or gene dosage. Once an environmental or genetic cue is received by the bipotential gonad, sex determination is initiated, the gonad begins to differentiate, and sex-specific characteristics begin to develop.

Among vertebrates, environmental sex determination is most commonly temperature-based. Temperature-based sex determination (TSD) has been observed in many reptiles, including all crocodilians, many turtles, and some lizard species. In TSD, the sex of the embryo is determined by a critical window of incubation during development at male or female-determining temperatures or temperature ranges. It has been shown that these environmental cues often initiate downstream gene regulatory networks and that these genetic mechanisms require initial input from the environment for gonad differentiation to proceed (Czerwinski et al., 2016; Ge et al., 2017, 2018; Mork et al., 2014; Schmahl et al., 2003; Weber et al., 2020; Yao & Capel, 2005).

Genetic sex determination in vertebrates employs mechanisms including gene presence, gene dosage, or gene expression differences, often occurring on specialized sex chromosomes. Vertebrate sex chromosomes can be homomorphic or heteromorphic, identical or visually distinct, respectively, and range from single-nucleotide differences between sexes (Kamiya et al., 2012) to highly evolved, degenerated sex chromosome systems (Bellott & Page, 2009; J.

A. Graves, 2006; Hirst et al., 2017, 2018; Lahn & Page, 1999; Stevens, 1905). For this review, I will focus on heteromorphic sex chromosome evolution and genetic sex determination mechanisms in vertebrates.

In genetic sex determination systems, the development of sexual characteristics is driven by sex-specific genomic differences of the sex chromosomes including genes and gene expression (Ioannidis et al., 2020; Kamiya et al., 2012; Peichel et al., 2020; Sinclair et al., 1990; Smith et al., 2009b). The accurate and timely initiation of these mechanisms is fundamental to species survival and reproductive success. In most vertebrates, primary genetic sex determination initiates the molecular cascade of gonadal sex differentiation, cueing the undetermined embryonic gonad to develop into either an ovary or a testis.

Previous studies have shown that many of the genes implicated in genetic sex determination pathways are conserved across vertebrate groups, while the timing and order of gene activation during gonad differentiation are highly variable (Bachtrog et al., 2014; Marshall Graves & Peichel, 2010; Sánchez-Baizán et al., 2024). Even more variable is the mechanism by which a genetic sex determination system is initiated. In some vertebrate groups, these primary sex determination genes are ancient and conserved across many related species, while in other groups, primary sex determination genes rapidly evolve, leading to high turnover of genetic sex determination systems (Bachtrog et al., 2014; Jeffries et al., 2018; Keating et al., 2021; Palmer et al., 2019). Despite its monumental importance, genetic sex determination systems have only been

carefully studied in a handful of model vertebrate species. The most well-studied genetic sex determination model systems, mammals and birds, rely on sex-specific differences between their highly evolved, ancient, and heteromorphic sex chromosome systems, XX/XY and ZZ/ZW, to initiate sex determination and trigger the downstream molecular mechanisms of gonad differentiation.

Sex chromosome evolution and dosage compensation mechanisms

Heteromorphic sex chromosomes evolve from a pair of homomorphic, or identical, autosomes when one chromosome acquires a sex-specific, primary sex-determination gene or genes (Charlesworth, 1991; Muller, 1914; Ohno, 1967). In vertebrates, this is the hypothesized evolutionary trajectory of the Y chromosome of mammals and the W chromosome of birds. This acquisition can result in progressive recombination suppression between sex chromosomes, leading to gene loss and chromosomal degeneration because of mutation accumulation on the Y or W chromosome. Thus, divergence between the heteromorphic sex chromosome pair increases rapidly, and deleterious mutants accumulate on the Y or W chromosome, likely leading to the degeneration of these chromosomes. The result is a heteromorphic sex chromosome pair differing in size, structure, and genetic content. Male (XX♀, XY♂) and female (ZZ♂, ZW ♀) heterogametic sex determination systems have evolved independently many times across vertebrate groups when an ancestral autosome acquired a primary sex determining locus (Bachtrog et al., 2014; J. Bull, 1983). Many vertebrate genetic sex determination systems maintain these highly degenerate heteromorphic sex chromosome systems for millions of years

without complete degeneration or sex chromosome turnover. In vertebrates, the most well-known and extensively studied ancient heteromorphic sex chromosome systems are found in the XX/XY genetic sex determination system of mammals and the ZZ/ZW genetic sex determination system of birds. The structural and genetic differences of the sex chromosomes ensure the maintenance of two sexes with dimorphic gametes essential for sexual reproduction and species survival but result in unequal gene expression important for fitness or vital for life. In response to these dosage disparities, many vertebrate species have subsequently evolved dosage compensation mechanisms to restore gene expression between the sexes, and in some cases, to ancestral autosomal levels.

In the past, heteromorphic sex chromosome systems were categorized based on cytogenetic evidence of physical size differences between sex chromosomes. In the genomic age, we now know that homomorphic, or cytologically indistinct, sex chromosomes can be extremely divergent in genetic content. The use of heteromorphy in this thesis will be used broadly when referring to genetic content, with the knowledge that in some lineages this has led to sex chromosome degeneration and heterogamety in one sex, while other lineages have maintained physically indistinguishable sex chromosomes with highly divergent gene content.

Dosage compensation has evolved to equilibrate the expression of genes between males and females, most often when a species has highly heteromorphic and genetically divergent sex chromosomes. In XX/XY systems,

XX females retain two alleles of a gene to one allele in XY males, and the opposite is true for ZZ/ZW systems. Dosage compensation mechanisms are often classified as complete or incomplete. Complete dosage compensation involves chromosome-wide regulatory machinery that adjusts expression of all or most genes on a sex chromosome. In contrast, incomplete dosage compensation regulates gene expression in a localized manner, often on a gene-by-gene basis.

Complete dosage compensation is achieved through diverse mechanisms, such as X chromosome inactivation in mammals and global upregulation of the male X in *Drosophila*, to ensure equal expression of X-linked genes between the sexes. Although the molecular pathways that initiate dosage compensation vary across taxa, many systems begin by recruiting protein complexes to specific binding sites or sequence motifs on the X chromosome. This recruitment facilitates epigenetic modifications to the chromatin landscape. For instance, DNA or histone methylation may decrease or inactivate X expression, while histone acetylation may increase X expression.

Current theories suggest that chromosome wide dosage compensation evolved through the co-option of existing regulatory networks to balance gene expression between the X chromosome and autosomes in both males and females (Marshall Graves, 2016). Long non-coding RNAs (lncRNAs) often play a central role by recruiting the protein complexes necessary for initiating and maintaining dosage compensation.

Our understanding of these mechanisms is largely derived from a few well-studied model systems, including mammals (Alfeghaly, 2025; Navarro-

Cobos, 2025), *C. elegans* (Albritton, 2018; Meyer, 2022), and *Drosophila* (Shevelyov, 2022). However, even in species with chromosome-wide dosage compensation, certain sex-linked genes escape regulation, often through mechanisms like those observed in incomplete dosage compensation.

In species with incomplete dosage compensation, chromosome-wide mechanisms do not evolve; instead, these species exhibit partial or gene-specific regulation. Dosage compensation is considered incomplete when the expression of sex-linked genes is not fully equalized between the sexes. In such cases, alternative regulatory strategies, such as gene-by-gene or regional control, and post-transcriptional mechanisms, are used. This localized approach can result in sex-biased expression of certain sex-linked genes.

Incomplete dosage compensation has been documented across diverse taxa, including the platypus (Deakin et al., 2008; Lister et al., 2024), the Monarch butterfly (Gu et al., 2019) and several moth species (Harrison et al., 2012; Suzuki et al., 1998).

To gain a deeper understanding of how dosage compensation is established and to begin to understand how diverse dosage compensation mechanisms truly are, we need to study dosage compensation across the tree of life. But first, I will briefly cover the most well-studied genetic sex determination systems to date—mammals and birds.

Genetic sex determination and dosage compensation in model species

Most of our knowledge about vertebrate genetic sex determination and gonadal sex differentiation comes from decades of research on the XX/XY

genetic sex determination system of mammals and, in more recent times, the ZZ/ZW genetic sex determination system of birds. Scientists have begun to understand how primary sex determination is initiated and how gonad differentiation is maintained to give rise to a sexually dimorphic population. With ever-growing diversity in the type of genes identified as primary initiators, the “usual suspects” genes of gonadal sex differentiation remain largely conserved across vertebrates (Bertho et al., 2021; Herpin & Schartl, 2015), though differences in the order of gene network pathways and expression patterns are starting to be identified and better understood. Mammals and birds remain the most well-studied systems for sex determination, and, with that, guide most of our thinking about the genetics underlying these mechanisms. While both genetic sex determination systems are ancient and deeply conserved within these amniote lineages, they highlight the differences and similarities of XX/XY and ZZ/ZW genetic sex determination systems.

The XX/XY genetic sex determination system in therian mammals is ancient, originating around 166 million years ago following the divergence of monotremes from the therian lineage (marsupials and placentals). The differentiation of the X and Y chromosomes occurred before the split between marsupials and placentals, approximately 148 million years ago (Marshall Graves, 1998; Lahn & Page, 1999; Veyrunes et al., 2008; Wallis et al., 2008). In the late 1950s, the Y chromosome was identified in eutherian mammals, initiating the search for a testis-determining factor or factors (*TDF*) (Ford et al., 1959). The search for the *TDF* followed five key principles. The *TDF* would be conserved

across mammals and located on the Y chromosome within the smallest known sex-determining region. This would also be the most ancient region of the Y. Its protein product would act cell-autonomously and be a primary regulator of other downstream genes. It would be expressed in the somatic cells of the testis early in XY gonad differentiation, and genetic manipulation of the *TDF* would result in complete sex reversal (Burgoyne et al., 1988; Koopman et al., 2016). Most, if not all, of these principles hold in the modern identification of primary sex determination loci across the tree of life and were essential to the project laid out in the 3rd chapter of this dissertation. Once these principles were identified, the race was on to identify the *TDF* of eutherian mammals.

In 1990, Sinclair and colleagues identified the gene **S**ex-determining **R**egion **Y**, or *SRY*, as the testis-determining factor in humans and mouse models. The presence of *SRY* on the male-specific Y chromosome initiates primary sex determination and the underlying downstream molecular mechanisms of testis differentiation in male mammals (Sinclair et al., 1990). *SRY* is not found in monotremes (Shearwin-Whyatt et al., 2025) and is estimated to have arisen ~130 million years ago when this gene landed on the eutherian Y and the translocation became fixed (J. A. Graves, 1998; Sinclair, 2001). This discovery, identified using chromosome walking of the human Y chromosome, propelled sex determination research and is the foundation for our current understanding of gonadal sex differentiation. Genomic sequences present in XX human males and absent in XY human females allowed researchers to identify a 35-kilobase region where the *SRY* (humans)/*Sry* (mouse) gene is located (Berta et al., 1990; Gubbay et al.,

1990; Koopman et al., 1990, 2016; Page et al., 1987; Palmer et al., 1989; Pritchard et al., 1987; Sinclair et al., 1990). Further research found that mutations in *SRY/Sry* resulted in XY female mice, and transgenic XX mice ectopically expressing *SRY/Sry* developed as males. Thus, *SRY/Sry* is required and sufficient to initiate male sex determination and testis differentiation in most mammals (Berta et al., 1990; Gubbay et al., 1990; Koopman et al., 1990, 1991, 2016; Sinclair, 2001). *SRY/Sry* is part of the Sox gene family. Related Sox genes (*Sox 8, Sox 9, Sox 10*) have been implicated in genetic sex determination initiation and downstream gonad differentiation mechanisms (Koopman, 2005). These genes usually express male-biased transcripts and are important for testis differentiation and development. This discovery and the decades of research since have made way for identifying primary sex determination genes in other vertebrates where *SRY/Sry* is absent, allowing us to further understand the evolution of genetic sex determination mechanisms (Koopman et al., 2016).

As a result of Y chromosome degeneration, the mammalian XX/XY genetic sex determination system undergoes a chromosome wide mechanism for dosage compensation. In mammals, XX females undergo X chromosome inactivation in which one X chromosome is silenced to match the singular X expression of XY males. The lncRNA, *XIST*, recruits a protein complex to initiate methylation of the X chromosome. The chromatin of the X chromosome is then tightly packed, condensed, and silenced to balance the expression of dosage-sensitive genes between the sexes (Loda & Heard, 2019; Monfort & Wutz, 2017; Disteche & Berletch, 2015).

While mammalian sex determination works in a gene presence vs absence mechanism, genetic sex determination can also be initiated through gene dosage differences between males and females. This sex determination mechanism has been most carefully studied in the ZZ/ZW system of birds. All bird species share a homologous ZZ/ZW genetic sex determination system in which males (ZZ) are the homomorphic sex and females (ZW) are the heteromorphic sex, opposite to what we see in mammalian sex determination. Although similarly ancient, the ZZ/ZW of birds arose independently from mammals via a different ancestral autosomal pair. The W chromosome of birds has undergone chromosome degeneration and gene loss, much like the mammalian Y chromosome. It was originally proposed that in the chicken, the W chromosome may contain an ovary determinant or primary sex determination locus or that the dosage of a Z-linked gene could be responsible for male sex determination and required in two copies. In 2009, Smith et al. proposed the Z-linked gene double sex and mab-3-related transcription factor 1, or *DMRT1,* as a testis-determining factor in birds. Using RNA interference (RNAi), researchers knocked down *DMRT1* in early chicken embryos to reduce overall expression. This reduction in ZZ male embryos led to feminization of the embryonic gonads and partial male-to-female sex reversal (Smith et al., 2009b). In birds, ZW female gonads develop asymmetrically with a large left ovary and the regression of the right ovary, while ZZ males have bilateral testes. In Smith et al. (2009), RNAi-treated ZZ males showed varying levels of gonad asymmetry. The larger left gonad displayed female-like histology, disorganized testicular cords, and

downregulation of testis marker genes. Additionally, the germ cells were found to be distributed in the female pattern. Thus, *DMRT1* was found to be required for testis determination in the chicken (Lambeth, 2014; Major, 2016; Raymond, 1999; Smith et al., 2009a). Supporting the Z dosage hypothesis, the two copies of *DMRT1* and higher expression in ZZ males drive male sex determination in avian species. This gene met the requirements for a primary sex determining locus as it is sex-linked, conserved across bird species, expressed exclusively in the urogenital system before gonad differentiation, expressed more highly in males, and when knocked out, resulted in partial sex reversal. *DMRT1* and its related gene family act as key regulators in gonad differentiation and initiate genetic sex determination in some vertebrate species (Augstenová & Ma, 2025). Ancestrally, *DMRT1* produces male-biased transcripts and plays a critical role in testis differentiation. However, in *Xenopus laevis,* a *DMRT1* paralog known as *DM-W* has been shown to direct female development (Yoshimoto et al., 2008, 2010)

The dosage of *DMRT1*, however, is just part of the story for genetic sex determination in birds. Gynandromorphic chickens, or chimeras, are half female/half male, indicating that, in birds, sexual phenotype is at least partly cell autonomous, with gonadal sex differentiation being only a small part of the overall sexual phenotype of an animal (Clinton et al., 2012; Hirst et al., 2018; Zhao et al., 2010). Using CRISPR-Cas9-based monoallelic targeting, Ioannidis et al. 2021 showed that mutations in *DMRT1* resulted in ZZ males that developed ovaries. The ovaries expressed typical female markers and were undergoing

follicular development, but externally, these chickens looked like wild-type males. This finding further supported cell-autonomous sex identity (CASI) in birds and confirmed *DMRT1* as the primary initiator of male sex determination and testis development. In addition, they blocked estrogen synthesis in wild-type ZW female embryos, which resulted in testis development. When estrogen production was blocked in *DMRT1* null female embryos, ovaries developed. This shows that estrogen plays a key role in primary sex determination, and its production is linked to *DMRT1* expression in birds (Ioannidis et al., 2020).

The W chromosome of birds has undergone massive gene loss and degeneration, leading to gene expression differences between males and females. Unlike the X chromosome of female mammals, however, the male Z chromosome does not undergo condensation or silencing, and it is not well understood how birds compensate for dosage differences (Sun et al., 2019). Without evidence of a chromosome wide dosage compensation mechanism, scientists have long thought that birds undergo dosage compensation on a gene-by-gene basis, and estimates of dosage compensation genes were ~20-45% (Ellegren et al., 2007; McQueen & Clinton, 2009; Wright et al., 2015). However, using chicken fibroblasts, Deviatiiarov et al., 2023 concluded that ~75% of Z chromosome genes are strictly compensated across avian species, a number much higher than previously thought and comparable to the fraction of dosage-compensated X genes in human fibroblasts (Carrel & Willard, 2005; San Roman et al., 2023). It is still unclear how avian species modulate Z chromosome dosage compensation. Dosage compensation could be modulated by the 2-fold

upregulation of the female Z chromosome, halving the expression of both male Z chromosomes, or a combination of these known mechanisms.

Reptilian sex determination: the XX/XY system of Pleurodont lizards

Unlike traditional model systems used to investigate sex determination, reptile lineages exemplify the diversity of sex determination mechanisms we see across the tree of life, making this group a remarkable system to study a wide breadth of sex determination systems. Reptiles encompass nearly every example of sex determination known to date, including XX/XY and ZZ/ZW genetic sex determination, environmental sex determination, polygenic sex determination, and genetic sex determination with homomorphic sex chromosome systems (Bachtrog et al., 2014; Zhu et al., 2025). This contrasts with mammalian and avian genetic sex determination, as both groups have very few species that do not use their ancient, conserved genetic sex determination systems (Saunders & Veyrunes, 2021) .

It was once thought that all species of reptiles would be subject to rapid sex chromosome turnover, as is seen in other vertebrate poikilotherms such as fish and amphibians, but with advancements in molecular and genomic techniques we now know that the evolutionary stability of sex determination systems among reptiles is as diverse as the species themselves (Rovatsos, Altmanová, et al., 2014; Rovatsos, Pokorná, et al., 2014). Within reptiles, ancient and evolutionarily stable genetic sex determination systems and young genetic sex determination systems with rapid sex chromosome turnover have been identified. With next-generation sequencing (NGS) becoming cheaper and more

attainable, reptile genomes are being published, and sex determination systems are being identified faster than ever before. However, research is still lacking to uncover the molecular mechanisms of the genetic pathways that make up these sex determination systems.

Why do some sex determination systems persist for millions of years, while others have turned over repeatedly? Studying genetic sex determination in reptiles can bridge these gaps in our understanding of how genetic sex determination evolved, how genetic sex determination systems are maintained, and what makes for a good primary sex determination locus. Since sex determination is fundamental to species survival, the ability to turn over sex chromosome systems and gain new primary sex determination gene(s) is essential. For ancient systems, though, it begs the question, what gives rise to evolutionarily stable genetic sex determination systems (Rovatsos, Altmanová, et al., 2014; Rovatsos, Pokorná, et al., 2014)? What genetic architecture allows some species to maintain sex determination systems for millions of years without turnover? The following chapters will explore the underlying genetic mechanisms of an ancient reptilian genetic sex determination system that has persisted for ~100 million years in over 1,200 lizard species.

The class Reptilia is made up of over 12,400 non-avian reptile species, with 12,000 of those belonging to the order Squamata, which encompasses all lizards and snakes (Uetz, P et al., 2025; The Reptile Database, (Keating et al., 2021b; Pinto et al., 2022)). Within Squamata, there are approximately 7,800 known lizard species, making it one of the largest and most diverse groups of

reptiles (Uetz, P et al., 2025; The Reptile Database, http://www.reptile-database.org). Among lizard species, genetic sex determination and environmental sex determination mechanisms have been identified. Some species groups, like geckos, experience rapid sex chromosome turnover (Keating et al., 2021; Pinto et al., 2022), while others, including the clade *Pleurodonta*, maintain an ancient and conserved genetic sex determination system (Gamble et al., 2014; Rovatsos, Altmanová, et al., 2014; Rovatsos, Pokorná, et al., 2014).

Pleurodonta, also cited in the literature as *Iguanomorpha* (DeMar et al., 2017), is a species-rich clade of over 1,200 lizard species across 12 families (Uetz, P et al., 2025; The Reptile Database, http://www.reptile-database.org). Of these species, only 9 species belonging to the family *Corytophanidae*, or the basilisk lizards, have experienced sex chromosome turnover (Acosta et al., 2019; Altmanová et al., 2018). The remaining species, including all iguanas and anoles, have retained an ancient XX/XY genetic sex determination system that has persisted for millions of years. This genetic sex determination system displays extensive stability of sex chromosomes, like what we see in other vertebrates such as mammals and birds. The pleurodont XX/XY sex determination system is hypothesized to have originated approximately 73-123 million years ago, with some estimates extending its emergence to around 160 million years ago. This system is thought to have arisen in the last common ancestor of pleurodont lizards, either shortly before or after their divergence from acrodont lineages (Ezaz et al., 2009; Lisachov et al., 2017; Marin et al., 2017; Rovatsos,

Altmanová, et al., 2014, 2014). The exact date that this system originated has been debated, but there is a consensus that this system is ancient and shared among all iguanas regardless of the precise timing of its origin (Ezaz et al., 2009; Lisachov et al., 2017; Marin et al., 2017; Rovatsos, Pokorná, et al., 2014). Among pleurodont lizards, homologous regions of the sex chromosomes have been identified across most of their member species. This is an evolutionarily stable XX/XY system derived from a single ancestral autosomal pair (Gamble et al., 2014). To date, the X and Y of pleurodont lizards represent the oldest known sex chromosomes among amniotic poikilothermic vertebrates (Rovatsos, Pokorná, et al., 2014). Among the subgroups within Pleurodonta, *Anolis* is one of the most diverse and species-rich representing the largest genus of terrestrial vertebrates (Giovannotti et al., 2017; Nicholson et al., 2012). Due to this, *Anolis* lizards make a stellar model for studying an array of biological processes.

Sex determination and dosage compensation in *Anolis* lizards

Anolis comprises more than 400 small to medium-sized lizard species, the result of an adaptive radiation that occurred >65 million years ago (Kichigin et al., 2016; Nicholson et al., 2012). These lizards are physically diverse in size, color, and ecological niche. They are distributed throughout the tropical and sub-tropical Americas, and across islands in the West Indies and eastern Pacific Ocean (Blankers et al., 2013; Geneva et al., 2022; Losos & Schneider, 2009). *Anolis* lizards have been used to study evolutionary ecology (Losos & Pringle, 2011; Pringle et al., 2019; Schoener & Schoener, 1980), behavior (Lapiedra et al., 2017, 2018), speciation (Ingram et al., 2016; Rabosky & Glor, 2010),

and convergent evolution (Arbuckle et al., 2014; Huie et al., 2021; Ord et al., 2013) for decades. More recently, due to advancements in sequencing technologies, they have become models for genetic (Cádiz et al., 2018; R. Reynolds et al., 2017; Tollis & Boissinot, 2013) and genomic (Rasys et al., 2019; Schneider, 2008; Tollis et al., 2012) studies as well.

Although anole lizards are phenotypically diverse, the X and Y sex chromosomes are homologous and shared across all anoles and most other Pleurodont lizards. Anole species exhibit tremendous variation in their chromosomal karyotypes. Their diploid chromosome numbers range from 26 to 44 and are a mix of macro and microchromosomes (Giovannotti et al., 2017). This variation is due to lineage-specific rearrangements, such as autosome and microchromosome fusion or fission events, that occurred during speciation. In some species, these rearrangements have included the sex chromosomes. Ancestrally, the X and Y were considered homomorphic micro sex chromosomes, meaning they were visually indistinguishable by karyotype. In the age of genomics, we now know that the pleurodont X and Y, while similar in size, are extremely divergent and differ greatly in genetic content. Some species of anoles, such as *Anolis carolinensis* (the green anole), have retained this micro-XX/XY ancestral karyotype. Other species, including *Anolis sagrei* (the brown anole), have undergone multiple fusion events resulting in a mid-sized heteromorphic XX/XY sex chromosome system. Additionally, there are some instances where the ancestral X is part of a multiple sex chromosome system, $X_1X_1X_2X_2/X_1X_2Y$ (Giovannotti et al., 2017). Although there is lineage-specific

variation in the X and Y sex chromosomes of *Anolis*, all species retain an ancestral X and Y homologous region. The micro sex chromosomes of *A. carolinensis* are often used as a proxy for the ancestral state of the *Anolis* X and Y. *A. carolinensis* has long been used as a model system. In 2011, Alfoldi et. al published the XX genome of the green anole, propelling non-avian reptiles into the world of genetics and genomics. Their study revealed a syntenic relationship between the *A. carolinensis* X and chicken microchromosome 15 and confirmed a male heterogametic XY system in *Anolis* (Alföldi et al., 2011).

In the years that followed, the green anole genome assembly paved the way for researchers to identify the ancestral origin of the pleurodont XX/XY system (Gamble et al., 2014; Rovatsos, Altmanová, et al., 2014; Rovatsos, Pokorná, et al., 2014), identify marker genes for use in PCR sex genotyping (Gamble 2014), identify novel X-linked genes (Rovatsos, Altmanová, et al., 2014; Rovatsos, Pokorná, et al., 2014), and gain insights into sex chromosome content and evolution (Giovannotti et al., 2017; Kichigin et al., 2016). In addition, studies were conducted to understand dosage compensation mechanisms in the green anole (Marin et al., 2017; Rupp et al., 2017).

Dosage compensation mechanisms evolve to equilibrate gene expression between the sexes in heteromorphic sex chromosome systems. The X and Y chromosomes of *Anolis* lizards are highly divergent from one another. As a result of recombination suppression and chromosomal rearrangements, the Y chromosome has degenerated and lost genetic content. To balance the expression of X genes in XY males with that of XX females, anole lizards evolved

a dosage compensation mechanism reminiscent of *Drosophila.* Our current understanding of this mechanism comes from studying the ancestral, micro sex chromosomes of the green anole.

In 2017, Rupp and colleagues looked for evidence of dosage compensation in *A. carolinensis* using transcriptome data from the regenerating tail. To identify signatures of dosage compensation, researchers looked at the expression ratio of male vs. female transcripts. In the absence of dosage compensation, this ratio would be ~0.5, with values closer to 1 indicating equal gene expression between sexes. Researchers analyzed the data in two groups, one proposed to be older and more differentiated (identified in Alföldi et al., 2011) and one containing newly proposed X genes thought to be younger. Median male to female relative expression varied from 0.97 in the older X-linked group to 0.82 across the younger set, suggesting that while many genes are compensated, it may not be complete across the entire *A. carolinensis* X chromosome. To uncover the dosage compensation mechanism, researchers compared absolute X expression with the autosomes. In both sexes, they found median expression for X-linked genes was lower than on the autosomes and that mean expression was significantly higher on the male X. They concluded that in the green anole, dosage compensation is modulated by the 2-fold upregulation of the male X (Rupp et al., 2017).

Marin et al. 2017 followed this work up with a larger and more expansive data set including genome, transcriptome, and histone modification sequencing. To assess dosage compensation in the green anole, researchers compared X

expression levels with ancestral levels they had inferred from autosomal ortholog expression in outgroup species (Cortez et al., 2014; Julien et al., 2012; Mank, 2013; Vicoso & Bachtrog, 2015). In their analyses, median X expression was indistinguishable from the inferred ancestral expression. This recapitulates the Rupp et al., 2016 finding that the male X is twofold upregulated, but researchers argue that this is a global mechanism indicating complete dosage compensation across the whole of the X chromosome. In *A. carolinensis,* XX females retain ancestral expression levels while XY males upregulate their X twofold to balance expression between sexes. X-upregulation in *Drosophila melanogaster* is achieved through global acetylation of H4K16 on the male X (Conrad & Akhtar, 2012; Hilfiker et al., 1997). To identify if global X-upregulation in the green anole is dependent on the same mechanism, researchers generated ChIP- sequencing data from the brain and liver. On the male X, they found that H4K16ac levels were substantially elevated, reminiscent of *D. melanogaster,* indicating male-specific chromatin machinery drives the global twofold upregulation of the male X in *Anolis* (Marin et al., 2017).

More recently, Tenorio et al. (2024) identified *MAYEX,* a male-specific, ancient lncRNA, that regulates dosage compensation in *A. carolinensis. MAYEX* lies in a large intergenic region opposite to the *MORC2* gene on the reverse strand. *MAYEX* and *MORC2* share a CpG promoter. Researchers also identified a female-specific locus, *FEREX*, located downstream of *MAYEX* in the same intergenic region. The male-to-female expression ratio indicated the presence of a chromosome-wide dosage compensation mechanism, and male-specific

hyperacetylation was found along the entire X chromosome. Additionally, the male X was found to have more topologically associated domains (TADs). Disruption of *MAYEX* in an *Anolis sagrei* cell line using CRISPRi revealed that X chromosome upregulation requires constant expression of the locus (Tenorio et al., 2024).

Advancing studies of *Anolis* sex chromosome biology using *A. sagrei*

Since the publication of the green anole genome, great strides have been made in understanding sex determination and dosage compensation mechanisms in reptiles. While this genome remains a vital resource to the field, it has become quickly outdated as sequencing technologies have continued to improve. *A. carolinensis* was chosen as the first non-avian reptile to have its genome sequenced due to its historical usage in epidemiology and neurobiology studies. In recent years, however, the brown anole, *Anolis sagrei*, has surpassed the green anole in publications per year, making this species an important emerging model (Baeckens et al., 2018; Bock et al., 2021; Geneva et al., 2022; Lapiedra et al., 2018; Sanger et al., 2008).

Native to Cuba and the Bahamas, the brown anole lizard, *Anolis sagrei,* is a medium-sized, ground-trunk anole. It is a pervasive invader with populations established on additional islands across the West Indies and the central Atlantic Ocean. *A. sagrei* has become abundant in the Southeastern United States from the Florida Everglades up to southern Georgia and as far west as Texas. Populations have been found in California and Hawaii as well. Due to their proclivity to invade, *A. sagrei* US populations are robust, often outcompeting the

native green anole. Wide native and invasive habitat range and high population abundance have made *A. sagrei* an important species for studying evolution and ecology. The brown anole boasts a short generation time (thirty days from egg lay to hatch and 6-8 months until adulthood) and year-round reproduction in captivity making it an ideal reptilian model for behavior (Driessens et al., 2017; Kabelik et al., 2014; Lapiedra et al., 2024; Logan et al., 2018; Pita-Aquino et al., 2023), development (Feiner et al., 2022; Hermyt et al., 2020; Kircher et al., 2024, 2025; Rasys et al., 2021, 2025; Weberling et al., 2025; Weronika et al., 2025), adaptation (Bock et al., 2023, 2024; Hall et al., 2020; Hall & Warner, 2021; R. G. Reynolds et al., 2020), and more recently, sex determination (Motley et al., Chapter 3). Recent advancements in sequencing technology and the development of genomic tools have propelled *A. sagrei* to model system status (Geneva et al., 2022; Rasys et al., 2019, 2021, 2025).

In 2019, Rasys et al. made history by successfully gene editing the brown anole using CRISPR-Cas9—the first reptile to undergo genome editing. In short, the gene editing procedure is performed by anesthetizing adult females and making an incision in the side of the animal to access the developing oocytes. CRISPR-Cas9 and guide RNAs are injected into the oocytes, and the female is closed. Once mated, eggs are collected as they are laid and incubated. Hatchlings are screened for mutations after emerging from the eggs. This is an extremely robust system, and many genes have been targeted successfully (Rasys et al., 2019, 2021, 2025; Menke Lab unpublished). This advancement

has allowed the brown anole to become a model system for studying reptilian gene function and evolutionary development in vivo.

In 2022, Geneva et al. published the highly complete and contiguous genome assembly of an XX brown anole female—an advancement long overdue for this emerging model. This assembly was generated through multiple rounds of iterative improvement using Illumina whole-genome shotgun sequencing, Hi-C scaffolding, and PacBio long-read sequencing. In this study, researchers identify the *A. sagrei* X chromosome and conduct synteny analyses with the *A. carolinensis* X to understand how the *A. sagrei* X has evolved (Geneva et al., 2022). Unlike the green anole that maintains the ancestral micro sex chromosomes, *Anolis sagrei* has undergone multiple autosome-to-sex chromosome fusion events. As a result, the X and Y of *A. sagrei* are mid-sized and relatively gene-rich due to these more recent additions. When fusion events occur with sex chromosomes, we refer to the new X and Y as neo-sex chromosomes. Neo-sex chromosome systems have historically been used to study sex chromosome degeneration and dosage compensation mechanisms (Altmanová et al., 2018; Gu & Walters, 2017). In addition to these newly added chromosomal regions, *A. sagrei* retains the homologous ancient X and Y shared across most pleurodont lizards. It is hypothesized that the brown anole sex chromosomes underwent three independent fusions of autosomes with the ancestral X and Y (Giovannotti et al., 2017; Lisachov et al., 2019), but the order and timing of these events have been debated.

In Giovannotti et al. (2017), researchers hypothesized that the *A. sagrei* ancestral X fused with ancestral micro chromosomes via 2 fusion events involving homologous *A. carolinensis* chromosomes 9 and 12. (Giovannotti et al., 2017). In a study by Kichigan and colleagues, researchers proposed three fusion events involving homologous *A. carolinensis* chromosomes 9, 12, and 18 (Kichigin et al., 2016). In 2022, Geneva and colleagues confirmed previous hypotheses that the *A. sagrei* neo-X chromosome is comprised of chromosomes homologous to *A. carolinensis* chromosomes 9, 12, 18, and the ancestral X (13). Due to the completeness of the newly assembled brown anole genome, a clear synteny prediction for the order of homologous chromosomes on the neo-X and the linkage groups of the ancestral X was made. To confirm male heterogamety, genome coverage was used to identify pseudoautosomal regions and the X-specific region. These PAR boundaries evolved after the chromosomal fusion events, as the ancestral PARs now sit in the middle of the X chromosome within the X-specific region. Lastly, Geneva and colleagues found evidence that X-Y divergence was higher on the ancestral X region as it has been sex linked the longest (Geneva et al., 2022). With genomic resources such as a well-annotated genome assembly and functional gene editing in vivo, *A. sagrei* has quickly become an enticing model to study developmental genetics and functional genomics.

A. sagrei as a model for studies of reproductive biology

In addition*, Anolis sagrei* is a well-suited model to study the genetic and evolutionary mechanisms of reproductive biology, sex determination, and gonad

differentiation. To this end, Kircher and colleagues described the female reproductive tract of *A. sagrei* in detail using hematoxylin and eosin staining, immunofluorescence staining, and micro-computed tomography (micro-CT) scanning. The female anole reproductive system consists of paired ovaries located next to paired reproductive tracts, consisting of the infundibulum, the glandular uterus, and the non-glandular uterus connected to the digestive tract and the cloaca. Kircher et al. generated a detailed anatomical atlas of the above reproductive tract, laying the groundwork for the exploration of genes involved in sexual differentiation (Kircher et al., 2024).

Over 1,200 species share the ancient, conserved XX/XY sex determination system of pleurodont lizards, including *Anolis sagrei*. The brown anole has quickly become an ideal model for developmental and evolutionary genetics, with unique biology allowing us to ask questions about sex chromosome evolution and dosage compensation in an ancient neo-sex chromosome system. Additionally, with the ability to conduct functional genomics, the brown anole has become an excellent model for studying sex determination and gonad differentiation in a reptile.

Research aims

The major goal of my dissertation was to uncover the genetic mechanisms underlying dosage compensation and sex determination in the brown anole lizard, *Anolis sagrei*. More specifically, I sought to identify the primary initiator of sex determination and to understand the relationship between gene loss on the Y chromosome and X chromosome dosage compensation. In Chapter 2, I examine

dosage compensation mechanisms and sex chromosome evolution. Using RNA-sequencing and a newly generated XY genome assembly, I investigate regional differences in dosage compensation across the neo-X chromosome. In Chapter 3, I generate an expansive RNA-sequencing data set to identify a candidate gene in my search for the primary determinant of sex in *A. sagrei*. Once identified, I functionally tested this candidate using CRISPR-Cas9-mediated gene editing surgeries, which resulted in complete sex reversal. From this, I concluded that *rpl6y* (ribosomal protein L6Y) is required for male sex determination in the brown anole. My work has uncovered interesting patterns of dosage compensation and deepened our understanding of how dosage compensation mechanisms evolve in neo-sex chromosome systems. Additionally, my work uncovered a novel mechanism for genetic sex determination that is likely used in over 1,200 lizard species and will fundamentally change how we think about primary sex determining genes. Lastly, in Chapter 4, I summarize the above findings and describe future directions.

REFERENCES

Acosta, A., Suárez-Varón, G., Rodríguez-Miranda, L. A., Lira-Noriega, A., Aguilar-Gómez, D., Gutiérrez-Mariscal, M., Hernández-Gallegos, O., Méndez-de-la-Cruz, F., & Cortez, D. (2019). Corytophanids Replaced the Pleurodont XY System with a New Pair of XY Chromosomes. *Genome Biol Evol*, *11*(9), 2666–2677. https://doi.org/10.1093/gbe/evz196

Agnese Loda, & Edith Heard. (2019). Xist RNA in action: Past, present, and future. *PLoS Genetics*, *15*(9). https://doi.org/10.1371/journal.pgen.1008333

Albritton, S. E. (2018). Caenorhabditis elegans Dosage Compensation: Insights into Condensin-Mediated Gene Regulation—PubMed. *Trends in Genetics : TIG*, *34*(1). https://doi.org/10.1016/j.tig.2017.09.010

Alfeghaly, C. R. (2025). X chromosome inactivation in mammals: General principles and species-specific considerations—PubMed. *EMBO Reports*, *26*(14). https://doi.org/10.1038/s44319-025-00499-1

Alföldi, J., Di Palma, F., Grabherr, M., Williams, C., Kong, L., Mauceli, E., Russell, P., Lowe, C. B., Glor, R. E., Jaffe, J. D., Ray, D. A., Boissinot, S., Shedlock, A. M., Botka, C., Castoe, T. A., Colbourne, J. K., Fujita, M. K., Moreno, R. G., ten Hallers, B. F., … Lindblad-Toh, K. (2011). The genome of the green anole lizard and a comparative analysis with birds and mammals. *Nature*, *477*(7366), 587–591. https://doi.org/10.1038/nature10390

Altmanová, M., Rovatsos M, Johnson Pokorná M, Veselý M, Wagner F, & Kratochvíl L. (2018). All iguana families with the exception of basilisks share sex chromosomes—PubMed. *Zoology (Jena, Germany)*, *126*. https://doi.org/10.1016/j.zool.2017.11.007

Arbuckle, K., Bennett, C. M., & Speed, M. P. (2014). A simple measure of the strength of convergent evolution. *Methods in Ecology and Evolution*, *5*(7), 685–693. https://doi.org/10.1111/2041-210X.12195

Asun Monfort, & Anton Wutz. (2017). Progress in understanding the molecular mechanism of Xist RNA function through genetics. *Philosophical Transactions of the Royal Society B: Biological Sciences*, *372*(1733). https://doi.org/10.1098/rstb.2016.0368

Augstenová, B., & Ma, W. J. (2025). Decoding Dmrt1: Insights into vertebrate sex determination and gonadal sex differentiation—PubMed. *Journal of Evolutionary Biology*. https://doi.org/10.1093/jeb/voaf031

Bachtrog, D., Mank, J. E., Peichel, C. L., Kirkpatrick, M., Otto, S. P., Ashman, T. L., Hahn, M. W., Kitano, J., Mayrose, I., Ming, R., Perrin, N., Ross, L., Valenzuela, N., & Vamosi, J. C. (2014). Sex determination: Why so many ways of doing it? *PLoS Biol*, *12*(7), e1001899. https://doi.org/10.1371/journal.pbio.1001899

Baeckens, S., Driessens, T., Huyghe, K., Vanhooydonck, B., & Van Damme, R. (2018). Intraspecific Variation in the Information Content of an Ornament: Why Relative Dewlap Size Signals Bite Force in Some, But Not All Island

Populations of Anolis sagrei. *Integrative and Comparative Biology*, *58*(1), 25–37. https://doi.org/10.1093/icb/icy012

Bellott, D. W., & Page, D. C. (2009). Reconstructing the evolution of vertebrate sex chromosomes—PubMed. *Cold Spring Harbor Symposia on Quantitative Biology*, *74*(0). https://doi.org/10.1101/sqb.2009.74.048

Berta, Hawkins, Sinclair, Taylor, Griffiths, Goodfellow, & Fellous. (1990). Genetic evidence equating SRY and the testis-determining factor. *Nature*, *348*(6300). https://doi.org/10.1038/348448A0

Bertho, S., Herpin A, Schartl M, & Guiguen Y. (2021). Lessons from an unusual vertebrate sex-determining gene—PubMed. *Philosophical Transactions of the Royal Society of London. Series B, Biological Sciences*, *376*(1832). https://doi.org/10.1098/rstb.2020.0092

Blankers, T., Townsend, T. M., Pepe, K., Reeder, T. W., & Wiens, J. J. (2013). Contrasting global-scale evolutionary radiations: Phylogeny, diversification, and morphological evolution in the major clades of iguanian lizards. *Biological Journal of the Linnean Society*, *108*(1), 127–143. https://doi.org/10.1111/j.1095-8312.2012.01988.x

Bock, D. G., Baeckens, S., Kolbe, J. J., & Losos, J. B. (2024). When adaptation is slowed down: Genomic analysis of evolutionary stasis in thermal tolerance during biological invasion in a novel climate. *Molecular Ecology*, *33*(10), e17075. https://doi.org/10.1111/mec.17075

Bock, D. G., Baeckens, S., Pita-Aquino, J. N., Chejanovski, Z. A., Michaelides, S. N., Muralidhar, P., Lapiedra, O., Park, S., Menke, D. B., Geneva, A. J.,

Losos, J. B., & Kolbe, J. J. (2021). Changes in selection pressure can facilitate hybridization during biological invasion in a Cuban lizard. *Proceedings of the National Academy of Sciences of the United States of America*, *118*(42), e2108638118. https://doi.org/10.1073/pnas.2108638118

Bock, D. G., Liu, J., Novikova, P., & Rieseberg, L. H. (2023). Long-read sequencing in ecology and evolution: Understanding how complex genetic and epigenetic variants shape biodiversity. *Molecular Ecology*, *32*(6), 1229–1235. https://doi.org/10.1111/mec.16884

Branco, A. T., Brito, R. M., & Lemos, B. (2017). Sex-specific adaptation and genomic responses to Y chromosome presence in female reproductive and neural tissues. *Proceedings. Biological Sciences*, *284*(1869), 20172062. https://doi.org/10.1098/rspb.2017.2062

Bull, J. (1983). *Evolution of Sex Determining Mechanisms*. Benjamin/Cummings Pub. Co.

Bull, J. J. (1985). Sex determining mechanisms: An evolutionary perspective—PubMed. *Experientia*, *41*(10). https://doi.org/10.1007/BF01952071

Burgoyne, Buehr, & McLaren. (1988). XY follicle cells in ovaries of XX----XY female mouse chimaeras—PubMed. *Development (Cambridge, England)*, *104*(4). https://doi.org/10.1242/dev.104.4.683

Cádiz, A., Nagata, N., Díaz, L. M., Suzuki-Ohno, Y., Echenique-Díaz, L. M., Akashi, H. D., Makino, T., Kawata, M., Cádiz, A., Nagata, N., Díaz, L. M., Suzuki-Ohno, Y., Echenique-Díaz, L. M., Akashi, H. D., Makino, T., & Kawata, M. (2018). Factors affecting interspecific differences in genetic

divergence among populations of Anolis lizards in Cuba. *Zoological Letters 2018 4:1*, *4*(1). https://doi.org/10.1186/s40851-018-0107-x

Carrel, L., & Willard, H. F. (2005). X-inactivation profile reveals extensive variability in X-linked gene expression in females. *Nature*, *434*(7031), 400–404. https://doi.org/10.1038/nature03479

Charlesworth, B. (1991). The evolution of sex chromosomes. *Science*, *251*(4997), 1030–1033. https://doi.org/10.1126/science.1998119

Clinton, M., Zhao, D., Nandi, S., & McBride, D. (2012). Evidence for avian cell autonomous sex identity (CASI) and implications for the sex-determination process? *Chromosome Research*, *20*(1), 177–190. https://doi.org/10.1007/s10577-011-9257-9

Conrad, T., & Akhtar, A. (2012). Dosage compensation in Drosophila melanogaster: Epigenetic fine-tuning of chromosome-wide transcription. *Nature Reviews. Genetics*, *13*(2), 123–134. https://doi.org/10.1038/nrg3124

Cortez, D., Marin, R., Toledo-Flores, D., Froidevaux, L., Liechti, A., Waters, P. D., Grützner, F., & Kaessmann, H. (2014). Origins and functional evolution of Y chromosomes across mammals. *Nature*, *508*(7497), 488–493. https://doi.org/10.1038/nature13151

Czerwinski, M., Natarajan, A., Barske, L., Looger, L. L., & Capel, B. (2016). A timecourse analysis of systemic and gonadal effects of temperature on sexual development of the red-eared slider turtle Trachemys scripta

elegans. *Dev Biol*, *420*(1), 166–177. https://doi.org/10.1016/j.ydbio.2016.09.018

Deakin, J. E., Hore, T. A., Koina, E., & Graves, J. A. M. (2008). The Status of Dosage Compensation in the Multiple X Chromosomes of the Platypus. *PLOS Genetics*, *4*(7), e1000140. https://doi.org/10.1371/journal.pgen.1000140

DeMar, D. G., Conrad, J. L., Head, J. J., Varricchio, D. J., & Wilson, G. P. (2017). A new Late Cretaceous iguanomorph from North America and the origin of New World Pleurodonta (Squamata, Iguania). *Proceedings. Biological Sciences*, *284*(1847), 20161902. https://doi.org/10.1098/rspb.2016.1902

Deviatiiarov, R., Nagai, H., Ismagulov, G., Stupina, A., Wada, K., Ide, S., Toji, N., Zhang, H., Sukparangsi, W., Intarapat, S., Gusev, O., & Sheng, G. (2023). Dosage compensation of Z sex chromosome genes in avian fibroblast cells. *Genome Biology*, *24*(1), 213. https://doi.org/10.1186/s13059-023-03055-z

Disteche, C. M., & Berletch, J. B. (2015). X-chromosome inactivation and escape—PubMed. *Journal of Genetics*, *94*(4). https://doi.org/10.1007/s12041-015-0574-1

Driessens, T., Baeckens S, Balzarolo M, Vanhooydonck B, Huyghe K, & Van Damme R. (2017). Climate-related environmental variation in a visual signalling device: The male and female dewlap in Anolis sagrei lizards—PubMed. *Journal of Evolutionary Biology*, *30*(10). https://doi.org/10.1111/jeb.13144

Dufresnes, C., & Crochet, P.-A. (2022). Sex chromosomes as supergenes of speciation: Why amphibians defy the rules? *Philosophical Transactions of the Royal Society B: Biological Sciences*, *377*(1856), 20210202. https://doi.org/10.1098/rstb.2021.0202

Ellegren, H., Hultin-Rosenberg, L., Brunström, B., Dencker, L., Kultima, K., & Scholz, B. (2007). Faced with inequality: Chicken do not have a general dosage compensation of sex-linked genes. *BMC Biology*, *5*, 40. https://doi.org/10.1186/1741-7007-5-40

Ezaz, T., Sarre, S. D., O'Meally, D., Graves, J. A. M., & Georges, A. (2009). Sex chromosome evolution in lizards: Independent origins and rapid transitions. *Cytogenetic and Genome Research*, *127*(2–4), 249–260. https://doi.org/10.1159/000300507

Feiner, N., Brun-Usan M, Andrade P, Pranter R, Park S, Menke DB, Geneva AJ, & Uller T. (2022). A single locus regulates a female-limited color pattern polymorphism in a reptile—PubMed. *Science Advances*, *8*(10). https://doi.org/10.1126/sciadv.abm2387

Ford, Jones, Polani, De Almeida, & Briggs. (1959). A sex-chromosome anomaly in a case of gonadal dysgenesis (Turner's syndrome)—PubMed. *Lancet (London, England)*, *1*(7075). https://doi.org/10.1016/s0140-6736(59)91893-8

Gamble, T., Geneva, A. J., Glor, R. E., & Zarkower, D. (2014). Anolis sex chromosomes are derived from a single ancestral pair. *Evolution*, *68*(4), 1027–1041. https://doi.org/10.1111/evo.12328

Ge C, Ye J, Weber C, Sun W, Zhang H, Zhou Y, Cai C, Qian G, & Capel B. (2018). The histone demethylase KDM6B regulates temperature-dependent sex determination in a turtle species—PubMed. *Science (New York, N.Y.)*, *360*(6389). https://doi.org/10.1126/science.aap8328

Ge C, Ye J, Zhang H, Zhang Y, Sun W, Sang Y, Capel B, & Qian G. (2017). Dmrt1 induces the male pathway in a turtle species with temperature-dependent sex determination—PubMed. *Development (Cambridge, England)*, *144*(12). https://doi.org/10.1242/dev.152033

Geneva, A. J., Park S, Bock DG, de Mello PLH, Sarigol F, Tollis M, Donihue CM, Reynolds RG, Feiner N, Rasys AM, Lauderdale JD, Minchey SG, Alcala AJ, Infante CR, Kolbe JJ, Schluter D, Menke DB, & Losos JB. (2022). Chromosome-scale genome assembly of the brown anole (Anolis sagrei), an emerging model species—PubMed. *Communications Biology*, *5*(1). https://doi.org/10.1038/s42003-022-04074-5

Giovannotti, M., Trifonov, V. A., Paoletti, A., Kichigin, I. G., O'Brien, P. C., Kasai, F., Giovagnoli, G., Ng, B. L., Ruggeri, P., Cerioni, P. N., Splendiani, A., Pereira, J. C., Olmo, E., Rens, W., Caputo Barucchi, V., & Ferguson-Smith, M. A. (2017). New insights into sex chromosome evolution in anole lizards (Reptilia, Dactyloidae). *Chromosoma*, *126*(2), 245–260. https://doi.org/10.1007/s00412-016-0585-6

Graves, J. A. (1998). Evolution of the mammalian Y chromosome and sex-determining genes. *J Exp Zool*, *281*(5), 472–481.

Graves, J. A. (2006). Sex chromosome specialization and degeneration in mammals. *Cell*, *124*(5). https://doi.org/10.1016/j.cell.2006.02.024

Graves, J. A. M. (2016). Evolution of vertebrate sex chromosomes and dosage compensation. *Nature Reviews Genetics*, *17*(1), 33–46. https://doi.org/10.1038/nrg.2015.2

Gu, L., Reilly, P. F., Lewis, J. J., Reed, R. D., Andolfatto, P., & Walters, J. R. (2019). Dichotomy of Dosage Compensation along the Neo Z Chromosome of the Monarch Butterfly. *Current Biology*, *29*(23), 4071-4077.e3. https://doi.org/10.1016/j.cub.2019.09.056

Gu, L., & Walters, J. R. (2017). Evolution of Sex Chromosome Dosage Compensation in Animals: A Beautiful Theory, Undermined by Facts and Bedeviled by Details. *Genome Biology and Evolution*, *9*(9), 2461–2476. https://doi.org/10.1093/gbe/evx154

Gubbay, Collignon, Koopman, Capel, Economou, Münsterberg, Vivian, Goodfellow, & Lovell-Badge. (1990). A gene mapping to the sex-determining region of the mouse Y chromosome is a member of a novel family of embryonically expressed genes—PubMed. *Nature*, *346*(6281). https://doi.org/10.1038/346245a0

Hall, J. M., Mitchell, T. S., Thawley, C. J., Stroud, J. T., & Warner, D. A. (2020). Adaptive seasonal shift towards investment in fewer, larger offspring: Evidence from field and laboratory studies. *The Journal of Animal Ecology*, *89*(5), 1242–1253. https://doi.org/10.1111/1365-2656.13182

Hall, J. M., & Warner, D. A. (2021). Thermal sensitivity of lizard embryos indicates a mismatch between oxygen supply and demand at near-lethal temperatures. *Journal of Experimental Zoology. Part A, Ecological and Integrative Physiology*, *335*(1), 72–85. https://doi.org/10.1002/jez.2359

Harrison, P. W., Mank, J. E., & Wedell, N. (2012). Incomplete sex chromosome dosage compensation in the Indian meal moth, Plodia interpunctella, based on de novo transcriptome assembly. *Genome Biology and Evolution*, *4*(11), 1118–1126. https://doi.org/10.1093/gbe/evs086

Hermyt, M., Janiszewska K, & Rupik W. (2020). Squamate egg tooth development revisited using three-dimensional reconstructions of brown anole (Anolis sagrei, Squamata, Dactyloidae) dentition—PubMed. *Journal of Anatomy*, *236*(6). https://doi.org/10.1111/joa.13166

Herpin, A., & Schartl, M. (2015). Plasticity of gene-regulatory networks controlling sex determination: Of masters, slaves, usual suspects, newcomers, and usurpators—PubMed. *EMBO Reports*, *16*(10). https://doi.org/10.15252/embr.201540667

Hilfiker, A., Hilfiker-Kleiner, D., Pannuti, A., & Lucchesi, J. C. (1997). Mof, a putative acetyl transferase gene related to the Tip60 and MOZ human genes and to the SAS genes of yeast, is required for dosage compensation in Drosophila. *The EMBO Journal*, *16*(8), 2054–2060. https://doi.org/10.1093/emboj/16.8.2054

Hirst, Major AT, Ayers KL, Brown RJ, Mariette M, Sackton TB, & Smith CA. (2017). Sex Reversal and Comparative Data Undermine the W

Chromosome and Support Z-linked DMRT1 as the Regulator of Gonadal Sex Differentiation in Birds—PubMed. *Endocrinology*, *158*(9). https://doi.org/10.1210/en.2017-00316

Hirst, Major AT, & Smith CA. (2018). Sex determination and gonadal sex differentiation in the chicken model—PubMed. *The International Journal of Developmental Biology*, *62*(1-2–3). https://doi.org/10.1387/ijdb.170319cs

Huie, J. M., Prates, I., Bell, R. C., & de Queiroz, K. (2021). Convergent patterns of adaptive radiation between island and mainland Anolis lizards. *Biological Journal of the Linnean Society*, *134*(1). https://doi.org/10.1093/biolinnean/blab072

Ingram, T., Harrison, A., Mahler, D. L., Castañeda, M. D. R., Glor, R. E., Herrel, A., Stuart, Y. E., & Losos, J. B. (2016). Comparative tests of the role of dewlap size in Anolis lizard speciation. *Proceedings. Biological Sciences*, *283*(1845), 20162199. https://doi.org/10.1098/rspb.2016.2199

Ioannidis, J., Taylor, G., Zhao, D., Liu, L., Idoko-Akoh, A., Gong, D., Lovell-Badge, R., Guioli, S., McGrew, M., & Clinton, M. (2020). Primary sex determination in chickens depends on DMRT1 dosage, but gonadal sex does not determine secondary sexual characteristics in adult birds. *bioRxiv*, 2020.09.18.303040. https://doi.org/10.1101/2020.09.18.303040

Jeffries, D. L., Lavanchy, G., Sermier, R., Sredl, M. J., Miura, I., Borzée, A., Barrow, L. N., Canestrelli, D., Crochet, P.-A., Dufresnes, C., Fu, J., Ma, W.-J., Garcia, C. M., Ghali, K., Nicieza, A. G., O'Donnell, R. P., Rodrigues, N., Romano, A., Martínez-Solano, Í., … Perrin, N. (2018). A rapid rate of

sex-chromosome turnover and non-random transitions in true frogs. *Nature Communications*, *9*(1), 4088. https://doi.org/10.1038/s41467-018-06517-2

Julien, P., Brawand, D., Soumillon, M., Necsulea, A., Liechti, A., Schütz, F., Daish, T., Grützner, F., & Kaessmann, H. (2012). Mechanisms and evolutionary patterns of mammalian and avian dosage compensation. *PLoS Biology*, *10*(5), e1001328. https://doi.org/10.1371/journal.pbio.1001328

Kabelik, D., Alix, V. C., Singh, L. J., Johnson, A. L., Choudhury, S. C., Elbaum, C. C., & Scott, M. R. (2014). Neural activity in catecholaminergic populations following sexual and aggressive interactions in the brown anole, Anolis sagrei. *Brain Research*, *1553*, 41–58. https://doi.org/10.1016/j.brainres.2014.01.026

Kamiya, Kai W, Tasumi S, Oka A, Matsunaga T, Mizuno N, Fujita M, Suetake H, Suzuki S, Hosoya S, Tohari S, Brenner S, Miyadai T, Venkatesh B, Suzuki Y, & Kikuchi K. (2012). A trans-species missense SNP in Amhr2 is associated with sex determination in the tiger pufferfish, Takifugu rubripes (fugu)—PubMed. *PLoS Genetics*, *8*(7). https://doi.org/10.1371/journal.pgen.1002798

Keating, S. E., Blumer, M., Grismer, L. L., Lin, A., Nielsen, S. V., Thura, M. K., Wood, P. L., Quah, E. S. H., & Gamble, T. (2021). Sex Chromosome Turnover in Bent-Toed Geckos (Cyrtodactylus). *Genes (Basel)*, *12*(1). https://doi.org/10.3390/genes12010116

Kichigin, I. G., Giovannotti, M., Makunin, A. I., Ng, B. L., Kabilov, M. R., Tupikin, A. E., Barucchi, V. C., Splendiani, A., Ruggeri, P., Rens, W., O'Brien, P. C., Ferguson-Smith, M. A., Graphodatsky, A. S., & Trifonov, V. A. (2016). Evolutionary dynamics of Anolis sex chromosomes revealed by sequencing of flow sorting-derived microchromosome-specific DNA. *Mol Genet Genomics*, *291*(5), 1955–1966. https://doi.org/10.1007/s00438-016-1230-z

Kircher, B. K., Liu B, Bramble MD, Moses MM, & Behringer RR. (2025). Gene expression profile analysis of subregions of the adult female reproductive tract in the brown anole, Anolis sagrei—PubMed. *Reproduction (Cambridge, England)*, *169*(2). https://doi.org/10.1530/REP-24-0062

Kircher, B. K., Stanley EL, & Behringer RR. (2024). Anatomy of the female reproductive tract organs of the brown anole (Anolis sagrei)—PubMed. *Anatomical Record (Hoboken, N.J. : 2007)*, *307*(2). https://doi.org/10.1002/ar.25293

Koopman, Gubbay, Vivian, Goodfellow, & Lovell-Badge. (1991). Male development of chromosomally female mice transgenic for Sry. *Nature*, *351*(6322). https://doi.org/10.1038/351117a0

Koopman, Münsterberg, Capel, Vivian, & Lovell-Badge. (1990). Expression of a candidate sex-determining gene during mouse testis differentiation—PubMed. *Nature*, *348*(6300). https://doi.org/10.1038/348450a0

Koopman, P. (2005). Sex determination: A tale of two Sox genes. *Trends Genet*, *21*(7), 367–370. https://doi.org/10.1016/j.tig.2005.05.006

Koopman, Sinclair, & Lovell-Badge. (2016). Of sex and determination: Marking 25 years of Randy, the sex-reversed mouse—PubMed. *Development (Cambridge, England)*, *143*(10). https://doi.org/10.1242/dev.137372

Lahn, & Page. (1999). Four evolutionary strata on the human X chromosome—PubMed. *Science (New York, N.Y.)*, *286*(5441). https://doi.org/10.1126/science.286.5441.964

Lambeth, L. S. (2014). Over-expression of DMRT1 induces the male pathway in embryonic chicken gonads. *Developmental Biology*, *389*(2). https://doi.org/10.1016/j.ydbio.2014.02.012

Lapiedra, O., Chejanovski, Z., & Kolbe, J. J. (2017). Urbanization and biological invasion shape animal personalities. *Global Change Biology*, *23*(2), 592–603. https://doi.org/10.1111/gcb.13395

Lapiedra, O., Morales, N., Yang, L. H., Fernández-Bellon, D., Michaelides, S. N., Giery, S. T., Piovia-Scott, J., Schoener, T. W., Kolbe, J. J., & Losos, J. B. (2024). Predator-driven behavioural shifts in a common lizard shape resource-flow from marine to terrestrial ecosystems. *Ecology Letters*, *27*(1), e14335. https://doi.org/10.1111/ele.14335

Lapiedra, O., Schoener, T. W., Leal, M., Losos, J. B., & Kolbe, J. J. (2018). Predator-driven natural selection on risk-taking behavior in anole lizards. *Science (New York, N.Y.)*, *360*(6392), 1017–1020. https://doi.org/10.1126/science.aap9289

Lisachov, A. P., Makunin, A. I., Giovannotti, M., Pereira, J. C., Druzhkova, A. S., Caputo Barucchi, V., Ferguson-Smith, M. A., & Trifonov, V. A. (2019).

Genetic Content of the Neo-Sex Chromosomes in Ctenonotus and Norops (Squamata, Dactyloidae) and Degeneration of the Y Chromosome as Revealed by High-Throughput Sequencing of Individual Chromosomes. *Cytogenet Genome Res*, *157*(1–2), 115–122. https://doi.org/10.1159/000497091

Lisachov, A. P., Trifonov VA, Giovannotti M, Ferguson-Smith MA, & Borodin PM. (2017). Heteromorphism of “Homomorphic” Sex Chromosomes in Two Anole Species (Squamata, Dactyloidae) Revealed by Synaptonemal Complex Analysis—PubMed. *Cytogenetic and Genome Research*, *151*(2). https://doi.org/10.1159/000460829

Lister, N. C., Milton, A. M., Patel, H. R., Waters, S. A., Hanrahan, B. J., McIntyre, K. L., Livernois, A. M., Horspool, W. B., Wee, L. K., Ringel, A. R., Mundlos, S., Robson, M. I., Shearwin-Whyatt, L., Grützner, F., Graves, J. A. M., Ruiz-Herrera, A., & Waters, P. D. (2024). Incomplete transcriptional dosage compensation of chicken and platypus sex chromosomes is balanced by post-transcriptional compensation. *Proceedings of the National Academy of Sciences*, *121*(32), e2322360121. https://doi.org/10.1073/pnas.2322360121

Logan, M. L., Curlis JD, Gilbert AL, Miles DB, Chung AK, McGlothlin JW, & Cox RM. (2018). Thermal physiology and thermoregulatory behaviour exhibit low heritability despite genetic divergence between lizard populations—PubMed. *Proceedings. Biological Sciences*, *285*(1878). https://doi.org/10.1098/rspb.2018.0697

Losos, J. B., & Pringle, R. M. (2011). Competition, predation and natural selection in island lizards. *Nature*, *475*(7355), E1-2; discussion E3. https://doi.org/10.1038/nature10140

Losos, J. B., & Schneider, C. J. (2009). Anolis lizards. *Current Biology: CB*, *19*(8), R316-318. https://doi.org/10.1016/j.cub.2009.02.017

Major, A. T. (2016). Sex Reversal in Birds—PubMed. *Sexual Development : Genetics, Molecular Biology, Evolution, Endocrinology, Embryology, and Pathology of Sex Determination and Differentiation*, *10*(5–6). https://doi.org/10.1159/000448365

Mank, J. E. (2013). Sex chromosome dosage compensation: Definitely not for everyone. *Trends in Genetics: TIG*, *29*(12), 677–683. https://doi.org/10.1016/j.tig.2013.07.005

Marin, R., Cortez, D., Lamanna, F., Pradeepa, M. M., Leushkin, E., Julien, P., Liechti, A., Halbert, J., Brüning, T., Mössinger, K., Trefzer, T., Conrad, C., Kerver, H. N., Wade, J., Tschopp, P., & Kaessmann, H. (2017). Convergent origination of a Drosophila-like dosage compensation mechanism in a reptile lineage. *Genome Res*, *27*(12), 1974–1987. https://doi.org/10.1101/gr.223727.117

Marshall Graves, J. A., & Peichel, C. L. (2010). Are homologies in vertebrate sex determination due to shared ancestry or to limited options? *Genome Biology*, *11*(4), 205. https://doi.org/10.1186/gb-2010-11-4-205

McQueen, H. A., & Clinton, M. (2009). Avian sex chromosomes: Dosage compensation matters. *Chromosome Research: An International Journal*

on the Molecular, Supramolecular and Evolutionary Aspects of Chromosome Biology, *17*(5), 687–697. https://doi.org/10.1007/s10577-009-9056-8

Meyer, B. J. (2022). The X chromosome in C. elegans sex determination and dosage compensation—PubMed. *Current Opinion in Genetics & Development*, *74*. https://doi.org/10.1016/j.gde.2022.101912

Mork, L., Czerwinski, M., & Capel, B. (2014). Predetermination of sexual fate in a turtle with temperature-dependent sex determination. *Dev Biol*, *386*(1), 264–271. https://doi.org/10.1016/j.ydbio.2013.11.026

Muller, H. J. (1914). A gene for the fourth chromosome of Drosophila. *Journal of Experimental Zoology*, *17*(3). https://doi.org/10.1002/jez.1400170303

Navarro-Cobos, M. B. (2025). Human XIST: Origin and Divergence of a cis-Acting Silencing RNA - PubMed. *Non-Coding RNA*, *11*(3). https://doi.org/10.3390/ncrna11030035

Nicholson, K. E., Crother, B. I., Guyer, C., & Savage, J. M. (2012). It is time for a new classification of anoles (Squamata: Dactyloidae). *Zootaxa*, *3477*(1). https://doi.org/10.11646/zootaxa.3477.1.1

Ohno, S. (1967). *Sex Chromosomes and Sex-Linked Genes*.

Ord, T. J., Stamps, J. A., & Losos, J. B. (2013). Convergent evolution in the territorial communication of a classic adaptive radiation: Caribbean *Anolis* lizards. *Animal Behaviour*, *85*(6), 1415–1426. https://doi.org/10.1016/j.anbehav.2013.03.037

Otto. (2009). The evolutionary enigma of sex. *The American Naturalist*, *174 Suppl 1*(S1). https://doi.org/10.1086/599084

Page, Mosher, Simpson, Fisher, Mardon, Pollack, McGillivray, de la Chapelle, & Brown. (1987). The sex-determining region of the human Y chromosome encodes a finger protein. *Cell*, *51*(6). https://doi.org/10.1016/0092-8674(87)90595-2

Palmer, D. H., Rogers, T. F., Dean, R., & Wright, A. E. (2019). How to identify sex chromosomes and their turnover. *Molecular Ecology*, *28*(21), 4709–4724. https://doi.org/10.1111/mec.15245

Palmer, Sinclair, Berta, Ellis, Goodfellow, Abbas, & Fellous. (1989). Genetic evidence that ZFY is not the testis-determining factor—PubMed. *Nature*, *342*(6252). https://doi.org/10.1038/342937a0

Peichel, C. L., McCann, S. R., Ross, J. A., Naftaly, A. F. S., Urton, J. R., Cech, J. N., Grimwood, J., Schmutz, J., Myers, R. M., Kingsley, D. M., White, M. A., Peichel, C. L., McCann, S. R., Ross, J. A., Naftaly, A. F. S., Urton, J. R., Cech, J. N., Grimwood, J., Schmutz, J., … White, M. A. (2020). Assembly of the threespine stickleback Y chromosome reveals convergent signatures of sex chromosome evolution. *Genome Biology 2020 21:1*, *21*(1). https://doi.org/10.1186/s13059-020-02097-x

Pinto, B. J., Keating, S. E., Nielsen, S. V., Scantlebury, D. P., Daza, J. D., & Gamble, T. (2022). Chromosome-Level Genome Assembly Reveals Dynamic Sex Chromosomes in Neotropical Leaf-Litter Geckos

(Sphaerodactylidae: Sphaerodactylus). *The Journal of Heredity*, *113*(3), 272–287. https://doi.org/10.1093/jhered/esac016

Pita-Aquino, J. N., Bock DG, Baeckens S, Losos JB, & Kolbe JJ. (2023). Stronger evidence for genetic ancestry than environmental conditions in shaping the evolution of a complex signalling trait during biological invasion—PubMed. *Molecular Ecology*, *32*(20). https://doi.org/10.1111/mec.17123

Pringle, R. M., Kartzinel, T. R., Palmer, T. M., Thurman, T. J., Fox-Dobbs, K., Xu, C. C. Y., Hutchinson, M. C., Coverdale, T. C., Daskin, J. H., Evangelista, D. A., Gotanda, K. M., A. Man in 't Veld, N., Wegener, J. E., Kolbe, J. J., Schoener, T. W., Spiller, D. A., Losos, J. B., & Barrett, R. D. H. (2019). Predator-induced collapse of niche structure and species coexistence. *Nature*, *570*(7759), 58–64. https://doi.org/10.1038/s41586-019-1264-6

Pritchard, Goodfellow, & Goodfellow. (1987). Mapping the limits of the human pseudoautosomal region and a candidate sequence for the male-determining gene—PubMed. *Nature*, *328*(6127). https://doi.org/10.1038/328273a0

Rabosky, D. L., & Glor, R. E. (2010). Equilibrium speciation dynamics in a model adaptive radiation of island lizards. *Proceedings of the National Academy of Sciences of the United States of America*, *107*(51), 22178–22183. https://doi.org/10.1073/pnas.1007606107

Rasys, A. M., Park, S., Ball, R. E., Alcala, A. J., Lauderdale, J. D., & Menke, D. B. (2019). CRISPR-Cas9 Gene Editing in Lizards through Microinjection of

Unfertilized Oocytes. *Cell Reports*, *28*(9), 2288-2292.e3. https://doi.org/10.1016/j.celrep.2019.07.089

Rasys, A. M., Pau SH, Irwin KE, Luo S, Kim HQ, Wahle MA, Trainor PA, Menke DB, & Lauderdale JD. (2021). Ocular elongation and retraction in foveated reptiles—PubMed. *Developmental Dynamics : An Official Publication of the American Association of Anatomists*, *250*(11). https://doi.org/10.1002/dvdy.348

Rasys, A. M., Pau SH, Irwin KE, Luo S, Menke DB, & Lauderdale JD. (2025). Histological analysis of anterior eye development in the brown anole lizard (Anolis sagrei)—PubMed. *Journal of Anatomy*, *247*(1). https://doi.org/10.1111/joa.14226

Raymond, C. S. (1999). Expression of Dmrt1 in the genital ridge of mouse and chicken embryos suggests a role in vertebrate sexual development—PubMed. *Developmental Biology*, *215*(2). https://doi.org/10.1006/dbio.1999.9461

Reynolds, R. G., Kolbe, J. J., Glor, R. E., López-Darias, M., Gómez Pourroy, C. V., Harrison, A. S., de Queiroz, K., Revell, L. J., & Losos, J. B. (2020). Phylogeographic and phenotypic outcomes of brown anole colonization across the Caribbean provide insight into the beginning stages of an adaptive radiation. *Journal of Evolutionary Biology*, *33*(4), 468–494. https://doi.org/10.1111/jeb.13581

Reynolds, R., Strickland, T., Kolbe, J., Falk, B., Perry, G., Revell, L., & Losos, J. (2017). Archipelagic genetics in a widespread Caribbean anole. *Journal of Biogeography*, *44*(11), 2631–2647. https://doi.org/10.1111/jbi.13072

Rovatsos, M., Altmanová, M., Pokorná, M., & Kratochvíl, L. (2014). Conserved sex chromosomes across adaptively radiated Anolis lizards. *Evolution*, *68*(7), 2079–2085. https://doi.org/10.1111/evo.12357

Rovatsos, M., Pokorná, M., Altmanová, M., & Kratochvíl, L. (2014). Cretaceous park of sex determination: Sex chromosomes are conserved across iguanas. *Biol Lett*, *10*(3), 20131093. https://doi.org/10.1098/rsbl.2013.1093

Rupp, S. M., Webster, T. H., Olney, K. C., Hutchins, E. D., Kusumi, K., & Wilson Sayres, M. A. (2017). Evolution of Dosage Compensation in Anolis carolinensis, a Reptile with XX/XY Chromosomal Sex Determination. *Genome Biol Evol*, *9*(1), 231–240. https://doi.org/10.1093/gbe/evw263

San Roman, A. K., Godfrey, A. K., Skaletsky, H., Bellott, D. W., Groff, A. F., Harris, H. L., Blanton, L. V., Hughes, J. F., Brown, L., Phou, S., Buscetta, A., Kruszka, P., Banks, N., Dutra, A., Pak, E., Lasutschinkow, P. C., Keen, C., Davis, S. M., Tartaglia, N. R., … Page, D. C. (2023). The human inactive X chromosome modulates expression of the active X chromosome. *Cell Genomics*, *3*(2), 100259. https://doi.org/10.1016/j.xgen.2023.100259

Sánchez-Baizán, N., Jarne-Sanz, I., Roco, Á. S., Schartl, M., & Piferrer, F. (2024). Extraordinary variability in gene activation and repression programs during gonadal sex differentiation across vertebrates. *Frontiers*

in Cell and Developmental Biology, *12*. https://doi.org/10.3389/fcell.2024.1328365

Sanger, T. J., Losos, J. B., & Gibson-Brown, J. J. (2008). A developmental staging series for the lizard genus Anolis: A new system for the integration of evolution, development, and ecology. *Journal of Morphology*, *269*(2), 129–137. https://doi.org/10.1002/jmor.10563

Saunders, P. A., & Veyrunes, F. (2021). Unusual Mammalian Sex Determination Systems: A Cabinet of Curiosities. *Genes*, *12*(11), 1770. https://doi.org/10.3390/genes12111770

Schmahl, J., Yao, H. H., Pierucci-Alves, F., & Capel, B. (2003). Colocalization of WT1 and cell proliferation reveals conserved mechanisms in temperature-dependent sex determination. *Genesis*, *35*(4), 193–201. https://doi.org/10.1002/gene.10176

Schneider, C. J. (2008). Exploiting genomic resources in studies of speciation and adaptive radiation of lizards in the genus Anolis. *Integrative and Comparative Biology*, *48*(4). https://doi.org/10.1093/icb/icn082

Schoener, T. W., & Schoener, A. (1980). Densities, Sex Ratios, and Population Structure in Four Species of Bahamian Anolis Lizards. *Journal of Animal Ecology*, *49*(1), 19–53. https://doi.org/10.2307/4276

Shearwin-Whyatt, L., Fenelon, J., Yu, H., Major, A., Qu, Z., Zhou, Y., Shearwin, K., Galbraith, J., Stuart, A., Adelson, D., Zhang, G., Pyne, M., Johnston, S., Smith, C., Renfree, M., Grützner, F., Shearwin-Whyatt, L., Fenelon, J., Yu, H., … Grützner, F. (2025). AMHY and sex determination in egg-laying

mammals. *Genome Biology 2025 26:1*, *26*(1). https://doi.org/10.1186/s13059-025-03546-1

Shevelyov, Y. U. (2022). Dosage Compensation in Drosophila: Its Canonical and Non-Canonical Mechanisms—PubMed. *International Journal of Molecular Sciences*, *23*(18). https://doi.org/10.3390/ijms231810976

Sinclair. (2001). Eleven years of sexual discovery—PubMed. *Genome Biology*, *2*(7). https://doi.org/10.1186/gb-2001-2-7-reports4017

Sinclair, A. H., Berta, P., Palmer, M. S., Hawkins, J. R., Griffiths, B. L., Smith, M. J., Foster, J. W., Frischauf, A. M., Lovell-Badge, R., & Goodfellow, P. N. (1990). A gene from the human sex-determining region encodes a protein with homology to a conserved DNA-binding motif. *Nature*, *346*(6281), 240–244. https://doi.org/10.1038/346240a0

Smith, C. A., Roeszler, K. N., Ohnesorg, T., Cummins, D. M., Farlie, P. G., Doran, T. J., & Sinclair, A. H. (2009a). The avian Z-linked gene DMRT1 is required for male sex determination in the chicken. *Nature*, *461*(7261), 267–271. https://doi.org/10.1038/nature08298

Smith, C. A., Roeszler, K. N., Ohnesorg, T., Cummins, D. M., Farlie, P. G., Doran, T. J., & Sinclair, A. H. (2009b). The avian Z-linked gene DMRT1 is required for male sex determination in the chicken—PubMed. *Nature*, *461*(7261). https://doi.org/10.1038/nature08298

Stevens, N. (1905). Studies in Spermatogenesis with Especial Reference to the Accessory Chromosome. *Carnegie Institution of Washington*.

Sun, D., Maney, D. L., Layman, T. S., Chatterjee, P., & Yi, S. V. (2019). Regional epigenetic differentiation of the Z Chromosome between sexes in a female heterogametic system. *Genome Research*, *29*(10), 1673–1684. https://doi.org/10.1101/gr.248641.119

Suzuki, M. G., Shimada, T., & Kobayashi, M. (1998). Absence of dosage compensation at the transcription level of a sex-linked gene in a female heterogametic insect, Bombyx mori. *Heredity*, *81*(3), 275–283. https://doi.org/10.1046/j.1365-2540.1998.00356.x

Tenorio M, Cruz-Ruiz S, Encarnación-Guevara S, Hernández M, Corona-Gomez JA, Sheccid-Santiago F, Serwatowska J, López-Perdomo S, Flores-Aguirre CD, Arenas-Moreno DM, Ossiboff RJ, Méndez-de-la-Cruz F, Fernandez-Valverde SL, Zurita M, Oktaba K, & Cortez D. (2024). MAYEX is an old long noncoding RNA recruited for X chromosome dosage compensation in a reptile—PubMed. *Science (New York, N.Y.)*, *385*(6715). https://doi.org/10.1126/science.adp1932

Thomas Lenormand, & Denis Roze. (2025). A single theory for the evolution of sex chromosomes and the two rules of speciation. *Science*, *389*(6756). https://doi.org/10.1126/science.ado9032

Tollis, M., Ausubel, G., Ghimire, D., & Boissinot, S. (2012). Multi-locus phylogeographic and population genetic analysis of Anolis carolinensis: Historical demography of a genomic model species. *PloS One*, *7*(6), e38474. https://doi.org/10.1371/journal.pone.0038474

Tollis, M., & Boissinot, S. (2013). Lizards and LINEs: Selection and Demography Affect the Fate of L1 Retrotransposons in the Genome of the Green Anole (Anolis carolinensis). *Genome Biology and Evolution*, *5*(9), 1754–1768. https://doi.org/10.1093/gbe/evt133

Uetz, P., Freed, P, Aguilar, R., Reyes, F., Kudera, J. & Hošek, J. (eds.) (2025) The Reptile Database, http://www.reptile-database.org, accessed August 2025.

Veyrunes, F., Waters, P. D., Miethke, P., Rens, W., McMillan, D., Alsop, A. E., Grützner, F., Deakin, J. E., Whittington, C. M., Schatzkamer, K., Kremitzki, C. L., Graves, T., Ferguson-Smith, M. A., Warren, W., & Marshall Graves, J. A. (2008). Bird-like sex chromosomes of platypus imply recent origin of mammal sex chromosomes—PubMed. *Genome Research*, *18*(6). https://doi.org/10.1101/gr.7101908

Vicoso, B., & Bachtrog, D. (2015). Numerous transitions of sex chromosomes in Diptera. *PLoS Biology*, *13*(4), e1002078. https://doi.org/10.1371/journal.pbio.1002078

Wallis, M. C., Waters PD, & Graves JA. (2008). Sex determination in mammals—Before and after the evolution of SRY - PubMed. *Cellular and Molecular Life Sciences : CMLS*, *65*(20). https://doi.org/10.1007/s00018-008-8109-z

Weber C, Zhou Y, Lee JG, Looger LL, Qian G, Ge C, & Capel B. (2020). Temperature-dependent sex determination is mediated by pSTAT3 repression of Kdm6b—PubMed. *Science (New York, N.Y.)*, *368*(6488). https://doi.org/10.1126/science.aaz4165

Weberling, A., Shylo, N. A., Kircher, B. K., Wilson, H., McClain, M., Marchini, M., Starr, K. B., Sanger, T. J., Hollfelder, F., & Trainor, P. A. (2025). Pre-oviposition development of the brown anole (Anolis sagrei). *Developmental Dynamics: An Official Publication of the American Association of Anatomists*. https://doi.org/10.1002/dvdy.70027

Weronika, R., Kowalska M, & Kaczmarek P. (2025). Comparative embryology of the squamate pancreas: Structural and 3D studies on the sand lizard (Lacerta agilis) and brown anole (Anolis sagrei)—PubMed. *Journal of Anatomy*. https://doi.org/10.1111/joa.14284

Wright, A. E., Zimmer, F., Harrison, P. W., & Mank, J. E. (2015). Conservation of Regional Variation in Sex-Specific Sex Chromosome Regulation. *Genetics*, *201*(2), 587–598. https://doi.org/10.1534/genetics.115.179234

Yao, H. H., & Capel, B. (2005). Temperature, genes, and sex: A comparative view of sex determination in Trachemys scripta and Mus musculus. *J Biochem*, *138*(1), 5–12. https://doi.org/10.1093/jb/mvi097

Yoshimoto, S., Ikeda N, Izutsu Y, Shiba T, Takamatsu N, & Ito M. (2010). Opposite roles of DMRT1 and its W-linked paralogue, DM-W, in sexual dimorphism of Xenopus laevis: Implications of a ZZ/ZW-type sex-determining system—PubMed. *Development (Cambridge, England)*, *137*(15). https://doi.org/10.1242/dev.048751

Yoshimoto, S., Okada E, Umemoto H, Tamura K, Uno Y, Nishida-Umehara C, Matsuda Y, Takamatsu N, Shiba T, & Ito M. (2008). A W-linked DM-domain gene, DM-W, participates in primary ovary development in Xenopus

laevis—PubMed. *Proceedings of the National Academy of Sciences of the United States of America*, *105*(7). https://doi.org/10.1073/pnas.0712244105

Zhao, D., McBride, D., Nandi, S., McQueen, H. A., McGrew, M. J., Hocking, P. M., Lewis, P. D., Sang, H. M., & Clinton, M. (2010). Somatic sex identity is cell autonomous in the chicken. *Nature*, *464*(7286), 237–242. https://doi.org/10.1038/nature08852

Zhou, Q., & Bachtrog, D. (2012). Sex-Specific Adaptation Drives Early Sex Chromosome Evolution in Drosophila. *Science*, *337*(6092), 341–345. https://doi.org/10.1126/science.1225385

Zhu, Z., Younas, L., & Zhou, Q. (2025). Evolution and regulation of animal sex chromosomes. *Nat Rev Genet*, *26*(1), 59–74. https://doi.org/10.1038/s41576-024-00757-3

CHAPTER 2

REGIONAL DIFFERENCES IN DOSAGE COMPENSATION ACROSS THE NEO-X CHROMOSOME OF *ANOLIS SAGREI*[1]

---

[1]**Motley, M. K.**, [1]Park, S., and Menke, D. B. *To be submitted to a peer-reviewed journal.*

ABSTRACT

In some species, sex chromosome evolution has led to highly divergent, heteromorphic systems, where one sex chromosome—typically the Y or W—undergoes degeneration and gene loss. In XX/XY sex determination systems, XX females retain two copies of each X-linked gene, while XY males are reduced to one, creating potential gene dosage imbalances that can impact fitness. To mitigate this, many species have evolved dosage compensation mechanisms that equalize gene expression between the sexes and, in some cases, restore ancestral expression levels. In *Anolis carolinensis*, previous studies have shown that the single X chromosome in males is upregulated twofold, suggesting a chromosome-wide dosage compensation mechanism. While *A. carolinensis* retains ancestral micro-sex chromosomes, *Anolis sagrei* has undergone multiple autosome-to-sex chromosome fusion events, giving rise to gene-rich, midsized neo-sex chromosomes. To investigate dosage compensation in *A. sagrei*, we sequenced the Y chromosome from an XY male and performed RNA-seq on XX and XY whole embryos at a developmental stage just prior to gonadal sex differentiation. Here, we present the Y chromosome assembly of *A. sagrei* and report regional differences in dosage compensation across its neo-X chromosome. We find that 89% of differentially expressed genes are strongly female-biased and are not fully dosage compensated in XY males. This includes more recently acquired regions of the X chromosome as well as genes on the ancient X. Further, we find that a small subset of X genes is strongly male-

biased. These male-biased genes are found in the most ancient region of the X chromosome and no longer have Y-linked gametologs.

This is the first study to investigate dosage compensation mechanisms in *A. sagrei*, a species with an old neo-sex chromosome system. Our findings provide new insights into the evolutionary dynamics and complexity of dosage compensation in XX/XY neo-sex chromosome systems.

Introduction

In genetic sex determination systems, an organism's sexual phenotype is governed by differences between the sex chromosomes. In some vertebrates, sex chromosomes have evolved from ancestral autosomes into highly divergent, heteromorphic pairs. This divergence is thought to result from sexually antagonistic selection and the accumulation of chromosomal inversions, which suppress recombination between the sex chromosomes (Bachtrog et al., 2014; B. Charlesworth, 1991; D. Charlesworth, 2001; Muller, 1918; Ohno, 1967; Rovatsos & Kratochvíl, 2021). This divergence can lead to gene loss, chromosome degeneration, and the establishment of a male heterogametic sex chromosome system—typically XX/XY, with XX females and XY males. In such systems, heteromorphic sex chromosomes differ significantly in size and gene content, often resulting in unequal gene expression between the sexes. While XX females retain two functional copies of X-linked genes, XY males only have one. To maintain viability and ensure proper gene function, many species have evolved dosage compensation mechanisms that balance gene expression

between the sexes. These mechanisms are particularly important in systems with highly heteromorphic and genetically divergent sex chromosomes.

Dosage compensation restores equal expression of X-linked genes between the sexes through a variety of epigenetic mechanisms. In placental mammals, this is achieved by X chromosome inactivation in females (Alfeghaly & Rougeulle, 2025; Harper, 2011; Lyon, 1974), while in *Drosophila,* it occurs through global upregulation of the male X chromosome (Muller, 1932; Shevelyov et al., 2022; Toups & Vicoso, 2025). In some systems, such as marsupials and *Anolis carolinensis*, dosage compensation also restores X-linked gene expression to levels comparable with the ancestral autosomes (Marin et al., 2017; Rens et al., 2010; Whitworth & Pask, 2016). However, much of our understanding of dosage compensation is based on a few well-studied groups, including mammals, *C. elegans*, and *Drosophila*. To better understand how dosage compensation is established and to fully appreciate the diversity of mechanisms that underlie this phenomenon, we need to study a wider range of species across the tree of life.

The *Anolis* species group includes over 400 diverse lizard species and has served as a model in ecology, evolution, genetics, and development (Arbuckle et al., 2014; Kircher et al., 2025; Losos & Pringle, 2011; Rasys et al., 2025). *Anolis* lizards possess a highly divergent, heteromorphic XX/XY genetic sex determination system, estimated to be over 100 million years old. This system originated in *Pleurodonta*, which includes more than 1,200 New World lizards such as iguanas and anoles (Gamble et al., 2014). Remarkably, the XX/XY

system is homologous across nearly all pleurodont lizards, making it the most ancient and conserved sex chromosome system identified in reptiles to date (Gamble et al., 2014; Rovatsos et al., 2014). Previous studies have identified *Drosophila*-like dosage compensation in the green anole, *Anolis carolinensis*, where the single male X chromosome upregulates gene expression twofold to match that of XX females (Marin et al., 2017; Rupp et al., 2017; Tenorio M et al., 2024). While the green anole retains the hypothesized ancestral state of micro sex chromosomes, the lineage leading to the brown anole, *Anolis sagrei,* has undergone multiple autosome-to-sex chromosome fusion events, resulting in midsized neo-sex chromosomes. These fusion events have added substantial gene-rich regions into the sex chromosomes, potentially influencing dosage compensation evolution in this species. Unlike the small micro sex chromosomes, neo-sex chromosomes contain greater genetic diversity and may require more complex regulatory mechanisms to balance gene expression between sexes. Studies in other systems have shown that neo-sex chromosomes can co-opt the ancestral dosage compensation machinery to achieve equal expression (Ellison & Bachtrog, 2019).

Geneva et al. (2022) proposed a new hypothesis for the sequence of autosome-to-sex chromosome fusion events in *A. sagrei,* based on detailed synteny analyses between the *A. carolinensis* and *A. sagrei* X chromosomes. More recently, our group has established the brown anole as a model system for studying developmental processes in reproductive biology, making it an ideal

species for investigating the evolution of dosage compensation across ancient neo-sex chromosomes.

In this study, we assembled the Y chromosome of the brown anole to uncover patterns of gene loss and degeneration across the Y-specific region. This assembly allows direct comparison between the X and Y chromosomes, offering new insights into sex chromosome evolution in ancient neo-sex chromosome systems. Using a gene-by-gene analysis, we reveal the nuanced regulation of expression across the neo-X chromosome and explore how dosage compensation evolves following sex chromosome-autosome fusion events. Taken together, our findings establish the brown anole as a powerful model for investigating sex chromosome evolution, dosage compensation, and sex determination.

RESULTS

Sequencing and assembly of the XY genome

We used high-fidelity (HiFi) PacBio long-read sequencing to assemble the genome of a male *A. sagrei* lizard from an invasive population in Orlando, Florida (Fig. 2.1A). The total assembly spans 3.75 Gb, approximately twice the expected haploid genome size for *A. sagrei*. Due to the highly polymorphic nature of wild-caught lizards, our XY assembly captures an almost fully diploid representation of the genome. Coverage depth averaged 30x across autosomes and 15x across sex chromosomes. We used chromosome conformation capture (Hi-C) sequencing combined with a proximity-guided method to assemble contigs into scaffolds. Previous karyotype analyses have determined that *A. sagrei*

possesses seven pairs of macrochromosomes and seven pairs of microchromosomes (2n=28) with the smallest pair of macrochromosomes (mid-sized) corresponding to the sex chromosomes (XX for females, XY for males). This assembly yielded 28 large scaffolds, representing 3.59 Gb or 95.6% of the total genome assembly (Fig. 2.1B).

To identify the Y chromosome scaffold, we performed a BLAST analysis on the XY genome assembly using previously reported *Anolis carolinensis* Y-linked genes (Marin et al., 2017). A similar approach was used to identify the scaffold corresponding to the X chromosome. We designated these scaffolds PGA Y and PGA X, respectively. In 2022, Geneva et. al. published a highly complete and contiguous XX genome of *A. sagrei* for which a high-quality NCBI-generated gene annotation is available. For our analyses, we generated a merged assembly by combining the haploid XX reference genome (*Anosag2.1*) with the newly annotated PGA Y.

Identification of the X-specific, Y-specific, and pseudoautosomal regions

Sex chromosomes evolve from autosomes through successive stages of recombination suppression. In XX/XY systems, the non-recombining portions of the sex chromosomes are known as the X- and Y-specific regions, while the regions that retain recombination are known as pseudoautosomal regions (PARs). To identify the X-specific region and adjacent PARs, we aligned whole-genome shotgun sequencing data from XX and XY individuals to the Anosag2.1 reference X chromosome (Geneva et al., 2022). We then examined the $\log_2$(XX/XY) read coverage ratio along the X chromosome to identify distinct

regions of coverage. A $\log_2$ ratio of 0 indicates equal coverage between the sexes, whereas a ratio of 1 indicates that the XX genome has twice the coverage of XY, consistent with hemizygosity in males.

Our analyses revealed two pseudoautosomal regions (XPAR1 & XPAR2), each approximately 20Mb in length, located at both ends of the X chromosome. These regions exhibited a $\log_2$ ratio near 0, indicating sequence homology and equal coverage in both sexes. Between the PARs, we identified a centrally located, ~70Mb X-specific region with a $\log_2$ ratio close to 1, indicating a reduction in XY read coverage (Fig. 2.2). The Y-specific region of the Y-scaffold was estimated to be ~50Mb, reflecting Y chromosome degeneration and gene loss.

Pleurodont lizards, including all *Anolis* species, share an ancient and conserved homologous X chromosome region. In the green anole, *Anolis carolinensis*, the X chromosome retains the proposed ancestral state as a microchromosome. In contrast, the sex chromosomes of *A. sagrei* have undergone multiple autosome-to-sex chromosome fusion events, adding newly evolving, gene-rich regions and giving rise to mid-sized neo-sex chromosomes. In our analyses, we have labeled the *A. sagrei* neo-X chromosome to reflect its homology with the *A. carolinensis* autosomes and X chromosome (Fig. 2.3; Geneva et al., 2022; Faircloth et al., unpublished).

Structural rearrangements and gene loss on the A. sagrei Y

In the absence of recombination, heteromorphic sex chromosomes (i.e., X & Y) no longer exchange genetic material, making the Y chromosome

susceptible to the accumulation of deleterious mutations and progressive gene loss. This evolutionary process can result in a small, degenerated Y chromosome. To investigate patterns of Y chromosome gene loss in *A. sagrei*, we performed a synteny analysis of X-Y gene pairs on the PGA X and Y. This analysis revealed Y-linked chromosomal rearrangements, including multiple inversions relative to the X. In addition, we observed widespread gene loss across the entire Y-specific region, with the most extensive degeneration occurring on the ancient Y (Fig. 2.3).

We find that the *A. sagrei* X-specific region contains approximately 1,100 genes, whereas only 340 genes are retained on the Y-specific region. Within the ancestral region of the X (Old X), 324 genes are present. In comparison, the ancestral Y chromosome region contains only 5 genes: *ccdc74by, rpl6y, gnazy, ube2l3y*, and *rsph14y.* Of these, only *rsph14* has lost its X homolog (Table 2.2; Fig. 2.3; Fig. 2.4).

To further assess Y chromosome gene loss, we compared the reference X chromosome (*Anosag2.1*; Geneva et al., 2022) to the PGA Y chromosome. Using open reading frame sequences (ORFs), we performed a BLAST analysis of annotated genes on the reference X chromosome. Of the 1,824 ORFs in our analysis, only 829 had a BLAST hit, indicating substantial gene loss across the Y-specific region. We found BLAST hits were concentrated in the pseudoautosomal region, as these regions still recombine between the Y and the X. As a control, we performed a BLAST analysis to compare the reference X chromosome to the PGA X. Of the 1,824 ORFs, we had BLAST hits to 1,791, indicating highly similar

X chromosomes. The ORFs without hits were constrained to the ends of the chromosome, possibly resulting from sequencing or assembly errors in repetitive telomeric regions (Fig. 2.4).

Our analyses reveal extensive genetic differences between the *A. sagrei* X and Y chromosomes, consistent with previous work that identified the Y chromosome as highly degenerate compared to the X (Rovatsos et al., 2014). As the X and Y chromosomes have been diverging for ~100 million years, Y-linked gene loss and degeneration are expected. We find that the pseudoautosomal regions have retained nearly complete homology, and the X chromosome has retained most of its gene content compared to the Y (Fig. 2.4).

The A. sagrei X chromosome does not show evidence of distinct evolutionary strata

To investigate the evolutionary history and divergence between the sex chromosomes, synonymous divergence (dS) was calculated between X and Y gametologs. Synonymous divergence is a measure of synonymous substitutions, or DNA sequence mutations that do not result in an amino acid change. We can compare these substitutions between the X and Y gametologs to estimate the timing of recombination suppression and understand divergence between gene pairs. Synonymous divergence has been used in other studies (Peichel et al., 2020) to identify strata, or the successive steps of recombination suppression, as is commonly seen in sex chromosome evolution (Olito & Abbott, 2025). Our analyses do not identify clear evolutionary strata indicating sex chromosome

evolution in *A. sagrei* may have been more gradual than in other vertebrate systems (Fig. 2.4), such as humans (Lahn & Page, 1999).

While our analyses do not reveal distinct strata on the Y, we do observe differences in median dS across ancient X/Y gene pairs when compared to X/Y gene pairs that have been more recently acquired through fusion events with autosomes. With only a few X/Y gene pairs remaining in the most ancient region of the X (X-specific region 3), we see the highest median dS in this ancient region. In newer regions, we find divergence rates match the order in which fusion events occurred (Geneva et al., 2022), with the oldest fusion region (X-specific region 2) displaying higher synonymous divergence than the more recent fusions (X-specific regions 1 and 4) (Fig. 2.4).

Regional differences in dosage compensation across the A. sagrei X chromosome

In highly heteromorphic XX/XY sex determination systems, XX females retain two copies of each X-linked gene, while XY males retain only one. This can cause potential gene dosage imbalances that can impact fitness or survival as Y gametologs are lost. As a result, dosage compensation mechanisms have evolved to equalize gene expression between the sexes. Previous studies have shown that in *A. carolinensis,* the male X chromosome is upregulated twofold, suggesting chromosome-wide dosage compensation (Marin et al., 2017; Rupp et al., 2017; Tenorio et al., 2024).

The *A. sagrei* X and Y sex chromosomes have undergone multiple autosome-to-sex chromosome fusion events, giving rise to a neo-sex

chromosome system. Previous studies have shown that neo-sex chromosome systems can co-opt ancestral dosage compensation machinery to evolve dosage compensation mechanisms (Ellison & Bachtrog, 2019). To explore dosage compensation patterns across the neo-X chromosome of *A. sagrei,* we performed RNA-seq on XX and XY stage 4 whole embryos (Sanger et al., 2008), an embryonic stage prior to sex determination initiation.

To understand regional differences of dosage compensation in *A. sagrei,* the $\log_2$ Fold Change ($\log_2$FC) of differentially expressed genes was plotted along the neo-X chromosome. If a gene has equal expression in XX and XY individuals, the $\log_2$FC will be close to 0, indicating complete dosage compensation between the sexes. In contrast, a $\log_2$FC close to -1 demonstrates two-fold lower expression in XY individuals relative to XX. This indicates a complete lack of dosage compensation. Consistent with findings in *A. carolinensis* (Marin et al., 2017; Rupp et al., 2017; Tenorio et al., 2024), our data suggest that dosage compensation in *A. sagrei* is also achieved through upregulation of the male X chromosome. However, we identified regional differences in dosage compensation across the neo-X, highlighting the complexity and nuance of this process.

Our stage 4 XX vs. XY differential expression analysis identified 332 differentially expressed genes (DEGs) (padj < 0.05; PAR genes excluded), of which 310 (93%) were located on the X-chromosome. Among these, 278 (89%), X-linked genes exhibited strong female-biased expression, indicating incomplete dosage compensation and higher expression in XX individuals. Interestingly, a

small subset of 32 (10%) X-linked genes was upregulated in XY individuals, suggesting that these genes are overcompensated in males (Fig. 2.5A).

To assess regional differences in dosage compensation, we calculated the proportion of DEGs within each X-specific region (XSR1-XSR4), where XSR1, XSR2, and XSR4 comprise the “new X”, and XSR3 represents the ancestral “old X”. Among the 278 female-biased genes, 93 (34%) were located on XSR1, 31 (11%) on XSR2, and 100 (36%) on XSR4, meaning 81% of XX-biased DEGS were found on the new X. In contrast, only 54 XX-biased DEGS (19%) were located on the old X (XSR3) (Table 2.4). Our XX-biased expression data suggest that dosage compensation in *A. sagrei* is more complete in the oldest X-specific regions (XSR3 and XSR2) compared to the youngest regions (XSR1 and XSR4). This pattern is consistent with the expectation that older genes have had more time to diverge and evolve dosage compensation mechanisms.

Similarly, we assessed regional patterns in our XY-biased DEGs. For the 32 male-biased genes, 1 (3%) was located on XSR1, 12 (38%) on XSR2, and 1 (3%) on XSR4, totaling 44% on the new X. Notably, 18 XY-biased DEGS (56%) were located on the old X, XSR3, indicating that male-biased overcompensation is more prevalent in the most ancestral region (Fig. 2.5A)

Next, we identified X-linked DEGs in our dataset that have retained Y-linked gametologs. If an X/Y gene pair is still present, there is less selection pressure to evolve dosage compensation, as expression from the Y gametolog supplements gene dosage in XY individuals. We found that X-linked DEGs with Y gametologs were concentrated in the youngest X-specific regions (XSR1 and

XSR4), near the PAR boundaries. Incomplete dosage compensation in these regions is most likely due to retained Y gametolog expression in males. In contrast, we identified a few XX-biased DEGs with Y gametologs on the ancient X (XSR3), suggesting that the upregulation of these genes in XX individuals may be important for fitness or female-specific biological processes. Additionally, none of the XY-biased X-linked DEGs retained a Y gametolog, suggesting that these genes may be dosage sensitive in XY individuals and have evolved to have higher expression in males (Fig. 2.5B).

To broadly investigate patterns of dosage compensation in *A. sagrei*, we calculated the $\log_2$ (XX/XY) gene expression ratio for all X-linked genes. Our analyses revealed that X-linked genes with Y gametologs exhibit significantly lower XX/XY expression ratios than those without gametologs, suggesting that these genes are less dosage compensated (Fig. 2.6A).

We further examined XX/XY expression ratios across different regions of the X chromosome: the newly evolved X-linked regions X (XSR1, XSR2, and XSR4), the ancestral X (XSR3), and the pseudoautosomal regions (PARs). Expression ratios differ significantly between the new and old X, suggesting the old X is more dosage compensated than the new X. Additionally, both the new and old X regions exhibited XX/XY expression ratios that were significantly different from those of the PARs. These differences highlight distinct regulatory patterns between the non-recombining X-specific regions and the recombining PARs (Fig. 2.6B).

XSR gene expression in XX embryos is higher than XY and ancestral levels

To further examine regional differences in dosage compensation in *A. sagrei*, we compared gene expression (in TPM) between XX and XY individuals across autosomes, the PARs, and the X-specific region (XSR). In XX embryos, autosomal gene expression (median=37.0 TPM) did not differ significantly from PAR expression (median=37.1 TPM). However, X-linked gene expression in XX embryos was significantly higher across the entire X-specific region (median=44.6 TPM), the new X (median=44.1 TPM), and the old X (median=46.4 TPM). These values represent a ~20% increase in expression compared to autosomes and PARs, indicating that X-linked genes in females have evolved elevated expression relative to the ancestral state (Fig. 2.7A).

In contrast, XY embryos showed no significant differences across autosomes (median=36.5 TPM), PARs (median=35.1 TPM), the entire XSR (median=36.9 TPM), the new X (median=35.3 TPM), or the old X (median=38.5 TPM). This suggests that, in XY individuals, the single male X chromosome expressed X-linked genes at levels comparable to the ancestral autosomal levels (Fig. 2.7B).

Finally, we compared gene expression between XX and XY embryos. As expected, there were no significant differences in expression for autosomal (XX median=37.0 TPM, XY median=36.5 TPM) or PAR genes (XX median=37.1 TPM, XY median=35.1 TPM), reflecting recombination in these regions. However, expression across the X-specific region differed significantly. The new X showed a substantial difference (XX median=44.1 TPM, XY median=35.3 TPM), while the old X had a smaller, non-significant difference (XX median=46.4

TPM, XY median=38.5 TPM). When the new X and the old X were combined (XSR), XX expression remained significantly higher than XY expression (XX median=44.6 TPM, XY median=36.9 TPM), suggesting that incomplete dosage compensation on the new X is driving expression differences observed (Fig. 2.7C).

Y gametolog expression influences dosage compensation in A. sagrei

To further understand the role of X and Y gametolog expression in dosage compensation in *A. sagrei*, we examined $\log_{10}$TPM gene expression levels for X/Y gametolog pairs. In XY individuals, X-linked gametologs (median=33.0 TPM) consistently exhibit higher expression than their Y-linked (median=9.40 TPM) counterparts (Fig. 2.8A). This pattern is consistent with partial Y chromosome degeneration and pseudogenization, driven by Y gametologs with minimal expression.

To contextualize these values, we measured X gametolog expression in XX individuals (median=51.3 TPM). This was significantly higher than both X and Y gametolog expression in XY individuals (Xmedian=33.0 TPM; Ymedian=9.40 TPM). However, the combined expression of the X and Y gametologs in XY embryos (X+Y median=48.7 TPM) was comparable to the expression of X gametologs in XX embryos (median=51.3 TPM), suggesting the additive expression of both gametologs in males contributes to overall dosage (Fig. 2.8B).

To quantify the relative contribution of Y gametologs to overall expression in XY individuals, we calculated relative expression ratios. The Y/X expression ratio for gametolog pairs in XY embryos was low (Y/X median=0.31, mean=0.41),

confirming that Y gametologs generally have lower expression than their X counterparts (Fig. 2.9 A). However, when we combined X and Y gametolog expression in XY individuals and compared it to X gametolog expression in XX individuals (X+Y/XX X), the resulting expression ratio was close to 1 (median=0.90, mean=0.96), indicating that total transcript levels are nearly equal between sexes. This suggests that although Y gametolog expression is often weak, its contribution is sufficient to equalize male and female expression

DISCUSSION

We present the first comprehensive analysis of dosage compensation in *Anolis sagrei*, a lizard species with ancient neo-sex chromosomes resulting from multiple autosome-to-sex chromosome fusion events. Our results reveal that dosage compensation in *A. sagrei* is regionally variable across the neo-X chromosome. Notably, gene expression is more balanced between the sexes in the ancestral X-specific region than in the more recently added neo-X regions. This pattern suggests that dosage compensation gradually evolves after chromosomal fusion events, with older X-linked genes having had more evolutionary time to develop regulatory mechanisms that restore expression balance between XX and XY individuals. Similar trajectories have been observed in other neo-sex chromosome systems, including some *Drosophila* species (Bachtrog et al., 2014). However, *A. sagrei* represents a unique opportunity to study dosage compensation mechanisms in a vertebrate with ancient, yet actively evolving sex chromosomes. Our results underscore that even in ancient systems, newly sex-linked regions may remain partially uncompensated.

Using genomic approaches, we identified chromosomal rearrangements and extensive gene loss across the Y-specific region of the *A. sagrei* Y chromosome. Y chromosome degeneration was most pronounced in the ancestral region, where only five genes remain (*ube2l3y, rpl6y, gnazy, ccdc74by,* & *rsph14y*). These results support the canonical model of Y chromosome degeneration, predicting that progressive gene loss is a result of recombination suppression and deleterious mutation accumulation (B. Charlesworth & D. Charlesworth, 2000; Miura et al., 2024). Further, our results suggest more complete dosage compensation in the oldest regions of the X chromosome, where Y gametologs have been lost, compared to younger X-linked regions where Y gametologs are still retained. The presence of a Y gametolog likely reduces selective pressure for X-linked upregulation. As these newer regions continue to diverge and Y-linked genes are lost, we hypothesize that X-linked genes will be subsequently selected upon to address dosage imbalances between the sexes.

Our gene expression analyses support the two-fold upregulation of the male X, mirroring the mechanism described in *A. carolinesis* (Marin et al., 2017; Rupp et al., 2017; Tenorio M et al., 2024). However, we observe that, in A. sagrei, X-linked gene expression in XX individuals is consistently higher than ancestral autosomal levels, suggesting a pattern of female-biased overexpression. This indicates that dosage compensation in A. sagrei may involve regulatory changes in both sexes. Interestingly, we identified a subset of XY-biased, differentially expressed X-linked genes located on the ancient X that

have lost their Y gametologs and appear to be undergoing overcompensation. These genes may be dosage sensitive or play critical roles in male-specific development. Their elevated expression in XY individuals may reflect adaptive regulatory evolution to compensate for Y gene loss. The evolutionary pressure to restore ancestral gene dosage in males may contribute to broader regulatory changes, including upregulation in XX and XY individuals. Male-specific regulatory elements are one possible mechanism, including the recently identified long non-coding RNA *MAYEX* in *A. carolinensis* (Tenorio et al., 2024). We also detected *MAYEX* expression in *A. sagrei,* suggesting a conserved role in *Anolis* dosage compensation.

Taken together, our findings establish the brown anole, *A. sagrei*, as an important model for studying neo-sex chromosome evolution and dosage compensation. Neo-sex chromosome systems, with ancient and recently added X-linked regions, allow for direct evolutionary comparisons within a single genome. The variability and regional complexity of *A. sagrei* dosage compensation highlight key differences of this mechanism from other model systems. Our study provides further evidence for the diverse nature of dosage compensation mechanisms across vertebrates.

CONCLUSION

Our findings add important nuance to the current understanding of chromosome-wide dosage compensation mechanisms, particularly within *Anolis* lizards (Marin et al., 2017; Rupp et al., 2017; Tenorio et al., 2024). This study provides the first in-depth characterization of dosage compensation in *Anolis*

sagrei, revealing variable, region-specific dosage compensation across its neo-X chromosome. These results offer insights into the evolutionary dynamics of gene regulation following sex chromosome-to-autosome fusion events and contribute to a broader understanding of vertebrate sex chromosome biology. The diverse and complex dosage compensation patterns observed in *A. sagrei* highlight the importance of studying dosage compensation in more diverse vertebrate systems to fully capture the diversity of regulatory mechanisms that evolve in response to sex chromosome differentiation.

Materials and Methods

Lizards

For genome sequencing, a single adult male *Anolis sagrei* was collected from Warren Park in Orlando, FL (28.46°N, 81.33°W). For RNA-sequencing, adult lizards were obtained from both Orlando and Miami, Florida. Animals were housed at our UGA facility in Athens, GA, in harem breeding cages containing one male and 5-7 females. Eggs were collected weekly and maintained at room temperature (~26°C) until dissection. Animal care, handling, and use strictly adhered to IACUC Animal Use Protocol #A2023-11-007-A9.

Anolis sagrei Y chromosome assembly

To confirm the genotypic sex of the male used for genome sequencing, PCR-based sex genotyping was performed using *Anolis*-specific primers *kank1* and *gnaz* (Gamble et al., 2014; Gamble & Zarkower, 2014; Table 2.1). The autosomal marker *kank1* is present in both XX and XY individuals, while the Y chromosome-specific marker *gnaz* is detected only in XY individuals. Thus, XY

samples produce two bands, whereas XX samples produce a single band. PCR reactions were prepared using DreamTaq PCR Master Mix (Thermo Scientific; Waltham, MA), nuclease-free water, and the above primers. Thermocycling conditions were as follows: 95°C for 2 mins, 35 cycles of 95°C for 30 secs/ 58°C for 30 secs/ 72°C for 30 secs, and 72°C for 2 minutes.

Following humane euthanasia via Tricaine injection (Conroy et al., 2009), high molecular weight (HMW) DNA was extracted from fresh forelimb and tail muscle tissue as previously described (Mayjonade et al., 2016). All remaining tissue was flash-frozen and stored at -80°C. All animal procedures were approved by and performed under UGA IACUC Animal Use Protocol #A2023-11-007-A9.

Extracted DNA was submitted to the Georgia Genomics and Bioinformatics Core (GGBC), where a single PacBio HiFi library was constructed and sequenced on the PacBio Sequel II platform (Menlo Park, CA). Frozen limb tissue was also sent to Phase Genomics (Seattle, WA), where a single Hi-C library was constructed, sequenced on the Illumina NovaSeq platform (San Diego, CA), and used for scaffolding via the Proximo Proximity-Guided Assembly platform.

PacBio HiFi reads were assembled using HiCanu (v.1.9; Nurk et al., 2020). For Hi-C-based assembly, contigs were clustered, ordered, and oriented onto chromosomes by Phase Genomics (Seattle, WA). Gene annotation was performed using BRAKER (v.2.1.2; Hoff et al., 2019) in conjunction with the NCBI

RefSeq database. Annotations were corrected manually using the Integrative Genome Viewer (IGV; Robinson et al., 2011).

To identify the scaffold containing the Y chromosome, we performed a BLAST analysis on the XY genome assembly using known Y-linked genes (Marin et al., 2017). The X and Y chromosomes in the new assembly are hereafter referred to as the PGA X and PGA Y. To determine the boundaries of the pseudoautosomal regions, whole-genome shotgun short read sequencing data from XX (Bahamian) and XY (Asord03; Concepción; provided by A. Geneva) *A. sagrei* individuals was aligned to the reference X chromosome (*Anosag2.1*; Geneva et al., 2022) to assess read coverage and the relative abundance of X-linked regions in each sample. For all downstream analyses, we used the highly complete, haploid XX female reference genome (*Anosag2.1*; Geneva et al., 2022) with the addition of the PGA Y chromosome.

Sex chromosome evolution analyses

To investigate sex chromosome evolution, the PGA X and Y chromosomes were aligned, and XY gene pairs were identified. Chromosomal rearrangements were visualized using the R package circlize (v.0.4.16; Gu et al., 2014). To examine Y chromosome gene loss and degeneration, the reference X chromosome (*Anosag2.1*;Geneva et al., 2022) was compared to the newly assembled PGA X and Y chromosomes. BLAST (v.2.12.0; Camacho et al., 2009) analyses were conducted using open reading frame sequences (ORFs) from annotated genes on the reference X (*Anosag2.1*; Geneva et al., 2022). The PGA X and PGA Y chromosomes were separately BLASTed against the reference X to

assess Y chromosome gene loss and X chromosome similarity. To investigate the evolutionary history and divergence between the sex chromosomes, synonymous divergence (dS) was calculated. Orthologs were detected with the R package orthologr (Drost et al., 2015) using Reciprocal Best Hit (RBH).

RNA-sequencing

Stage 4 embryos of *Anolis sagrei* (Sanger et al., 2008) were collected for RNA sequencing. Eggs were dissected in 1X Phosphate-Buffered Saline (PBS) solution (137mM NaCl, 10mM Na_2PO_4, 2.7mM KCl, 2mM KH_2PO_4). A small tail clip was collected from each embryo for DNA extraction and sex genotyping using the primers described above (Table 2.1). Tail clips were placed in 500µL of DNA lysis buffer (100mM Tris, 5mM EDTA, 0.2% SDS, 200mM NaCl, pH 8.5) with 2.5µL of Proteinase K (ThermoFisher; Waltham, MA). Samples were digested at 55°C for 24 hours. Following digestion, samples were centrifuged for 10 minutes at 15,000rpm, and 500µL of isopropanol was added to precipitate DNA. Samples were then centrifuged again for 10 minutes at 15,0000rpm. The supernatant was removed, 200µL of 70% EtOH was added, and samples were centrifuged for 5 minutes at 15,000rpm. After EtOH removal, DNA pellets were air dried for 10 minutes. DNA was resuspended in 300-500µL of TE buffer (10mM Tris-HCl, 1mM EDTA, pH 8.0) and incubated for 1 hour at 55°C. DNA concentration was measured via NanoDrop (ThermoFisher; Waltham, MA). Samples were stored at -20°C until sex genotyping by PCR, which was performed as described above.

Stage 4 whole embryos were placed in 200ul of the mirVana™ miRNA isolation kit lysis buffer (Invitrogen; Waltham, MA), homogenized using a motorized pestle, and stored at -80°C until RNA extraction and library preparation. Total RNA was extracted using the mirVana™ miRNA isolation kit (Invitrogen; Waltham, MA) following the manufacturer's protocol. RNA concentration was quantified using the High Sensitivity RNA Qubit kit (Invitrogen; Waltham, MA). RNA-sequencing libraries were prepared in-house using the Illumina® Stranded mRNA Prep kit (San Diego, CA) with an input of 1000ng of total RNA per sample. Libraries were amplified using 14 cycles of PCR.

Five biological replicates per sex were made, resulting in a total of 10 libraries. Indexed libraries were pooled and sequenced on the Illumina NovaSeq X Plus platform (Illumina; San Diego, CA) at Novogene (Sacramento, CA). Sequencing was performed using a P2 flow cell, generating 150bp pair-end reads.

Dosage compensation analyses

To investigate dosage compensation in the brown anole, differentially expressed X-linked genes were plotted along the X chromosome using R. We then assessed which DEGs on the X chromosome had corresponding Y-linked gametologs using R. All boxplots and dotplots were generated using ggplot2 (v.3.5.2; Wickham, 2016). For regional gene expression analyses, only genes with a TPM value ≥10 were included. For relative expression comparisons between gametologs, only X-linked gametologs with TPM ≥ 10 were considered.

FIGURES

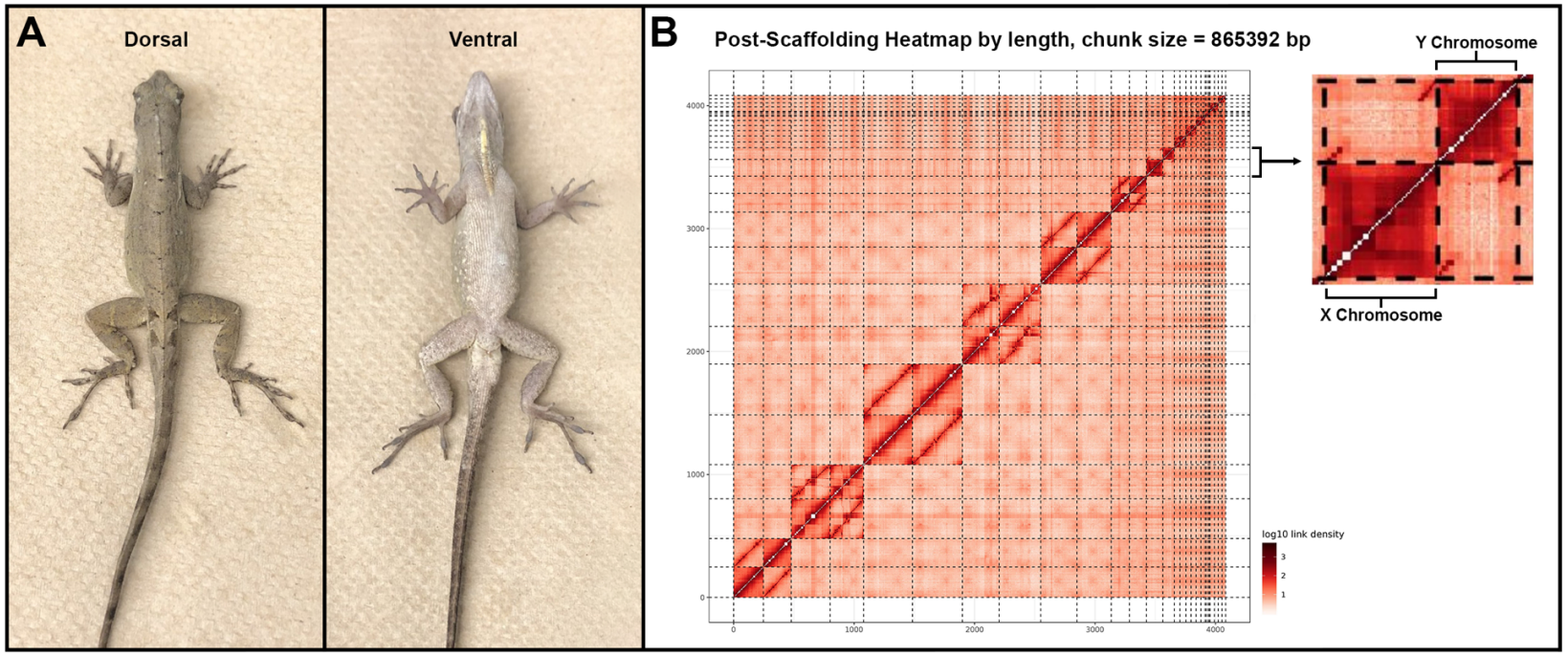

Figure 2.1. Genome assembly of an XY *A. sagrei* adult male. (A) Dorsal and ventral views of the sequenced male. (B) Hi-C chromosome conformation capture sequencing generated 28 chromosome-level scaffolds representing a diploid XY genome. The Hi-C contact matrix displays a strong enrichment of interactions along the diagonal, indicating proximity between contigs. Parallel off-diagonal lines reflect interactions between homologous chromosomes. The X and Y chromosomes were assembled as separate scaffolds, with detectable Interactions in the pseudoautosomal regions.

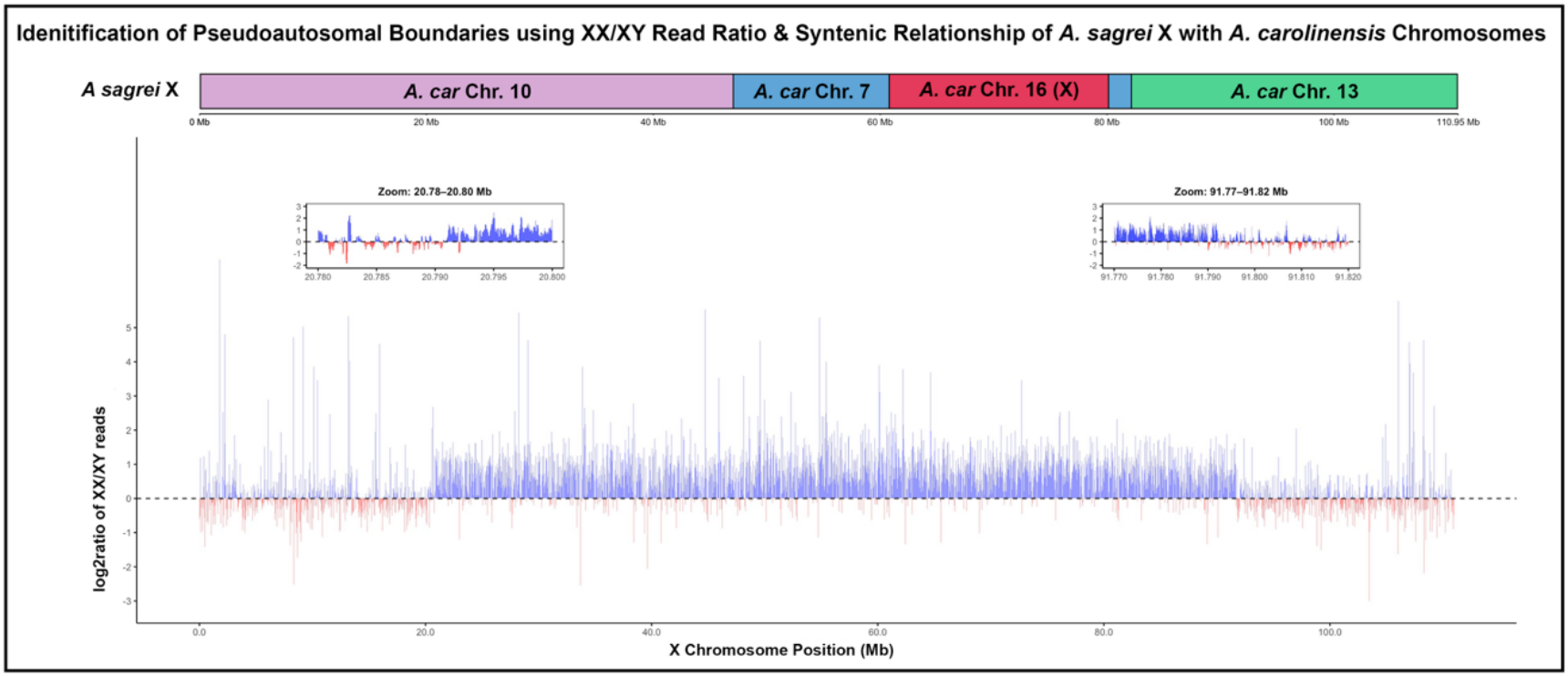
Idenitification of Pseudoautosomal Boundaries using XX/XY Read Ratio & Syntenic Relationship of A. sagrei X with A. carolinensis Chromosomes
A sagrei X
A. car Chr. 10
A. car Chr. 7
A. car Chr. 16 (X)
A. car Chr. 13
0 Mb
20 Mb
40 Mb
60 Mb
80 Mb
100 Mb
110.95 Mb
Zoom: 20.78–20.80 Mb
Zoom: 91.77–91.82 Mb
log2ratio of XX/XY reads
X Chromosome Position (Mb)

Figure 2.2. Identification of the X-specific region and pseudoautosomal boundaries. Whole genome shotgun sequence from XX and XY individuals was aligned to the XX reference genome (*Anosag2.1*; Geneva et al., 2022) to examine the $\log_2$(XX/XY) read coverage ratio along the *A. sagrei* X chromosome. A $\log_2$ ratio of 0 indicates equal coverage between the sexes, while a ratio of 1 indicates that the XX genome has twice the coverage of XY, consistent with hemizygosity. The pseudoautosomal regions (PARs) are located at both ends of the X chromosome and exhibit a $\log_2$ ratio near 0, indicating shared sequence and coverage in both sexes. In contrast, the centrally located X-specific region shows a $\log_2$ ratio near 1, indicating a reduction in XY read coverage. Regions with greater XX coverage are in blue and regions with greater coverage in XY are in red. At the top, the syntenic relationships between the *A. sagrei* X chromosome and *A. carolinensis* autosomes and X chromosome are illustrated (adapted from Geneva et al., 2022; Faircloth et al., unpublished).

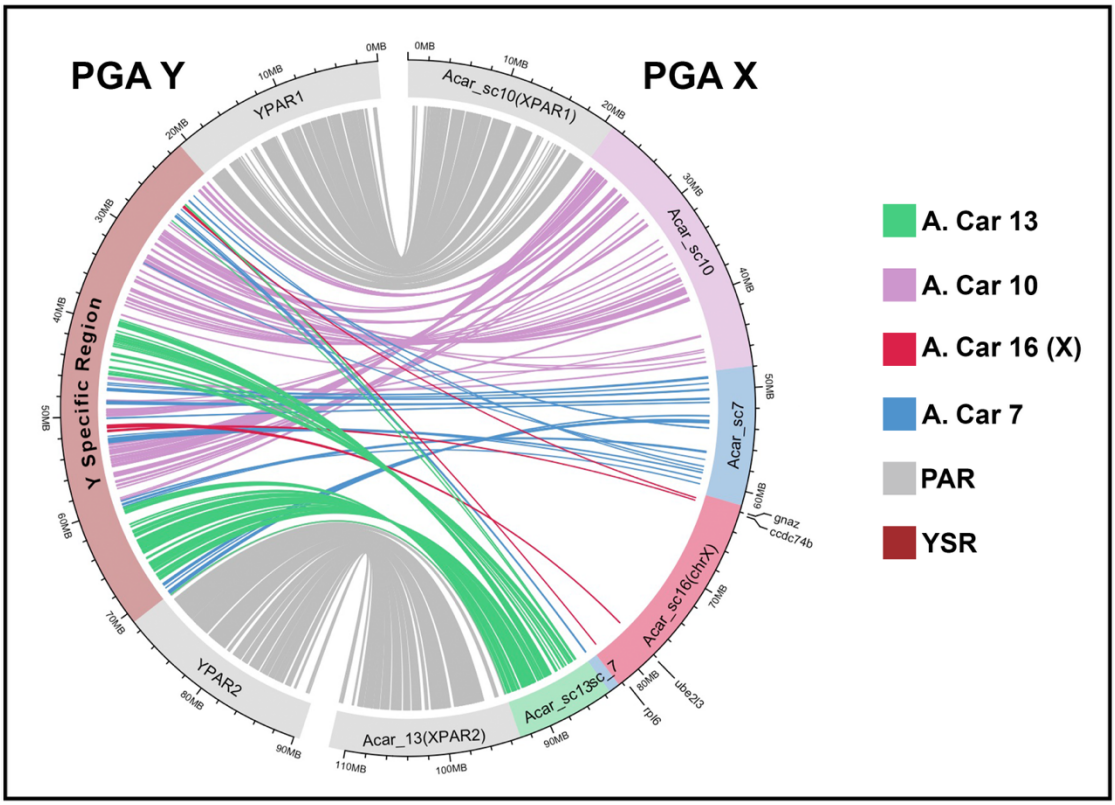

Figure 2.3. Synteny analyses of the X and Y gene pairs. A Circos plot displaying the positions of X/Y gene pairs on the PGA Y chromosome (left) and the PGA X chromosome (right) reveals extensive gene loss on the Y chromosome and multiple Y-linked inversions relative to the X. Only four Y-linked genes remain within the most ancient region of the Y chromosome. These genes are annotated and aligned to their corresponding positions on the ancestral X (*A. carolinensis* Chr.16; Faircloth, unpublished). The X-specific region is color-coded and labeled according to syntenic relationship with *A. carolinensis* chromosomes.

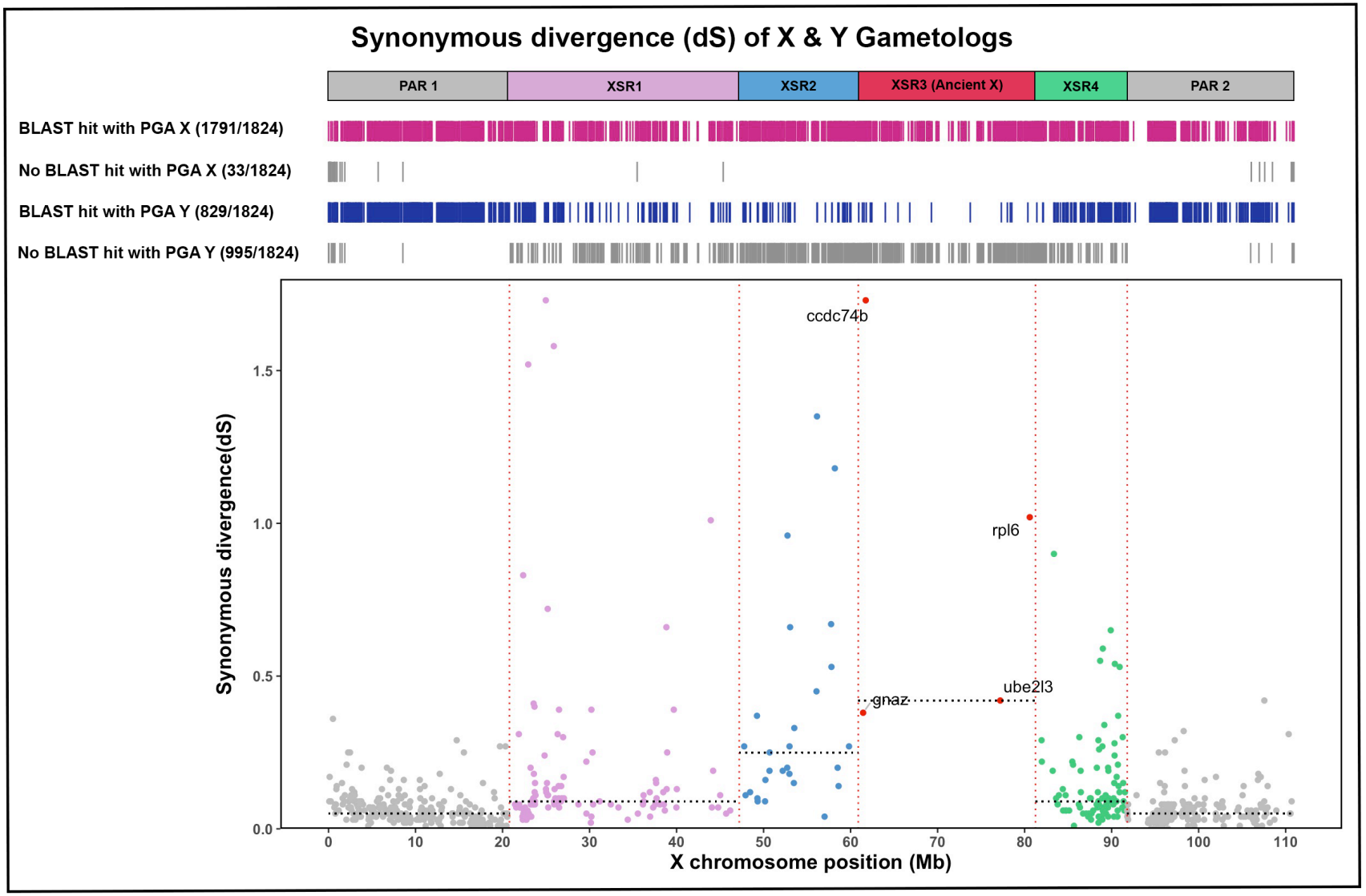
Synonymous divergence (dS) of X & Y Gametologs
PAR 1
XSR1
XSR2
XSR3 (Ancient X)
XSR4
PAR 2
BLAST hit with PGA X (1791/1824)
No BLAST hit with PGA X (33/1824)
BLAST hit with PGA Y (829/1824)
No BLAST hit with PGA Y (995/1824)
ccdc74b
rpl6
ube2l3
gnaz
Synonymous divergence(dS)
0.0
0.5
1.0
1.5
0
10
20
30
40
50
60
70
80
90
100
110
X chromosome position (Mb)

Figure 2.4. Y chromosome gene loss and synonymous divergence of XY gene pairs in *A. sagrei*. (Top) Genes annotated on the reference X chromosome assembly (*Anosag2.1*; Geneva et al., 2022) were BLAST comparisons against the newly assembled PGA X and Y chromosomes. BLAST hits recovered on the PGA X chromosome are shown in pink, hits on the PGA Y chromosome are shown in blue, and hits not found are shown in gray. The PGA Y chromosome exhibits massive gene loss across the non-recombining region, consistent with Y chromosome degeneration. (Bottom) Synonymous divergence (dS) was estimated for retained XY gene pairs. The *A. sagrei* X chromosome shows no clear evidence of distinct evolutionary strata. The top panel depicts the *A. sagrei* X chromosome, color-coded by X-specific regions (XSR1-XSR4) and their syntenic relationships to *A. carolinensis* chromosomes. The corresponding dS values are plotted below, ordered by X chromosome position (in Mb) and color-coded as above. Median dS for each X-specific region is indicated by a dotted black line. Red dashed lines mark X region boundaries. The four-remaining ancient XY gene pairs are labeled on the plot.

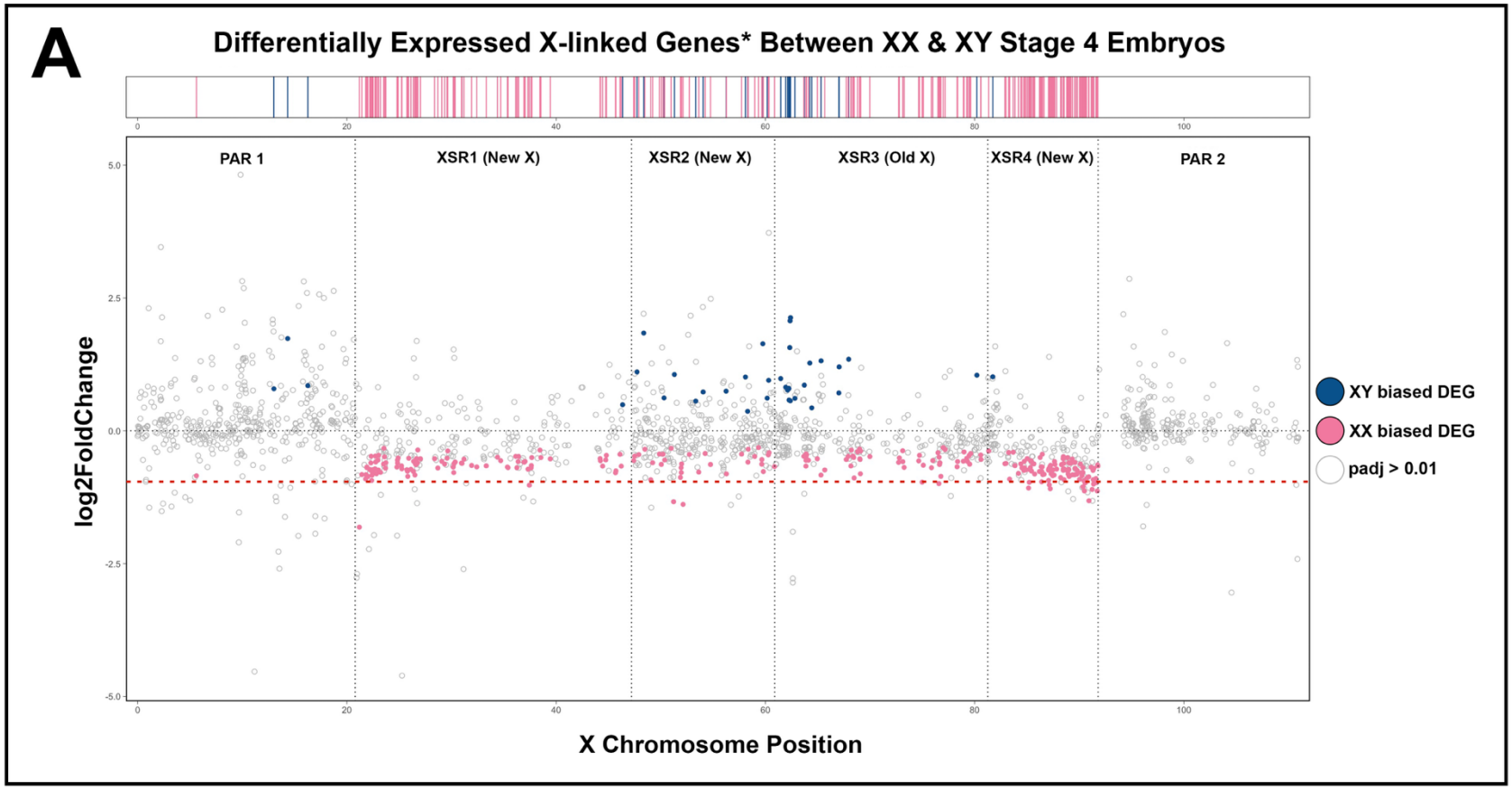
A
Differentially Expressed X-linked Genes* Between XX & XY Stage 4 Embryos
PAR 1
XSR1 (New X)
XSR2 (New X)
XSR3 (Old X)
XSR4 (New X)
PAR 2
log2FoldChange
X Chromosome Position
XY biased DEG
XX biased DEG
padj > 0.01

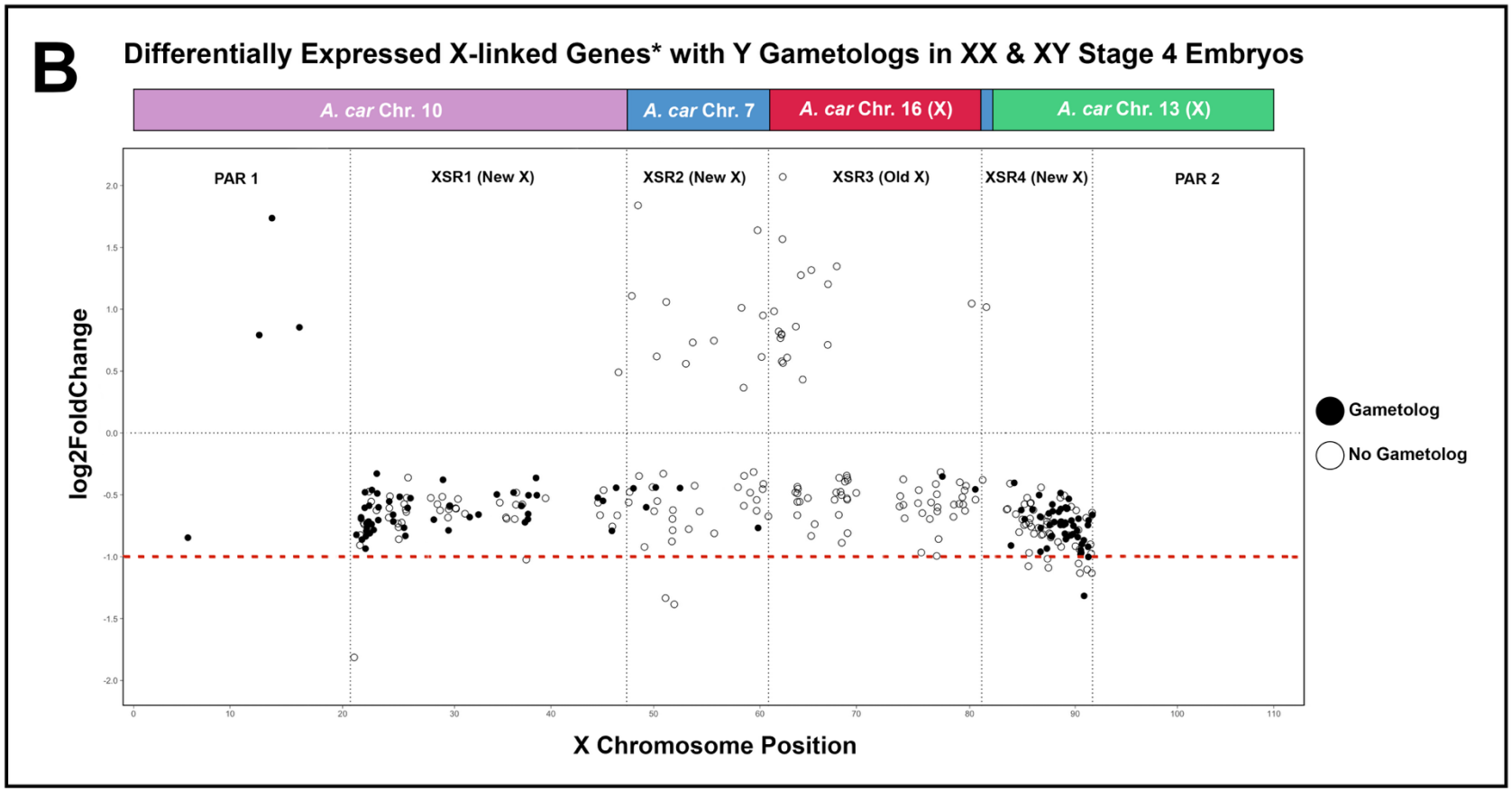
B
Differentially Expressed X-linked Genes* with Y Gametologs in XX & XY Stage 4 Embryos
A. car Chr. 10
A. car Chr. 7
A. car Chr. 16 (X)
A. car Chr. 13 (X)
PAR 1
XSR1 (New X)
XSR2 (New X)
XSR3 (Old X)
XSR4 (New X)
PAR 2
log2FoldChange
X Chromosome Position
Gametolog
No Gametolog

Figure 2.5. A genome-wide view of dosage compensation across the X chromosome in *A. sagrei*. (A) Log_2 fold change (log_2FC) values of differentially expressed genes (DEGs, padj > 0.05) between XX and XY stage 4 embryos are plotted along the X chromosome (in Mb). Genes significantly upregulated in XX embryos are shown in pink, while those upregulated in XY embryos are shown in blue. Genes that are not significantly differentially expressed are shown in gray (padj > 0.01). The top panel displays a tick mark representation of the DEGs, color-coded as above. (B) Log_2FC values of significant DEGs with and without Y chromosome gametologs are plotted along the X chromosome (in Mb). X-linked genes with a Y gametolog are shown as solid black circles, while those without a Y gametolog are shown as open black circles. The top panel illustrates the X chromosome, color-coded by syntenic relationships to *A. carolinensis*. A log_2FC of 0 indicates equal expression between the sexes, consistent with complete dosage compensation. A log_2FC of -1 demonstrates two-fold lower expression in XY relative to XX, indicating a lack of dosage compensation. In both plots, a red dashed line is present at $log_2FC = -1$.

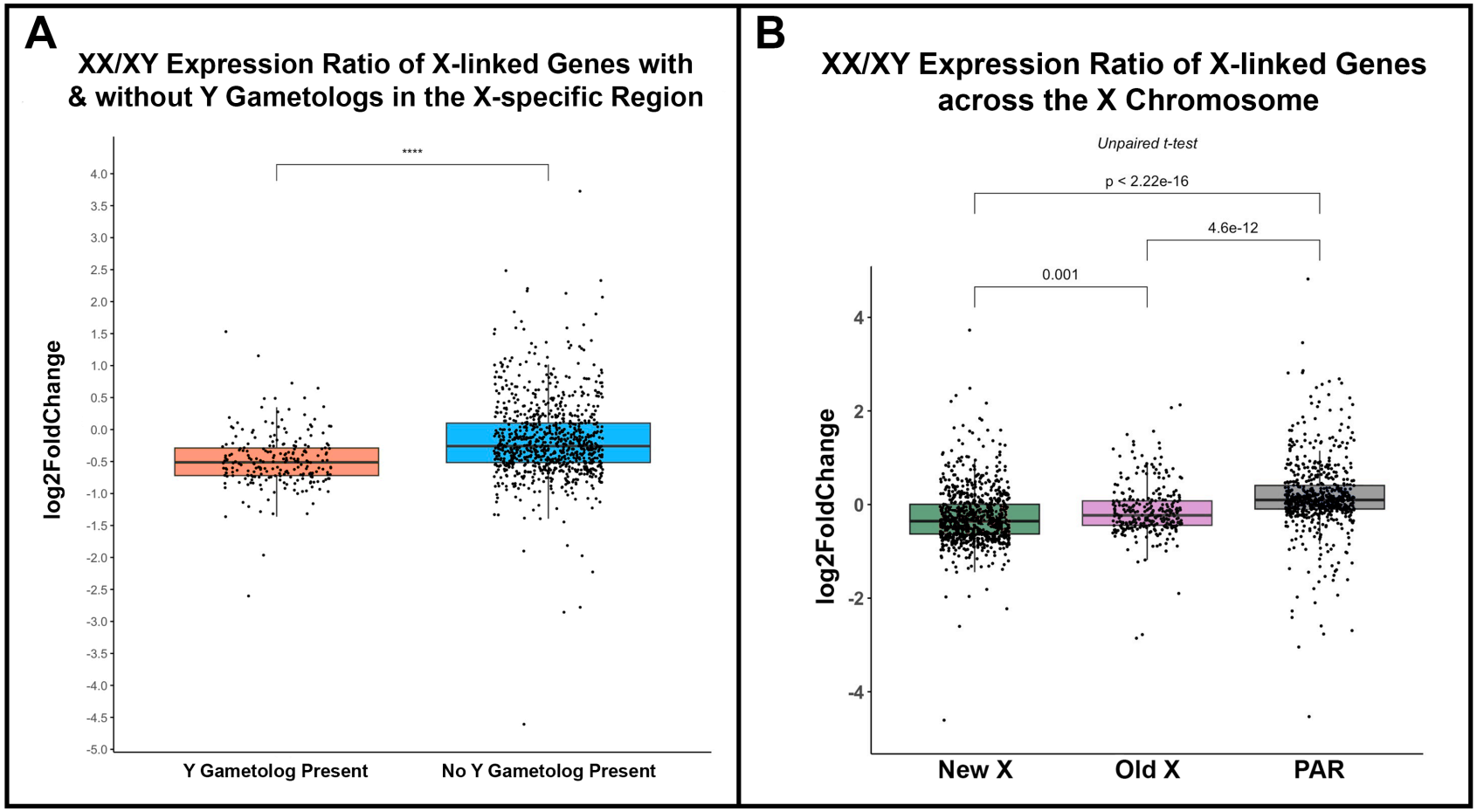
A
XX/XY Expression Ratio of X-linked Genes with & without Y Gametologs in the X-specific Region
log2FoldChange
****
Y Gametolog Present
No Y Gametolog Present
B
XX/XY Expression Ratio of X-linked Genes across the X Chromosome
Unpaired t-test
p < 2.22e-16
4.6e-12
0.001
log2FoldChange
New X
Old X
PAR

Figure 2.6. XX/XY gene expression ratio analyses to examine general dosage compensation patterns in *A. sagrei.* (A) Log_2(XX/XY) expression ratios were calculated for X-linked genes, grouped by presence or absence of a Y-linked gametolog. X-linked genes with Y gametologs (orange) exhibit lower XX/XY ratios overall, indicating reduced dosage compensation relative to X-linked genes without Y gametologs (blue). (B) Log_2(XX/XY) expression ratios of X-linked genes are plotted across different regions of the X chromosome, including the newly evolved regions (New X: XSR1, XSR2, and XSR4), the ancient, conserved X (Old X: XSR3), and the PARs. Expression ratios differ significantly between the new and old X, with the old X showing stronger evidence of dosage compensation. Additionally, expression ratios in both the new and old X-specific regions differ significantly from those in the PARs, highlighting key differences in expression between the recombining and non-recombining regions.

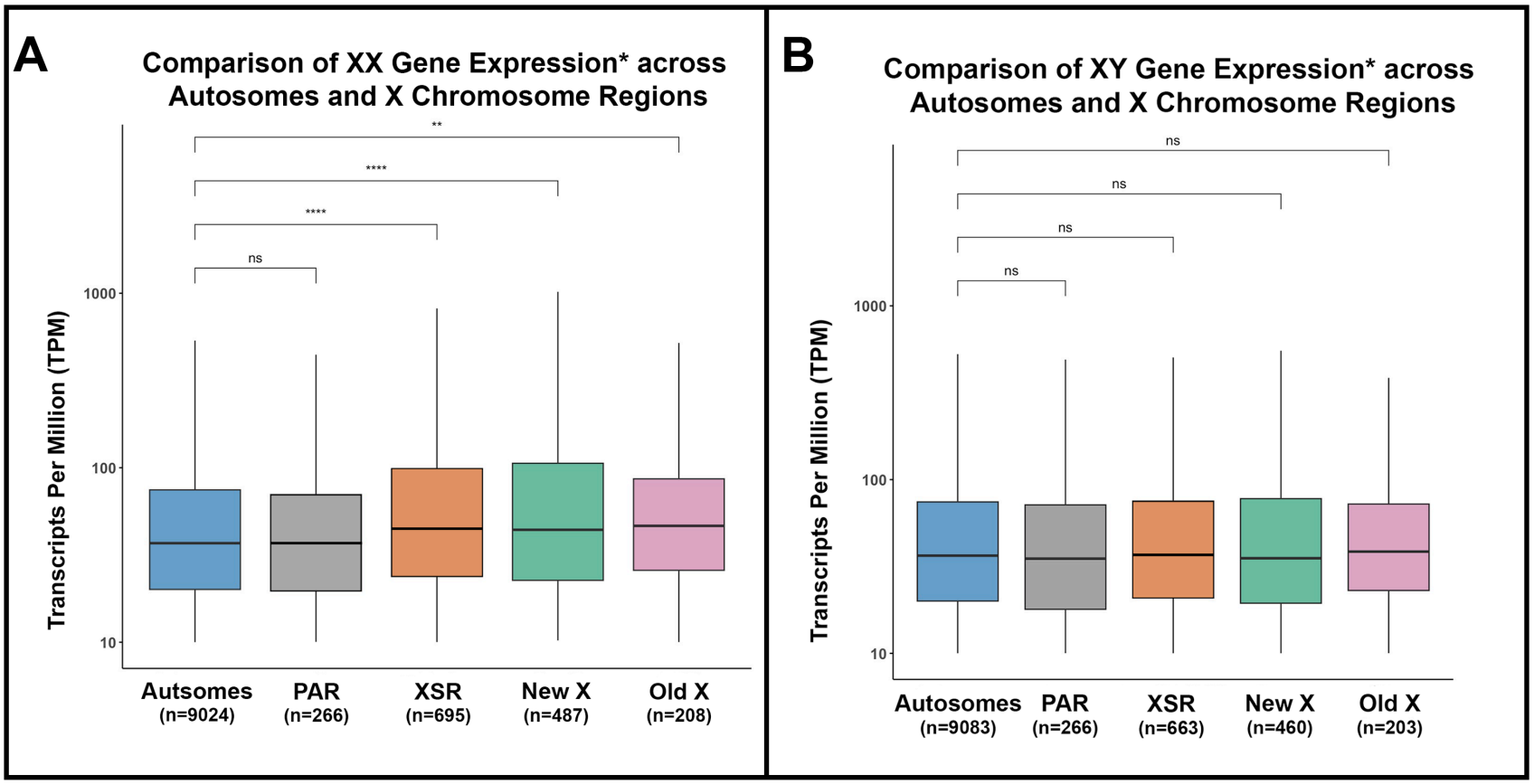
A
Comparison of XX Gene Expression* across Autosomes and X Chromosome Regions
Transcripts Per Million (TPM)
1000
100
10
**
****
****
ns
Autsomes (n=9024)
PAR (n=266)
XSR (n=695)
New X (n=487)
Old X (n=208)
B
Comparison of XY Gene Expression* across Autosomes and X Chromosome Regions
Transcripts Per Million (TPM)
1000
100
10
ns
ns
ns
ns
Autosomes (n=9083)
PAR (n=266)
XSR (n=663)
New X (n=460)
Old X (n=203)

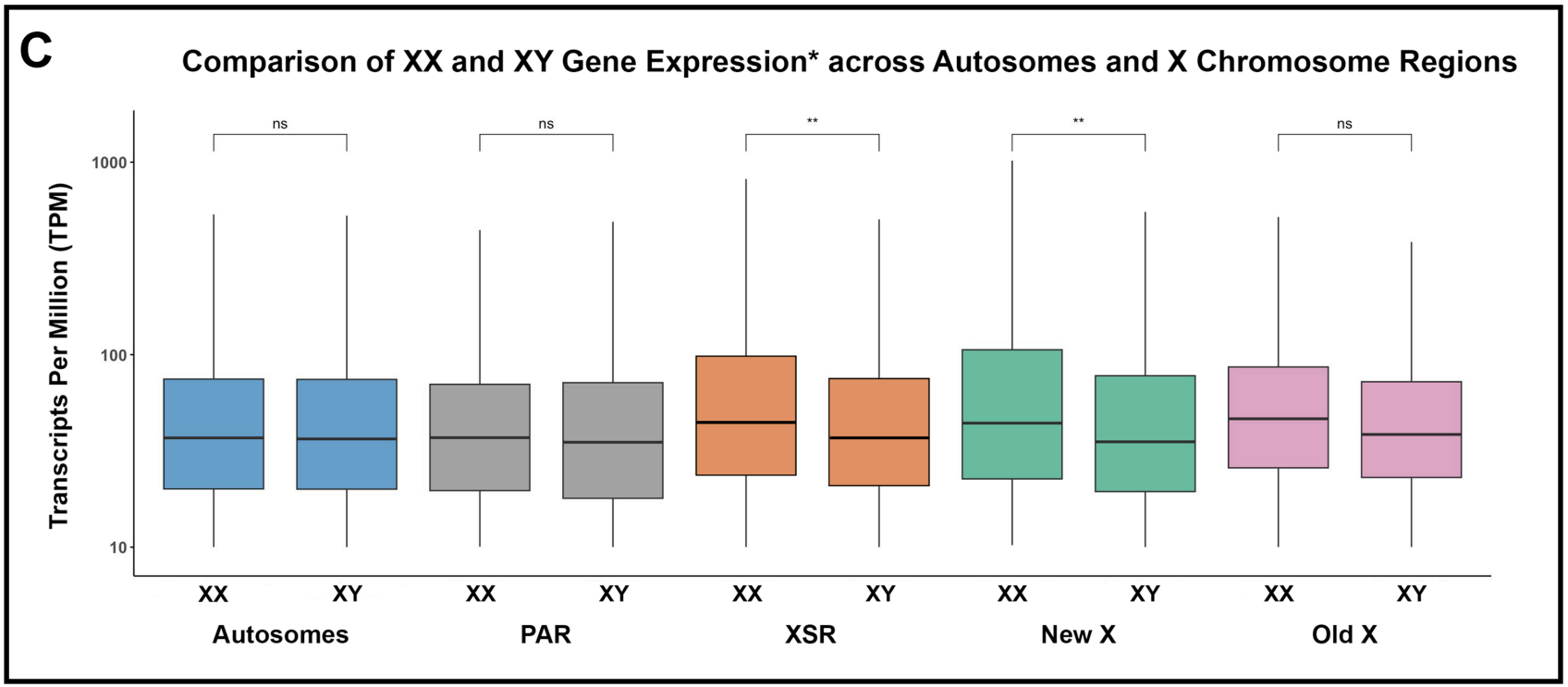
C
Comparison of XX and XY Gene Expression* across Autosomes and X Chromosome Regions
Transcripts Per Million (TPM)
1000
100
10
ns
ns
**
**
ns
XX
XY
XX
XY
XX
XY
XX
XY
XX
XY
Autosomes
PAR
XSR
New X
Old X

Figure 2.7. Gene expression comparisons to gain a deeper understanding of dosage compensation in *A. sagrei.* (A) Gene expression (in TPM) was measured in XX embryos across the autosomes and various regions of the X chromosome including the psuedoautosomal regions (PARs), the X-specific region (XSR = New X + Old X), the new X, and the old X. Expression of genes in old and new sections of the XSR were significantly higher than autosomal and PAR genes, indicating elevated X-linked gene expression in XX embryos. (B) The same analysis in XY embryos showed no significant differences in gene expression between the autosomes and the X chromosome, suggesting balanced expression across the XY genome. (C) Comparisons of gene expression between XX and XY embryos revealed no significant differences on the autosomes, PARs, or the old X. However, XX embryos exhibit significantly higher expression of the new X and the combined XSR compared to XY embryos, indicating variable dosage compensation in *A. sagrei*.

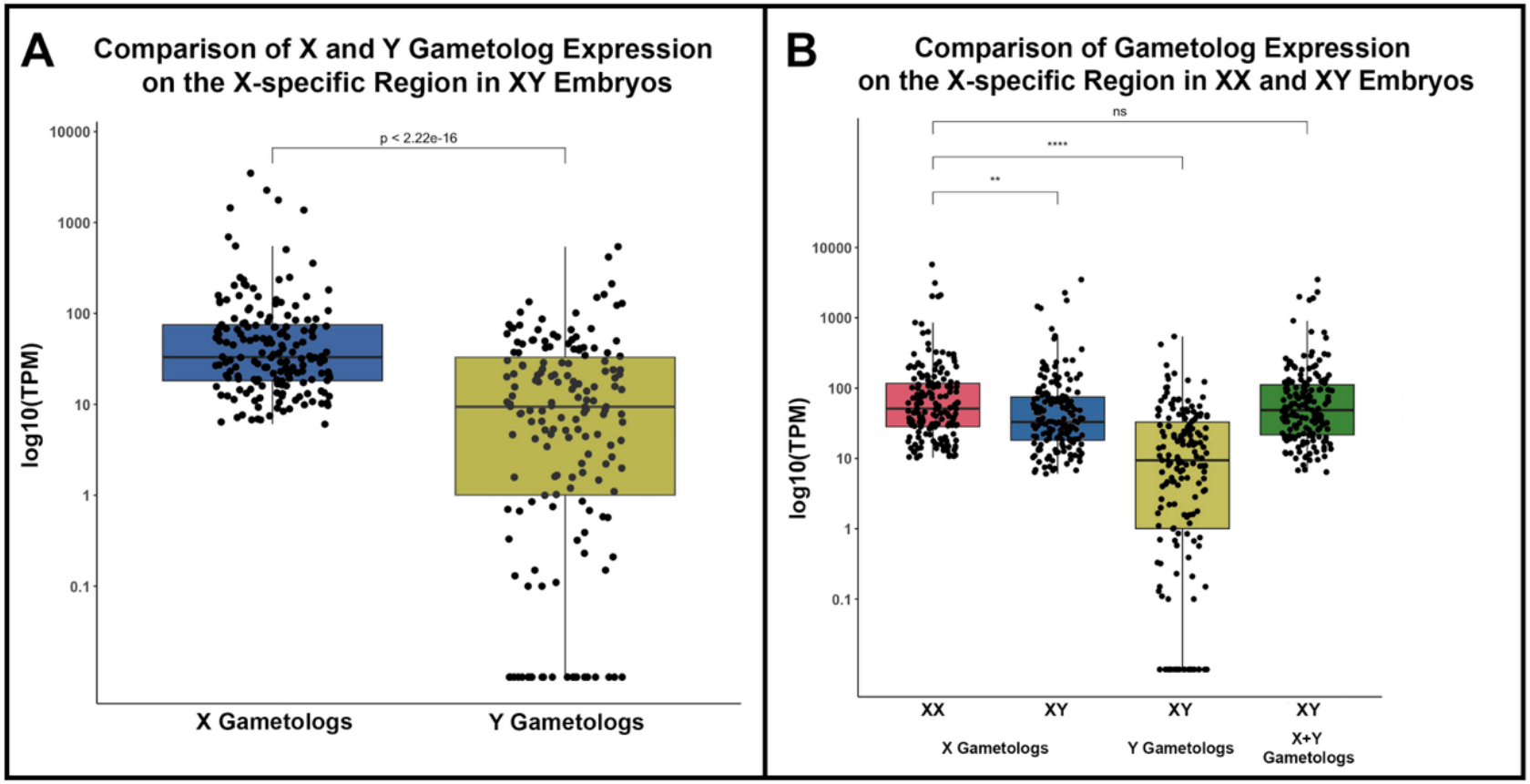
A
Comparison of X and Y Gametolog Expression on the X-specific Region in XY Embryos
p < 2.22e-16
log10(TPM)
10000
1000
100
10
1
0.1
X Gametologs
Y Gametologs
B
Comparison of Gametolog Expression on the X-specific Region in XX and XY Embryos
ns
****
**
log10(TPM)
10000
1000
100
10
1
0.1
XX
XY
XY
XY
X Gametologs
Y Gametologs
X+Y Gametologs

Figure 2.8. Investigation of Y gametolog expression in XY embryos. (A) The $\log_{10}$ of transcripts per million (TPM) was calculated for X and Y gametolog expression in XY embryos. X gametologs exhibit significantly higher expression levels compared to their Y counterparts, suggesting that many Y gametologs are either non-functional or undergoing degeneration. (B) To further assess this pattern, $\log_{10}$(TPM) values were also calculated for X gametologs in XX embryos and for the combined X+Y gametolog expression in XY embryos. X gametolog expression in XX embryos differs significantly from both X and Y gametolog expression in XY embryos. However, when X and Y gametolog expression are combined in XY embryos, expression differences are no longer significant, indicating partial dosage compensation through Y gametolog expression.

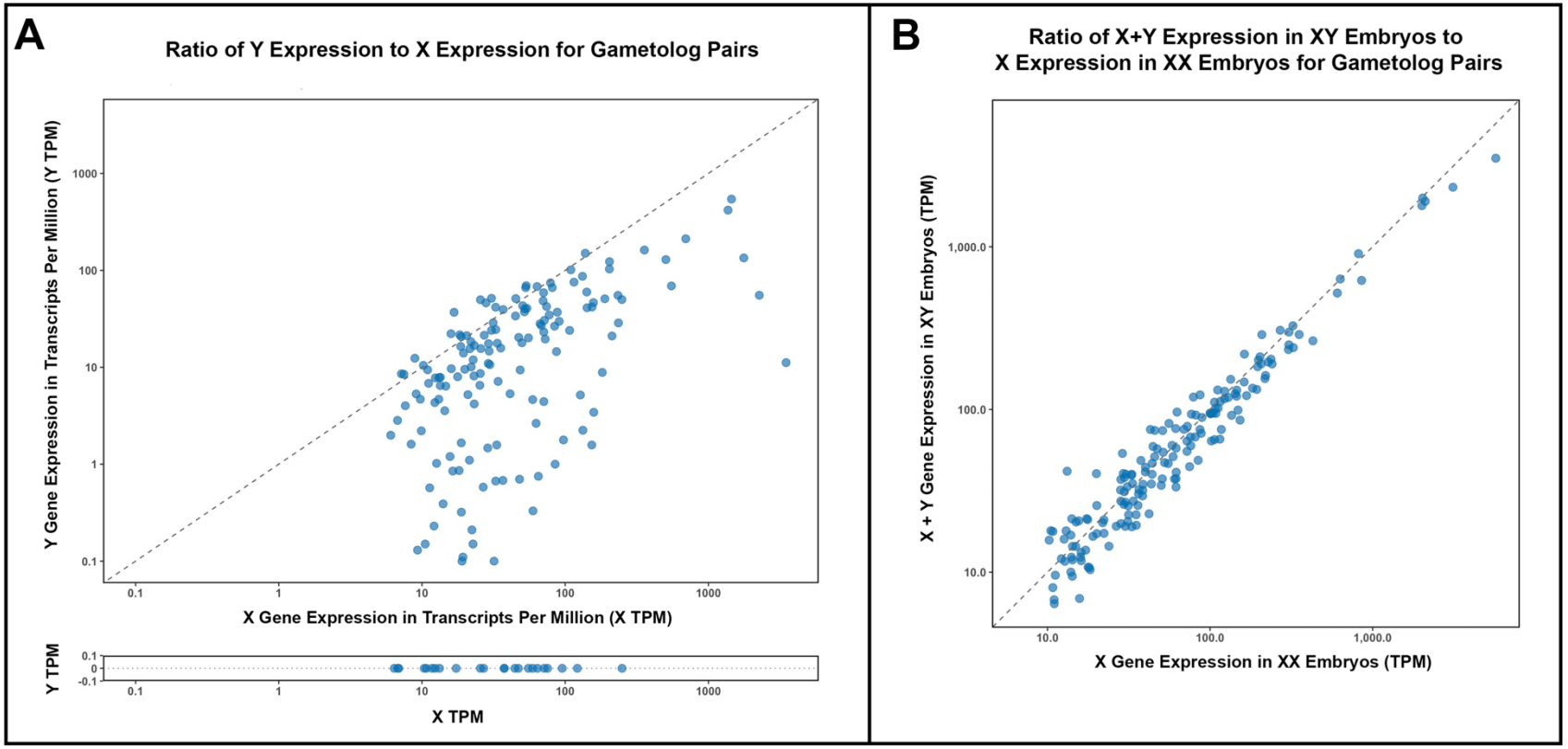
A
Ratio of Y Expression to X Expression for Gametolog Pairs
Y Gene Expression in Transcripts Per Million (Y TPM)
1000
100
10
1
0.1
0.1
1
10
100
1000
X Gene Expression in Transcripts Per Million (X TPM)
Y TPM
0.1
0
-0.1
0.1
1
10
100
1000
X TPM
B
Ratio of X+Y Expression in XY Embryos to
X Expression in XX Embryos for Gametolog Pairs
X + Y Gene Expression in XY Embryos (TPM)
1,000.0
100.0
10.0
10.0
100.0
1,000.0
X Gene Expression in XX Embryos (TPM)

Figure 2.9. Gametolog expression analysis to assess the role of X and Y gametologs in dosage compensation. (A) Expression levels (in TPM) of X and Y gametolog pairs in XY embryos were plotted to evaluate their relative expression. The dotted diagonal line indicates equal expression from both gametologs. Points below the line represent genes with higher expression from the X gametolog, while those above the line reflect higher Y gametolog expression. The bottom panel highlights instances where the Y gametolog is not expressed (< 0.1 TPM), further supporting the observation that X gametologs generally exhibit higher expression than Y gametologs in XY embryos. (B) The combined expression (X+Y) of gametologs in XY embryos was plotted against the expression of X gametologs in XX embryos. The alignment of points along the diagonal indicates that total gametolog expression in males is comparable to that of X expression in females.

TABLES

Table 2.1. Sex genotyping primer sequences

Gene:	Primer:	Sequence
kank 1	forward	5’-CCTTCCTTTGTAGGATCCAGTG-3'
kank1	reverse	5’-GGAGCACAGGGATAGTTTTGAC-3'
gnazy	forward	5’-GTGGTGGGTTCAACCTAGAGG-3'
gnazy	reverse	5’-CGTAGGATGTCCTCCACTGTG-3’

Table 2.2. Gene count on sex chromosomes

Sex Chromosome Region:	Gene Number:
Entire X-specific region	1,100
Old X-specific region	324
Entire Y-specific region	340
Old Y-specific region	5

Table 2.3. Differentially expressed genes in XX and XY stage 4 embryos

Total DEGS (padj < 0.05)	336
Total DEGs on X chromosome	314 (93%)
XX biased DEGs on X	279 (89%)
XY biased DEGs on X	35 (11%)

Table 2.4. Stage 4 differentially expressed X-chromosome genes by X-specific region

XX biased DEGs (excluding PAR)	XSR1	XSR2	XSR3	XSR4	New X	Old X
278	93 (34%)	31 (11%)	54 (19%)	100 (36%)	224 (81%)	54 (19%)
XY biased DEGs (excluding PAR)	XSR1	XSR2	XSR3	XSR4	New X	Old X
32	1 (3%)	12 (38%)	18 (56%)	1 (3%)	14 (44%)	18 (56%)

REFERENCES

Alföldi, J., Di Palma, F., Grabherr, M., Williams, C., Kong, L., Mauceli, E., Russell, P., Lowe, C. B., Glor, R. E., Jaffe, J. D., Ray, D. A., Boissinot, S., Shedlock, A. M., Botka, C., Castoe, T. A., Colbourne, J. K., Fujita, M. K., Moreno, R. G., ten Hallers, B. F., … Lindblad-Toh, K. (2011). The genome of the green anole lizard and a comparative analysis with birds and mammals. *Nature*, *477*(7366), 587–591. https://doi.org/10.1038/nature10390

Anirudhan, A., Angulo-Bejarano, P. I., Paramasivam, P., Manokaran, K., Kamath, S. M., Murugesan, R., Sharma, A., & Ahmed, S. S. S. J. (2021). RPL6: A Key Molecule Regulating Zinc- and Magnesium-Bound Metalloproteins of Parkinson's Disease. *Frontiers in Neuroscience*, *15*, 631892. https://doi.org/10.3389/fnins.2021.631892

Arbuckle, K., Bennett, C. M., & Speed, M. P. (2014). A simple measure of the strength of convergent evolution. *Methods in Ecology and Evolution*, *5*(7), 685–693. https://doi.org/10.1111/2041-210X.12195

Bachtrog, D., Mank, J. E., Peichel, C. L., Kirkpatrick, M., Otto, S. P., Ashman, T. L., Hahn, M. W., Kitano, J., Mayrose, I., Ming, R., Perrin, N., Ross, L., Valenzuela, N., & Vamosi, J. C. (2014). Sex determination: Why so many ways of doing it? *PLoS Biol*, *12*(7), e1001899. https://doi.org/10.1371/journal.pbio.1001899

Baeckens, S., Driessens, T., Huyghe, K., Vanhooydonck, B., & Van Damme, R. (2018). Intraspecific Variation in the Information Content of an Ornament:

Why Relative Dewlap Size Signals Bite Force in Some, But Not All Island Populations of Anolis sagrei. *Integrative and Comparative Biology*, *58*(1), 25–37. https://doi.org/10.1093/icb/icy012

Bai, D., Zhang, J., Xiao, W., & Zheng, X. (2014). Regulation of the HDM2-p53 pathway by ribosomal protein L6 in response to ribosomal stress. *Nucleic Acids Research*, *42*(3), 1799–1811. https://doi.org/10.1093/nar/gkt971

Bertho, S., Herpin A, Schartl M, & Guiguen Y. (2021). Lessons from an unusual vertebrate sex-determining gene—PubMed. *Philosophical Transactions of the Royal Society of London. Series B, Biological Sciences*, *376*(1832). https://doi.org/10.1098/rstb.2020.0092

Bitgood, M. J., Shen, L., & McMahon, A. P. (1996). Sertoli cell signaling by Desert hedgehog regulates the male germline. *Current Biology: CB*, *6*(3), 298–304. https://doi.org/10.1016/s0960-9822(02)00480-3

Bock, D. G., Baeckens, S., Pita-Aquino, J. N., Chejanovski, Z. A., Michaelides, S. N., Muralidhar, P., Lapiedra, O., Park, S., Menke, D. B., Geneva, A. J., Losos, J. B., & Kolbe, J. J. (2021). Changes in selection pressure can facilitate hybridization during biological invasion in a Cuban lizard. *Proceedings of the National Academy of Sciences of the United States of America*, *118*(42), e2108638118. https://doi.org/10.1073/pnas.2108638118

Bull, J. (1983). *Evolution of Sex Determining Mechanisms*. Benjamin/Cummings Pub. Co.

Burgoyne, Buehr, & McLaren. (1988). XY follicle cells in ovaries of XX----XY female mouse chimaeras—PubMed. *Development (Cambridge, England)*, *104*(4). https://doi.org/10.1242/dev.104.4.683

Capel, B. (2017). Vertebrate sex determination: Evolutionary plasticity of a fundamental switch. *Nature Reviews. Genetics*, *18*(11), 675–689. https://doi.org/10.1038/nrg.2017.60

Capel, B. (2019). WOMEN IN REPRODUCTIVE SCIENCE: To be or not to be a testis. *Reproduction*, *158*(6), F101-f111. https://doi.org/10.1530/rep-19-0151

Charlesworth, B. (1996). The evolution of chromosomal sex determination and dosage compensation—PubMed. *Current Biology : CB*, *6*(2). https://doi.org/10.1016/s0960-9822(02)00448-7

Concordet, J.-P., & Haeussler, M. (2018). CRISPOR: Intuitive guide selection for CRISPR/Cas9 genome editing experiments and screens. *Nucleic Acids Research*, *46*(W1), W242–W245. https://doi.org/10.1093/nar/gky354

Cortez, D., Marin, R., Toledo-Flores, D., Froidevaux, L., Liechti, A., Waters, P. D., Grützner, F., & Kaessmann, H. (2014). Origins and functional evolution of Y chromosomes across mammals. *Nature*, *508*(7497), 488–493. https://doi.org/10.1038/nature13151

Ezaz, T., Sarre, S. D., O'Meally, D., Graves, J. A. M., & Georges, A. (2009). Sex chromosome evolution in lizards: Independent origins and rapid transitions. *Cytogenetic and Genome Research*, *127*(2–4), 249–260. https://doi.org/10.1159/000300507

Feiner, N., Brun-Usan M, Andrade P, Pranter R, Park S, Menke DB, Geneva AJ, & Uller T. (2022). A single locus regulates a female-limited color pattern polymorphism in a reptile—PubMed. *Science Advances*, *8*(10). https://doi.org/10.1126/sciadv.abm2387

Felsenstein, J. (1985). CONFIDENCE LIMITS ON PHYLOGENIES: AN APPROACH USING THE BOOTSTRAP. *Evolution; International Journal of Organic Evolution*, *39*(4), 783–791. https://doi.org/10.1111/j.1558-5646.1985.tb00420.x

Ford, Jones, Polani, De Almeida, & Briggs. (1959). A sex-chromosome anomaly in a case of gonadal dysgenesis (Turner's syndrome)—PubMed. *Lancet (London, England)*, *1*(7075). https://doi.org/10.1016/s0140-6736(59)91893-8

Gamble, T., Geneva, A. J., Glor, R. E., & Zarkower, D. (2014). Anolis sex chromosomes are derived from a single ancestral pair. *Evolution*, *68*(4), 1027–1041. https://doi.org/10.1111/evo.12328

Gao, Y., Wang, Z., Long, Y., Yang, L., Jiang, Y., Ding, D., Teng, B., Chen, M., Yuan, J., & Gao, F. (2024). Unveiling the roles of Sertoli cells lineage differentiation in reproductive development and disorders: A review. *Frontiers in Endocrinology*, *15*, 1357594. https://doi.org/10.3389/fendo.2024.1357594

Geneva, A. J., Park S, Bock DG, de Mello PLH, Sarigol F, Tollis M, Donihue CM, Reynolds RG, Feiner N, Rasys AM, Lauderdale JD, Minchey SG, Alcala AJ, Infante CR, Kolbe JJ, Schluter D, Menke DB, & Losos JB. (2022).

Chromosome-scale genome assembly of the brown anole (Anolis sagrei), an emerging model species—PubMed. *Communications Biology*, *5*(1). https://doi.org/10.1038/s42003-022-04074-5

Genuth, N. R., & Barna, M. (2018a). Heterogeneity and specialized functions of translation machinery: From genes to organisms. *Nature Reviews. Genetics*, *19*(7), 431–452. https://doi.org/10.1038/s41576-018-0008-z

Genuth, N. R., & Barna, M. (2018b). The Discovery of Ribosome Heterogeneity and Its Implications for Gene Regulation and Organismal Life. *Molecular Cell*, *71*(3), 364–374. https://doi.org/10.1016/j.molcel.2018.07.018

Giovannotti, M., Trifonov, V. A., Paoletti, A., Kichigin, I. G., O'Brien, P. C., Kasai, F., Giovagnoli, G., Ng, B. L., Ruggeri, P., Cerioni, P. N., Splendiani, A., Pereira, J. C., Olmo, E., Rens, W., Caputo Barucchi, V., & Ferguson-Smith, M. A. (2017). New insights into sex chromosome evolution in anole lizards (Reptilia, Dactyloidae). *Chromosoma*, *126*(2), 245–260. https://doi.org/10.1007/s00412-016-0585-6

Hopes, T., Norris, K., Agapiou, M., McCarthy, C. G. P., Lewis, P. A., O'Connell, M. J., Fontana, J., & Aspden, J. L. (2022). Ribosome heterogeneity in Drosophila melanogaster gonads through paralog-switching. *Nucleic Acids Research*, *50*(4), 2240–2257. https://doi.org/10.1093/nar/gkab606

Huie, J. M., Prates, I., Bell, R. C., & de Queiroz, K. (2021). Convergent patterns of adaptive radiation between island and mainland Anolis lizards. *Biological Journal of the Linnean Society*, *134*(1). https://doi.org/10.1093/biolinnean/blab072

Jones, D. T., Taylor, W. R., & Thornton, J. M. (1992). The rapid generation of mutation data matrices from protein sequences. *Computer Applications in the Biosciences: CABIOS*, *8*(3), 275–282. https://doi.org/10.1093/bioinformatics/8.3.275

Kamiya, Kai W, Tasumi S, Oka A, Matsunaga T, Mizuno N, Fujita M, Suetake H, Suzuki S, Hosoya S, Tohari S, Brenner S, Miyadai T, Venkatesh B, Suzuki Y, & Kikuchi K. (2012). A trans-species missense SNP in Amhr2 is associated with sex determination in the tiger pufferfish, Takifugu rubripes (fugu)—PubMed. *PLoS Genetics*, *8*(7). https://doi.org/10.1371/journal.pgen.1002798

Keating, S. E., Blumer, M., Grismer, L. L., Lin, A., Nielsen, S. V., Thura, M. K., Wood, P. L., Quah, E. S. H., & Gamble, T. (2021). Sex Chromosome Turnover in Bent-Toed Geckos (Cyrtodactylus). *Genes (Basel)*, *12*(1). https://doi.org/10.3390/genes12010116

Kichigin, I. G., Giovannotti, M., Makunin, A. I., Ng, B. L., Kabilov, M. R., Tupikin, A. E., Barucchi, V. C., Splendiani, A., Ruggeri, P., Rens, W., O'Brien, P. C., Ferguson-Smith, M. A., Graphodatsky, A. S., & Trifonov, V. A. (2016). Evolutionary dynamics of Anolis sex chromosomes revealed by sequencing of flow sorting-derived microchromosome-specific DNA. *Mol Genet Genomics*, *291*(5), 1955–1966. https://doi.org/10.1007/s00438-016-1230-z

Kim, D., Paggi, J. M., Park, C., Bennett, C., & Salzberg, S. L. (2019). Graph-based genome alignment and genotyping with HISAT2 and HISAT-

genotype. *Nature Biotechnology*, *37*(8), 907–915. https://doi.org/10.1038/s41587-019-0201-4

Kircher, B. K., Liu, B., Bramble, M. D., Moses, M. M., & Behringer, R. R. (2024). Gene expression profile analysis of subregions of the adult female reproductive tract in the brown anole, Anolis sagrei. *Reproduction (Cambridge, England)*, *169*(2), e240062. https://doi.org/10.1530/REP-24-0062

Kircher, B. K., McCown MA, Scully DM, Behringer RR, & Larina IV. (2024). Structural analysis of the female reptile reproductive system by micro-computed tomography and optical coherence tomography†—PubMed. *Biology of Reproduction*, *110*(6). https://doi.org/10.1093/biolre/ioae039

Kircher, B. K., Stanley EL, & Behringer RR. (2024). Anatomy of the female reproductive tract organs of the brown anole (Anolis sagrei)—PubMed. *Anatomical Record (Hoboken, N.J. : 2007)*, *307*(2). https://doi.org/10.1002/ar.25293

Koopman, Sinclair, & Lovell-Badge. (2016). Of sex and determination: Marking 25 years of Randy, the sex-reversed mouse—PubMed. *Development (Cambridge, England)*, *143*(10). https://doi.org/10.1242/dev.137372

Kumar, S., Stecher, G., Suleski, M., Sanderford, M., Sharma, S., & Tamura, K. (2024). MEGA12: Molecular Evolutionary Genetic Analysis Version 12 for Adaptive and Green Computing. *Molecular Biology and Evolution*, *41*(12), msae263. https://doi.org/10.1093/molbev/msae263

Lahn, & Page. (1999). Four evolutionary strata on the human X chromosome—PubMed. *Science (New York, N.Y.)*, *286*(5441). https://doi.org/10.1126/science.286.5441.964

Lapiedra, O., Chejanovski, Z., & Kolbe, J. J. (2017). Urbanization and biological invasion shape animal personalities. *Global Change Biology*, *23*(2), 592–603. https://doi.org/10.1111/gcb.13395

Lapiedra, O., Schoener, T. W., Leal, M., Losos, J. B., & Kolbe, J. J. (2018). Predator-driven natural selection on risk-taking behavior in anole lizards. *Science (New York, N.Y.)*, *360*(6392), 1017–1020. https://doi.org/10.1126/science.aap9289

Li, D., & Wang, J. (2020). Ribosome heterogeneity in stem cells and development. *The Journal of Cell Biology*, *219*(6), e202001108. https://doi.org/10.1083/jcb.202001108

Li, H., Handsaker, B., Wysoker, A., Fennell, T., Ruan, J., Homer, N., Marth, G., Abecasis, G., Durbin, R., & 1000 Genome Project Data Processing Subgroup. (2009). The Sequence Alignment/Map format and SAMtools. *Bioinformatics (Oxford, England)*, *25*(16), 2078–2079. https://doi.org/10.1093/bioinformatics/btp352

Li, H., Huo, Y., He, X., Yao, L., Zhang, H., Cui, Y., Xiao, H., Xie, W., Zhang, D., Wang, Y., Zhang, S., Tu, H., Cheng, Y., Guo, Y., Cao, X., Zhu, Y., Jiang, T., Guo, X., Qin, Y., & Sha, J. (2022). A male germ-cell-specific ribosome controls male fertility. *Nature*, *612*(7941), 725–731. https://doi.org/10.1038/s41586-022-05508-0

Liao, Y., Smyth, G. K., & Shi, W. (2014). featureCounts: An efficient general purpose program for assigning sequence reads to genomic features. *Bioinformatics (Oxford, England)*, *30*(7), 923–930. https://doi.org/10.1093/bioinformatics/btt656

Lisachov, A. P., Trifonov VA, Giovannotti M, Ferguson-Smith MA, & Borodin PM. (2017). Heteromorphism of “Homomorphic” Sex Chromosomes in Two Anole Species (Squamata, Dactyloidae) Revealed by Synaptonemal Complex Analysis—PubMed. *Cytogenetic and Genome Research*, *151*(2). https://doi.org/10.1159/000460829

Losos, J. B., & Pringle, R. M. (2011). Competition, predation and natural selection in island lizards. *Nature*, *475*(7355), E1-2; discussion E3. https://doi.org/10.1038/nature10140

Love, M. I., Huber, W., & Anders, S. (2014). Moderated estimation of fold change and dispersion for RNA-seq data with DESeq2. *Genome Biology*, *15*(12), 550. https://doi.org/10.1186/s13059-014-0550-8

Marin, R., Cortez, D., Lamanna, F., Pradeepa, M. M., Leushkin, E., Julien, P., Liechti, A., Halbert, J., Brüning, T., Mössinger, K., Trefzer, T., Conrad, C., Kerver, H. N., Wade, J., Tschopp, P., & Kaessmann, H. (2017). Convergent origination of a Drosophila-like dosage compensation mechanism in a reptile lineage. *Genome Res*, *27*(12), 1974–1987. https://doi.org/10.1101/gr.223727.117

McClive, P. J., & Sinclair, A. H. (2003). Type II and type IX collagen transcript isoforms are expressed during mouse testis development. *Biology of*

Reproduction, *68*(5), 1742–1747. https://doi.org/10.1095/biolreprod.102.008235

Moser, T. V., Bond, D. M., & Hore, T. A. (2025). Variant ribosomal DNA is essential for female differentiation in zebrafish. *Philosophical Transactions of the Royal Society of London. Series B, Biological Sciences*, *380*(1921), 20240107. https://doi.org/10.1098/rstb.2024.0107

Muller H. 1932. Further studies on the nature and causes of gene mutations. In *Proceedings of the 6th International Congress of Genetics*, Vol. **1** (ed. D.F. Jones), pp. 213-215. Menasha, WI: Banta.

Nicholson, K. E., Crother, B. I., Guyer, C., & Savage, J. M. (2012). It is time for a new classification of anoles (Squamata: Dactyloidae). *Zootaxa*, *3477*(1). https://doi.org/10.11646/zootaxa.3477.1.1

Ord, T. J., Stamps, J. A., & Losos, J. B. (2013). Convergent evolution in the territorial communication of a classic adaptive radiation: Caribbean *Anolis* lizards. *Animal Behaviour*, *85*(6), 1415–1426. https://doi.org/10.1016/j.anbehav.2013.03.037

Pierucci-Alves, F., Clark, A. M., & Russell, L. D. (2001). A developmental study of the Desert hedgehog-null mouse testis. *Biology of Reproduction*, *65*(5), 1392–1402. https://doi.org/10.1095/biolreprod65.5.1392

Pinto, B. J., Keating, S. E., Nielsen, S. V., Scantlebury, D. P., Daza, J. D., & Gamble, T. (2022). Chromosome-Level Genome Assembly Reveals Dynamic Sex Chromosomes in Neotropical Leaf-Litter Geckos

(Sphaerodactylidae: Sphaerodactylus). *The Journal of Heredity*, *113*(3), 272–287. https://doi.org/10.1093/jhered/esac016

Pringle, R. M., Kartzinel, T. R., Palmer, T. M., Thurman, T. J., Fox-Dobbs, K., Xu, C. C. Y., Hutchinson, M. C., Coverdale, T. C., Daskin, J. H., Evangelista, D. A., Gotanda, K. M., A. Man in 't Veld, N., Wegener, J. E., Kolbe, J. J., Schoener, T. W., Spiller, D. A., Losos, J. B., & Barrett, R. D. H. (2019). Predator-induced collapse of niche structure and species coexistence. *Nature*, *570*(7759), 58–64. https://doi.org/10.1038/s41586-019-1264-6

Rasys, A. M., Park, S., Ball, R. E., Alcala, A. J., Lauderdale, J. D., & Menke, D. B. (2019). CRISPR-Cas9 Gene Editing in Lizards through Microinjection of Unfertilized Oocytes. *Cell Rep*, *28*(9), 2288-2292.e3. https://doi.org/10.1016/j.celrep.2019.07.089

Rovatsos, M., Altmanová, M., Pokorná, M., & Kratochvíl, L. (2014). Conserved sex chromosomes across adaptively radiated Anolis lizards. *Evolution*, *68*(7), 2079–2085. https://doi.org/10.1111/evo.12357

Rovatsos, M., Pokorná, M., Altmanová, M., & Kratochvíl, L. (2014). Cretaceous park of sex determination: Sex chromosomes are conserved across iguanas. *Biol Lett*, *10*(3), 20131093. https://doi.org/10.1098/rsbl.2013.1093

Saitou, N., & Nei, M. (1987). The neighbor-joining method: A new method for reconstructing phylogenetic trees. *Molecular Biology and Evolution*, *4*(4), 406–425. https://doi.org/10.1093/oxfordjournals.molbev.a040454

Sanger, T. J., Losos, J. B., & Gibson-Brown, J. J. (2008). A developmental staging series for the lizard genus Anolis: A new system for the integration

of evolution, development, and ecology. *Journal of Morphology*, *269*(2), 129–137. https://doi.org/10.1002/jmor.10563

Schindelin, J., Arganda-Carreras, I., Frise, E., Kaynig, V., Longair, M., Pietzsch, T., Preibisch, S., Rueden, C., Saalfeld, S., Schmid, B., Tinevez, J.-Y., White, D. J., Hartenstein, V., Eliceiri, K., Tomancak, P., & Cardona, A. (2012). Fiji: An open-source platform for biological-image analysis. *Nature Methods*, *9*(7), 676–682. https://doi.org/10.1038/nmeth.2019

Schoener, T. W., & Schoener, A. (1980). Densities, Sex Ratios, and Population Structure in Four Species of Bahamian Anolis Lizards. *Journal of Animal Ecology*, *49*(1), 19–53. https://doi.org/10.2307/4276

Shah, A. N., Leesch, F., Lorenzo-Orts, L., Grundmann, L., Novatchkova, M., Haselbach, D., Calo, E., & Pauli, A. (2024). A dual ribosomal system in the zebrafish soma and germline. *bioRxiv: The Preprint Server for Biology*, 2024.08.29.610041. https://doi.org/10.1101/2024.08.29.610041

Stecher, G., Tamura, K., & Kumar, S. (2020). Molecular Evolutionary Genetics Analysis (MEGA) for macOS. *Molecular Biology and Evolution*, *37*(4), 1237–1239. https://doi.org/10.1093/molbev/msz312

Stöck M, Kratochvíl L, Kuhl H, Rovatsos M, Evans BJ, Suh A, Valenzuela N, Veyrunes F, Zhou Q, Gamble T, Capel B, Schartl M, & Guiguen Y. (2021). A brief review of vertebrate sex evolution with a pledge for integrative research: Towards ' sexomics'—PubMed. *Philosophical Transactions of the Royal Society of London. Series B, Biological Sciences*, *376*(1832). https://doi.org/10.1098/rstb.2020.0426

Tang, Y. P., & Wade, J. (2010). Sex- and age-related differences in ribosomal proteins L17 and L37, as well as androgen receptor protein, in the song control system of zebra finches. *Neuroscience*, *171*(4), 1131–1140. https://doi.org/10.1016/j.neuroscience.2010.10.014

Uetz, P., Freed, P, Aguilar, R., Reyes, F., Kudera, J. & Hošek, J. (eds.) (2025) The Reptile Database, http://www.reptile-database.org, accessed August 2025.

Wagner, S., Whiteley, S. L., Castelli, M., Patel, H. R., Deveson, I. W., Blackburn, J., Holleley, C. E., Marshall Graves, J. A., & Georges, A. (2023). Gene expression of male pathway genes sox9 and amh during early sex differentiation in a reptile departs from the classical amniote model. *BMC Genomics*, *24*(1), 243. https://doi.org/10.1186/s12864-023-09334-0

Weberling, A., Shylo NA, Kircher BK, Wilson H, McClain M, Marchini M, Starr KB, Sanger TJ, Hollfelder F, & Trainor PA. (2025). Pre-oviposition development of the brown anole (Anolis sagrei)—PubMed. *Developmental Dynamics : An Official Publication of the American Association of Anatomists*. https://doi.org/10.1002/dvdy.70027

Wickham H (2016). *ggplot2: Elegant Graphics for Data Analysis*. Springer-Verlag New York. ISBN 978-3-319-24277-4, https://ggplot2.tidyverse.org.

Xue, S., & Barna, M. (2012). Specialized ribosomes: A new frontier in gene regulation and organismal biology. *Nature Reviews. Molecular Cell Biology*, *13*(6), 355–369. https://doi.org/10.1038/nrm3359

Yang, C., Zang, W., Ji, Y., Li, T., Yang, Y., & Zheng, X. (2019). Ribosomal protein L6 (RPL6) is recruited to DNA damage sites in a poly(ADP-ribose) polymerase-dependent manner and regulates the DNA damage response. *The Journal of Biological Chemistry*, *294*(8), 2827–2838. https://doi.org/10.1074/jbc.RA118.007009

Zhang, J., Ma, Q., Han, Y., Wen, H., Zhang, Z., Hao, Y., Xiao, F., & Liang, C. (2022). Downregulated RPL6 inhibits lung cancer cell proliferation and migration and promotes cell apoptosis by regulating the AKT signaling pathway. *Journal of Thoracic Disease*, *14*(2), 507–514. https://doi.org/10.21037/jtd-22-116

Zhu, Z., Younas, L., & Zhou, Q. (2025). Evolution and regulation of animal sex chromosomes. *Nat Rev Genet*, *26*(1), 59–74. https://doi.org/10.1038/s41576-024-00757-3

AUTHOR CONTRIBUTIONS

Megan Motley contributed to conceptualization, molecular work, data analysis, figure generation, funding acquisition, and writing. Sungdae Park contributed to molecular work, data analysis, and figure generation. Douglas Menke contributed to conceptualization, writing, funding acquisition, supervision, and editing.
All Co-authors agree that the work may be included in this thesis or dissertation.

CHAPTER 3

A Y-LINKED RIBOSOMAL GENE IS REQUIRED FOR SEX DETERMINATION IN THE BROWN ANOLE LIZARD, *ANOLIS SAGREI* [1]

---

[1] **Motley, M. K.**, Park, S., Roman, B., Mohan, S., Osman, R., Bellot, D.W., Burslie, M., Iouchmanov, A., Al-Shurafa, N., Page, D., Lauderdale, J. D., and Menke, D. B. *To be submitted to a peer-reviewed journal.*

ABSTRACT

The accurate initiation of sex determination is fundamental to reproductive success. Despite its importance, genetic sex determination remains poorly understood in reptiles. The *Anolis* XX/XY sex chromosome system arose ~100 mya and is conserved in over 1,200 pleurodont lizard species. We report a Y-linked ribosomal gene, *rpl6y*, as the primary determinant of sex in *Anolis sagrei*. This gene is among a small number of ancient Y genes conserved across most pleurodonts and encodes a highly diverged version of RPL6, a core protein component of the ribosome. During testis differentiation, expression of *rpl6y* is elevated in XY gonads, while its X chromosome paralog, *rpl6x*, is downregulated in XX and XY gonads. To investigate the role of *rpl6y*, we generated a *rpl6y* frameshift mutant using CRISPR/Cas9 gene editing. The external and internal anatomy of the XY *rpl6y* mutant resembled that of a wild-type XX female, confirming that loss of *rpl6y* results in complete male-to-female sex reversal. In addition, we have uncovered a potential regulatory mechanism in which *rpl6x* is downregulated in males and females by a gonad-specific *rpl6x* antisense mRNA transcript, *astra*. We speculate that anoles and most other pleurodonts may use the ribosomal protein encoded by *rpl6y* as part of a translation-based mechanism to determine sex. This would represent a novel sex-determining mechanism, distinct from previously identified vertebrate genetic sex determination systems.

INTRODUCTION

An organism's sex determination system, comprised of sex-specific variation in downstream molecular pathways, tells the developing embryo which sex to become. The accurate and timely initiation of sex determination and gonad differentiation mechanisms is fundamental to species survival and reproductive success (Bachtrog et al., 2014; Bull, 1983; Capel, 2017; Charlesworth, 1996). In vertebrates, primary sex determination is initiated environmentally, via temperature, or genetically, via sex-specific genetic differences on specialized sex chromosomes. Vertebrate sex chromosomes can be homomorphic or heteromorphic, and sex-specific genetic differences can range from a single nucleotide polymorphism, as seen in the Fugu pufferfish (Kamiya et al., 2012) to highly evolved, diverged sex chromosome systems, as seen in mammals and birds (Zhu et al., 2025). Once sex determination is initiated, the bipotential gonad will begin to differentiate into either a testis or an ovary to produce sperm or eggs, respectively (Bachtrog et al., 2014; Capel, 2017). Sex-specific differentiation pathways depend upon the underlying mechanisms of an organism's sex determination system.

In genetic sex determination, the development of sexual characteristics is driven by sex-specific genomic differences of the sex chromosomes, genes, or gene expression. While the underlying genetic mechanisms of gonad differentiation are highly conserved across vertebrates, the genetic initiators of primary sex determination are as diverse as the species themselves, and, to date, very few have been identified (Bachtrog et al., 2014). In some vertebrate

groups, primary sex determination genes evolve rapidly, leading to sex chromosome turnover (Keating et al., 2021; Pinto et al., 2022), while in other groups, primary sex determination genes and their sex chromosome systems are ancient and highly conserved (Cortez et al., 2014; Lahn & Page, 1999). We know a lot about how these mechanisms function in model systems such as mammals and birds (Capel, 2017, 2019; Stöck M et al., 2021), but our knowledge of reptilian sex determination mechanisms remains extremely limited. Unlike mammals and birds, reptile lineages exemplify the diversity of sex determination systems we see across vertebrates, making reptiles a powerful system for studying sex determination. With over 12,000 squamate (lizards and snakes) reptile species (Uetz et al., 2025; reptile-database.org), this group represents an excellent opportunity to more deeply understand vertebrate sex determination biology. Since lizards comprise over half of all squamate species (Uetz et al., 2025; reptile-database.org), uncovering the genetic mechanisms underlying sex determination in these lineages is of high priority. Among these, Pleurodont lizards are ideal for investigating sex determination due to their abundance and the stability of their sex chromosome system.

Pleurodonta represents a species-rich clade of over 1,200 lizard species, where most have maintained a deeply conserved XX/XY sex determination system. Current evidence suggests that this sex chromosome system originated ~100 mya from a single ancestral autosomal pair (Ezaz et al., 2009; Gamble et al., 2014; Marin et al., 2017; Rovatsos, Altmanová, et al., 2014; Rovatsos, Pokorná, et al., 2014). Pleurodont lizards include the family *Anolis,* which is the

largest genus of terrestrial vertebrates (Giovannotti et al., 2017; Nicholson et al., 2012). *Anolis* comprises over 400 lizard species—the result of an ancient adaptive radiation event (Nicholson et al., 2012). Anole lizards have long been used to study convergent evolution (Arbuckle et al., 2014; Huie et al., 2021; Ord et al., 2013), ecology (Losos & Pringle, 2011; Pringle et al., 2019; Schoener & Schoener, 1980), and behavior (Lapiedra et al., 2017, 2018) among other things, with the green anole, *A. carolinensis*, being the first non-avian reptile to have its genome sequenced (Alföldi et al., 2011).

In more recent years, due to advancements in genomic and genetic tools, the brown anole, *A. sagrei*, has become an important model for investigating gene function in squamates (Baeckens et al., 2018; Bock et al., 2021; Geneva et al., 2022; Lapiedra et al., 2018; Rasys et al., 2019; Sanger et al., 2008). The brown anole is a medium-sized, ground-trunk anole native to Cuba and the Bahamas. It is a pervasive invader known for its robust populations and expansive distribution in the southeastern United States, California, and islands in the West Indies and Atlantic and Pacific oceans. As the first reptile to have its genome edited, *A. sagrei* has become a useful model to study developmental genetics and functional genomics (Rasys et al., 2019). In addition, the publication of a highly complete and contiguous XX reference genome and the more recent Y chromosome assembly have made the brown anole an exciting model for studying sex determination biology (Geneva et al., 2022; Chapter 2).

Here, we report a Y-linked ribosomal gene, *rpl6y*, as a primary determinant of sex in *A. sagrei*. Using CRISPR/Cas9 gene editing, we confirmed that loss of

rpl6y results in complete male-to-female sex reversal. Additionally, we report a potential regulatory mechanism in which the X chromosome paralog, *rpl6x,* is downregulated by a gonad-specific *rpl6x* antisense mRNA transcript. We were able to identify *rpl6y* orthologs in additional *Anolis* species and other close relatives and believe that *rpl6y* may initiate male development in over 1,000 pleurodont lizards. Taken together, we hypothesize that anoles and related species may use a translation-based mechanism to determine sex via the ribosomal protein encoded by *rpl6y*. This would represent a novel sex-determining mechanism, distinct from any other previously identified vertebrate sex determination systems.

RESULTS

Initiation of sex determination and gonad differentiation in Anolis

During embryogenesis, sex determination initiates the bipotential gonad to take on a male or female fate. As such, primary sex determination genes are expected to be expressed during the initial phases of gonadal sex differentiation. To assess X and Y gene expression during anole gonad development, RNA-seq was conducted on XX and XY embryonic gonadal tissue at three developmental time points—stages 7, 8, and 9 (staging based on Sanger et al., 2008; Fig. 3.1 A & C). Until stage 8, XX and XY embryonic gonads are morphologically indistinguishable; therefore, we focused our analyses starting at stage 7. Additional libraries were constructed using stage 5 mesonephros (embryonic kidney) tissue to serve as a non-gonadal control (Fig. 3.1 A & B). Differential expression analysis revealed several hundred differentially expressed genes

(DEGs) between the sexes at each gonadal time point. As expected, fewer genes were differentially expressed at embryonic stage 7 than at stages 8 or 9. At stage 7, our analyses identified 1,506 DEGs with more DEGs expressed in our male samples (47% XX-biased, 53% XY-biased). At stage 8, a total of 3,338 DEGs were identified (43% XX-biased, 57% XY-biased), and at stage 9, a total of 2,753 DEGs were identified (54% XX-biased, 46% XY-biased) (Table 3.2).

Among the XY-biased DEGs at stage 7 were collagen genes *col9a1, col9a2, and col9a3,* Desert hedgehog, or *dhh,* and known testis differentiation genes including *sox9, amh,* and *dmrt1* (Table 3.3). In mice, *COL9A* genes are expressed in the Sertoli cells of differentiating testicular cords (McClive & Sinclair, 2003), and *Dhh* is critical for seminiferous tubule development, among other testis-specific functions (Bitgood et al., 1996; Pierucci-Alves et al., 2001). The significant differential expression of these genes, in addition to known male-biased genes, in XY libraries at stage 7 tells us that gonadal sex differentiation is already well underway. For our stage 7 XX libraries, female differentiation genes, *foxl2* and *wnt4,* were identified, among others, as being differentially expressed (Table 3.3). Again, the differential expression of female-biased genes in our XX libraries tells us that, while visually indistinguishable, stage 7 gonads have already adopted a male or female fate. For stages 8 and 9, additional known sex differentiation genes were found to be male and female-biased, including the XX-biased gene, *cyp19a1*, which is tremendously upregulated by stage 8. (Table 3.3). Taken together, our results indicate that sex determination is initiated before stage 7 in *A. sagrei*.

Primary sex determination is not initiated by a known sex determination gene in A. sagrei

Most often, when identifying primary sex determination genes, a few key principles are followed based on what we know from well-studied groups such as mammals and birds. These genes are often ancient, expressed during a critical window of early gonadogenesis, and are conserved across species that share a homologous sex chromosome system (Burgoyne et al., 1988; Koopman et al., 2016). Most Pleurodont lizards, including all iguanas and anoles, share an ancient XX/XY sex determination system that is approximately 100 million years old (Ezaz et al., 2009; Gamble et al., 2014; Lisachov et al., 2017; Marin et al., 2017; Rovatsos, Altmanová, et al., 2014; Rovatsos, Pokorná, et al., 2014). A strong candidate gene for sex determination in *A. sagrei* would also be conserved in related lizard species.

To identify a candidate gene for primary sex determination in *A. sagrei*, we first examined the expression of known sex differentiation genes present on the X and Y sex chromosomes at stage 7. The genes *sox8* and *rspo1* are present on the X and Y sex chromosomes, although the latter appears to be undergoing pseudogenization on the Y. We found evidence that the *rspo1y* open reading frame has been disrupted and is severely truncated (data not shown). Additionally, the genes *amh* and *foxl2* are present on the X chromosome. The sex chromosomes of *A. sagrei* have undergone multiple autosome-to-sex chromosome fusion events, resulting in a mid-sized neo-sex chromosome system (Geneva et al., 2022; Giovannotti et al., 2017; Kichigin et al., 2016). Due

to these fusion events, *sox8, rspo1*, and *amh* are all more recent additions to the sex chromosomes. Under the assumption that a primary sex determination gene would be ancient and shared across pleurodonts, these newly added genes are unlikely candidates. Additionally, we examined the expression profiles of these genes to further rule them out. At stage 7, *sox8y* and *rspo1y* have minimal expression in XY gonads in addition to *rspo1y's* disrupted open reading frame. *sox8x* and *rspo1x* are not differentially expressed until stage 9, indicating they function during a later stage of gonad differentiation and not primary initiation. *amhy* has been lost on the Y chromosome, but *amhx* has XY-biased expression at stage 7. As *amh* is known to play a role in testis differentiation, it is an unlikely X-dosage candidate for primary sex determination. early stages of gonadogenesis, all the above known sex determination genes were ruled out as candidates for primary sex determination.

Analysis of ancient Y chromosome genes reveals rpl6y as a candidate for sex determination in A. sagrei

As sex chromosomes evolve and recombination is suppressed, Y chromosomes often degenerate and lose genes. Genes retained on the Y are often critical for male-specific functions, such as primary sex determination or spermatogenesis, or are retained because they are dosage sensitive and critical for maintaining equivalent expression between the sexes.

A recent assembly of the *A. sagrei* Y chromosome revealed that only 5 genes remain in the most ancient region of the Y chromosome (Chapter 2). The

most ancient regions of the X and Y are homologous across more than 1,200 Pleurodont lizard species (Gamble et al., 2014; Rovatsos, Altmanová, et al., 2014; Rovatsos, Pokorná, et al., 2014), making genes in this region especially exciting to examine for primary sex determination candidates. We investigated the expression of the 5 ancient Y genes, *rsph14y, ccdc74by, gnazy, ube2l3y,* and *rpl6y* in our stage 7 XY RNA-seq libraries. Additionally, we determined whether an X chromosome paralog exists and, if present, calculated the percent protein sequence identity between the paralogs. If a Y protein coding gene has evolved a new function, i.e., sex determination initiation, we might expect amino acid changes to have accumulated between the paralogs. Lastly, we looked for evidence of gene conservation in 11 other Pleurodont species. Given that the XX/XY system is shared among nearly all pleurodont lizards, we believe the sex determination gene of *A. sagrei* is likely to be conserved in the more than 1,200 other species that share the homologous XX/XY system.

rsph14y (Radial Spoke Head 14 Homolog) is known to play a role in sperm motility (Roderick et al., 1974; Zhang et al., 2022) and, in *A. sagrei*, has lost its X paralog. Although conserved across related species, there is minimal evidence of expression in embryonic stage 7 XY gonads (0.1 TPM) (Table 3.4). This gene likely plays a role in *Anolis* spermatogenesis later in development. *ccdc74by* (coiled-coil domain containing 74B) is associated with protein binding (Kawai et al., 2001; Eom et al., 2024). We found that, while the Y protein has significantly diverged from the X paralog (X/Y protein identity = 76%), *ccdc74by* shows minimal evidence of expression in XY gonads (0.2 TPM) and is not

conserved in related species. (Table 3.4). *gnazy* (G protein subunit alpha z) codes for a protein thought to be involved in G-protein-mediated signaling (Roderick et al., 1974; Adams et al., 2024). It has a high amino acid sequence identity (X/Y protein identity = 96%) with its X paralog and shows minimal evidence of expression (0.04 TPM) at stage 7 (Table 3.4). *ube2l3y* (ubiquitin-conjugating enzyme E2L 3), which codes for an enzyme that plays a role in the ubiquitination process (Matuschewski et al., 1996; Mishra et al., 2023), shows weak expression at stage 7 (16 TPM). By comparison, *rpl6y* (ribosomal protein L6), which codes for a core protein component of the ribosome and plays a role in DNA damage response (Roderick et al., 1974; Yang et al., 2019; Zhang et al., 2022), shows strong expression (Table 3.4). In vertebrates, both *ube2l3y* and *rpl6y* are known to be broadly expressed across tissues (human protein atlas), with ancestral protein function critical for cellular processes. We identified X chromosome paralogs for both genes and calculated X/Y protein identity to determine whether their protein function has potentially diverged. The UBE2L3X amino acid sequence is identical to UBE2L3Y (X/Y protein identity = 100%; Table 3.4). When compared to human UBE2L3, no amino acid changes were observed, suggesting *ube2l3y* may be retained due to dosage sensitivity. In contrast, when RPL6X and RPL6Y protein sequences were compared, we found them to be significantly diverged (X/Y protein identity = 70%; Table 3.4). When compared to human RPL6, we found that RPL6Y has undergone much more amino acid sequence divergence than RPL6X (*A sagrei* RPL6Y protein identity to human RPL6Y = 59%; *A. sagrei* RPL6X protein identity to human RPL6 = 72%;

Table 3.4). This finding suggests that the RPL6Y protein function may have diverged from its X counterpart. Based on these lines of evidence, we identified *rpl6y* as a strong candidate for male sex determination in *A. sagrei*.

Protein evolution and mRNA expression reveal key differences between rpl6x and rpl6y

Using the complete coding sequences of *rpl6x* and *rpl6y* identified from 11 XY Pleurodont lizard genomes, we constructed a protein sequence tree to better understand RPL6X and RPL6Y protein evolution. Included in our analysis are genomes from 3 Pleurodont families—*Dactyloidae* (5 species; Fig. 3.2), *Iguanidae* (2 species; Fig. 3.2), and *Phrynosomatidae* (4 species; Fig. 3.2). Our results show that among pleurodonts, RPL6Y (Fig. 3.2, bottom) is diverging much faster than RPL6X (Fig. 3.2, top). Shorter branch lengths indicate that RPL6X has undergone much less amino acid divergence in the same amount of time (Fig. 3.2, bottom). These results further support different levels of functional constraint between *rpl6x* and *rpl6y*.

In *Anolis*, as in other amniotes, the embryonic gonad develops as a long, thin genital ridge atop the mesonephros, or embryonic kidney (Fig. 3.1). The gonadal ridge is formed by stage 5 and condenses into a round gonad during differentiation (Fig. 3.1). We quantified *rpl6y* expression using transcriptome data from stages 7, 8, and 9 XY gonads, and stage 5 XY mesonephroi (Fig. 3.1). In the embryonic gonads, *rpl6y* is strongly upregulated compared to the mesonephroi. *rpl6y* is most strongly expressed at stage 7 (Mean=116 TPM, SD 12.3), and tapers downward in stages 8 (Mean=109 TPM, SD 30.4) and 9

(Mean=61, SD 13.8) as testis differentiation proceeds. In comparison, stage 5 mesonephroi have a mean *rpl6y* expression of 10 TPM (SD 10) (Fig. 3.3A).

We next wanted to assess *rpl6x* expression in males and females. Overall, *rpl6x* is more highly expressed than *rpl6y* in all XY tissues examined (Fig. 3.3B and data not shown). Surprisingly, we found that *rpl6x* is significantly downregulated in XX and XY gonadal samples by approximately 2-fold compared to the non-gonadal mesonephroi (Fig. 3.3B). In XY gonads, the relative amounts of *rpl6x* are 6-7X more than *rpl6y,* but strikingly, the relative amounts of *rpl6x* are 144X more than *rpl6y* in XY mesonephroi (Fig. 3.3B). As *rpl6x* is downregulated in XX and XY gonads, *rpl6y* is upregulated in XY gonads. This is opposite to XY non-gonadal tissues where expression of *rpl6x* remains high and *rpl6y* remains low (Fig. 3.3 A & B). Additionally, *rpl6x* is differentially expressed (XX-biased) in our gonad libraries (Fig. 3.3B).

Discovery of astra—an Anti-sense transcript for rpl6x in Anolis

Ribosomal proteins are essential components of ribosome biogenesis, a process linked to cell growth and division and often have additional functions beyond protein translation (Yang et al., 2019). RPL6 is a core protein component of the 60S large ribosomal subunit and has been implicated in DNA damage repair in humans (Yang et al., 2019). Thus, the ~2-fold downregulation of *rpl6x* in both XX and XY gonads of *A. sagrei* might have important functional consequences and warrants further investigation. Aligning XX and XY embryonic gonad RNA-seq data to the *A. sagrei* reference genome revealed evidence of a highly expressed anti-sense RNA transcript complementary to *rpl6x* on the X

chromosome. We named this transcript *Anti-sense transcript for rpl6x in Anolis*, or *astra*. The protein-coding gene*, ptpn11,* sits to the 5' side of *rpl6x* in a head-to-head orientation and is transcribed in the opposite direction. Initiated from the 3' side of *rpl6x*, the antisense transcript, *astra,* is transcribed in male and female embryonic gonads. We discovered that *astra* is part of a *ptpn11* mRNA isoform consisting of alternative 5' untranslated region (UTR) exons and is produced from an alternative, gonad-specific *ptpn11* promoter (Fig. 3.4). In other tissues, *ptpn11* is transcribed from a different promoter and does not produce *astra* transcripts. Based on RNA-seq data from various tissues, including eye, skin, heart, liver, limbs, brain, mesonephroi, and stage 4 whole embryos, we conclude that *astra* is gonad-specific, with minimal expression detected in other tissues (Fig. 3.5 A, B; data not shown).

Next, we investigated whether the *rpl6x* anti-sense transcript is conserved in related species. Using a recently generated *A. carolinensis* XY genome (Faircloth et al., unpublished) along with published RNA-seq data from stage 6 *A. carolinensis* embryos, we compared *astra* structure between *A. sagrei* and *A. carolinensis.* Although no conserved reading frame was found within the *astra* exons, the 5' UTR splice sites were perfectly conserved (Fig. 3.6), confirming *astra* expression in the green anole. Given the estimated 40 million years of divergence between *A. sagrei* and *A. carolinensis*, our findings suggest that *astra* has been conserved for at least that long. Additionally, we searched for *astra* transcripts in published RNA-seq datasets from bearded dragon (*Pogona vitticeps*) embryonic gonads, a non-pleurodont lizard with a ZZ/ZW sex

chromosome system (Wagner et al., 2023). Since *astra* was not detected, we hypothesize that *rpl6x* downregulation in the gonads is driven by *astra* expression in *Anolis* and potentially other Pleurodont lizards (Fig. 3.5 B; Fig. 3.7).

Based on these findings, we propose a novel genetic sex determination mechanism in *A. sagrei* where initiation of testis differentiation by *rpl6y* depends on the prior downregulation of *rpl6x* (Fig. 3.7). In our model, *astra,* produced from the gonad specific *ptpn11* promoter, downregulates *rpl6x* expression in both XX and XY gonads, preparing the system for sex determination. The subsequent upregulation of *rpl6y* in XY gonads then initiates male sex determination and drives testis differentiation (Fig. 3.7).

Loss of rpl6y results in complete male-to-female sex reversal in Anolis sagrei

To test whether *rpl6y* acts as the primary sex determining gene in *A. sagrei*, we disrupted its open reading frame. To generate out-of-frame mutations, we targeted the second coding exon (exon 3) of *rpl6y* using CRISPR-mediated gene editing (Table 3.1). Our initial efforts yielded a single *rpl6y* XY mutant that underwent complete male-to-female sex reversal (Fig. 3.8, left). Sanger sequencing identified a -32bp deletion that fully disrupted the open reading frame (Fig. 3.8, right). Two additional in-frame mutants generated from our initial efforts did not undergo sex reversal (data not shown). The external and internal anatomy of the *rpl6y* mutant XY female closely resembled that of a wild-type XX female. The mutant was raised to adulthood (6 months), after which detailed phenotypic analyses were conducted (Fig. 3.9, Fig. 3.10). For comparison, 3 wildtype XY males and 3 wildtype XX females were also characterized.

Male and female wildtype brown anoles exhibit clear sexual dimorphism in several external traits. Males have a longer, bulkier body and a large, colorful dewlap used in male-specific behaviors. They can weigh over 6g and reach an adult body length of approximately 5-6cm (nose to the base of the tail). Below the cloacal opening, males have two enlarged post anal scales. In contrast, females typically weigh less than 3g and measure around 4-5cm, have a much smaller dewlap, and lack post anal scales. Males and females also exhibit distinct differences in dorsal (back) pigmentation patterns.

Female anoles can have either a “diamond-back” or a “chevron-back” pigmentation pattern, whereas male anoles always have a chevron-back pattern, regardless of their underlying genotype (Fig. 3.9C). This sexual dimorphism is influenced by the gene *CCDC170,* which sits adjacent to and is co-expressed with the gene *Estrogen receptor 1.* Feiner et al., 2022 demonstrated that a female-limited polymorphism regulates the diamond-back pattern in females. The diamond-back pattern ranges from well-defined diamonds to a broad stripe, also referred to as “bar”. The striking physical differences between males and females were documented for the *rpl6y* XY mutant female and wild-type controls.

Overall, the external morphology of the *rpl6y* XY mutant female strongly resembles that of wild-type control females across all listed sexually dimorphic traits. Our analyses show that the *rpl6y* XY mutant female’s weight (2.3g) and body length (4.0cm) more closely resemble those of wildtype female controls (mean weight=2.9g, SD=0.6g; mean length=4.4cm, SD=0.4cm) than wildtype male controls (mean weight =6.0g, SD0.8g; mean length =5.6cm, SD=0.2cm)

(Fig. 3.9 A, B). Wildtype controls were ~6-7 months old when characterized. Similarly, the mutant's dewlap length (1.3cm) and width (0.6cm) more closely resemble those of wildtype females (mean length =1.0cm, SD=0.1cm; mean width=0.5cm, SD=0.1cm) than wildtype males (mean length =2.0cm, SD=0.2cm; mean width=1.3cm, SD=0.0cm) (Fig. 3.9 D). Notably, the *rpl6y* XY mutant female has a prominent diamond/bar-back pattern and lacks post anal scales, both characteristic of wild-type females (Fig. 3.9 C, E). Taken together, these findings indicate that the external morphology of the XY mutant is extremely XX female-like.

To further assess the completeness of the XY sex reversal, we examined the internal reproductive anatomies of the mutant alongside wildtype XX females and XY males. We began by examining the reproductive anatomy of wildtype XY males. Male anoles possess paired testes, epididymides, and vasa deferentia. The vasa deferentia extend caudally, connecting to the paired hemipenes and the cloaca (Fig. 3.10, left). The male reproductive tract is responsible for producing sperm and testosterone, storing sperm, and transporting sperm during mating. Next, we examined the reproductive anatomy of wild-type XX females. Female anoles possess paired ovaries, infundibula, and both glandular and non-glandular uteri. The non-glandular uteri connect caudally to the paired hemiclitores and the cloaca (Fig. 3.10, right). The female reproductive tract is responsible for oocyte development and the production of female hormones such as estrogen. The *Anolis* ovaries consist of developing follicles, and once the oocytes within each follicle mature and are fertilized, the infundibula guide these

fertilized oocytes into the glandular uteri (GU). The GU are thick, elongated tubes where young eggs continue to develop. The non-glandular uteri (NGU) are shorter, muscular tubes with heterogeneous morphology along their length. Kircher and colleagues describe the posterior portion of the NGU as a “cervix” and the anterior portion as a “vagina”, based on similarities to mammalian reproductive tracts. Additionally, females can store sperm within isolated lumens of the NGU (Kircher, Liu, et al., 2024; Kircher, McCown MA, et al., 2024; Kircher, Stanley EL, et al., 2024; Weberling et al., 2025). Finally, we examined the reproductive anatomy of the *rpl6y* XY mutant female. Consistent with female-like external morphology extern, internal anatomy of the *rpl6y* XY mutant female closely resembled that of a wildtype female, with well-developed ovaries, yolky oocytes, infundibula, and uteri. Based on both external and internal observations, we conclude that loss of *rpl6y* function results in complete XY male-to-female sex reversal in *A. sagrei.* To further support and extend these findings, we performed histological analysis of the *rpl6y* mutant reproductive tract alongside wild-type controls.

To investigate the sex reversal phenotype at the cellular level, we performed Hematoxylin and Eosin (H&E) staining on the reproductive tracts of the *rpl6y* XY mutant and wild-type XX and XY controls. In wildtype XY males, cross sections of the testis reveal seminiferous tubules where spermatogenesis occurs. Within the outer tubule layers, spermatogonia and primary and secondary spermatocytes—the precursors to mature sperm—are visible. Sertoli cells, which support developing sperm, are found within the germinal epithelium.

Adjacent to these, dense rows of spermatids (immature sperm) await spermiogenesis. At the center of the tubules lies the lumen and mature spermatozoa. Outside of the tubules, Leydig cells are responsible for producing male-specific androgens are present. Sections of the epididymis and vas deferens show masses of mature sperm cells surrounded by epithelial tissue (Fig. 3.11 A). In wildtype XX females, cross sections of the ovary reveal developing follicles. The germ cell, or oocyte, sits centrally, surrounded by a layer of granulosa cells within the developing antrum. Granulosa cells are essential for follicle growth and hormone production. Surrounding these, along the outer layer, are theca cells, which support the follicle structure and produce female-specific androgens. Sections of the infundibulum show a highly ciliated epithelium. In the glandular uterus, histological sections reveal a muscular lumen patterned with epithelial ducts and acinar structures. Sections of the non-glandular uterus display folded, ciliated epithelium (Fig. 3.11 C). Histological analysis of the *rpl6y* mutant XY female revealed a striking resemblance to wild-type XX tissue samples. Most notably, ovary sections showed a developing oocyte with a visible germinal vesicle—the oocyte's nucleus (Fig. 3.11 B). Due to the estimated age of the *Anolis* XX/XY system and the high divergence between the X and Y sex chromosomes, we anticipated that complete sex reversal would likely result in sterility. Although we did not attempt to breed the mutant, based on the morphology and histology of its reproductive tract, we believe *rpl6y* sex-reversed lizards may retain fertility. To gain deeper insight into the molecular basis of this

phenotype, we investigated the cellular localization pattern of *astra* in XY *A. sagrei* gonads.

astra and amh are colocalized in embryonic XY A. sagrei gonads

The cellular localization patterns of *astra* and *amh* were visualized using HCR RNA-FISH. Preliminary results from a stage 6 XY gonad show that *astra* expression colocalizes with *amh* (Fig. 3.12). Since *amh* is known to be expressed in the somatic cells of the XY gonad in other systems (Gao et al., 2024), we hypothesize that both *amh* and *astra* are expressed in somatic cells in *Anolis*.

DISCUSSION

Sex determination initiation and the downstream molecular mechanisms of gonad differentiation are essential for maintaining two sexes and, therefore, species survival (Bachtrog et al., 2014). However, our current understanding of the genes that initiate these pathways is highly limited, with most known examples falling into a narrow group of transcription factors and signaling molecules—the so-called “usual suspects” (Bertho et al., 2021). This limited framework constrains our ability to identify novel sex-determining genes in other vertebrate systems. The work presented here fundamentally changes our understanding of vertebrate sex determination initiation mechanisms. This study is the first to functionally identify a primary sex determination gene in a reptile and the first to implicate a ribosomal protein gene, *rpl6y*, as a primary initiator of sex determination in vertebrates.

Using transcriptomic, genomic, and molecular approaches, we identified a novel sex determination mechanism in *Anolis*. Furthermore, we propose that this mechanism is conserved across more than 1,200 Pleurodont lizard species (Gamble et al., 2014; Rovatsos, Altmanová, et al., 2014; Rovatsos, Pokorná, et al., 2014). We hypothesize that the antisense transcript *astra* downregulates *rpl6x* expression in both XX and XY embryonic gonads, in preparation for the subsequent upregulation of *rpl6y* in XY gonads. Our results show that loss of *rpl6y* function results in complete male-to-female sex reversal in an XY individual, demonstrating that *rpl6y* is required for male sex determination in *A. sagrei*. Although the identification of *rpl6y* as a primary sex determination gene may be unexpected, it aligns with many of the key characteristics typically associated with primary initiators such as *SRY*. *rpl6y* is an ancient and deeply conserved Y-linked gene among Pleurodont species. We found that *rpl6y* is highly expressed in XY gonads during a critical window of early development, and its loss of function leads to complete sex reversal. While *rpl6y* is not a “usual suspect”, its discovery followed a similar pattern to other known primary sex determination genes (Ford et al., 1959). Although *rpl6y* meets the traditional criteria for a primary sex determinant, it is neither a transcription factor nor a signaling molecule, raising the key question: how does a ribosomal protein initiate sex determination and drive testis development?

rpl6y encodes a highly diverged version of RPL6, a core protein component of the 60S large ribosomal subunit. *RPL6* is essential for protein synthesis and has been implicated in DNA damage repair (Yang et al., 2019), cell

cycle regulation (Zhang et al., 2022), cancer development (Zhang et al., 2022), Parkinson's disease (Anirudhan et al., 2021), and p53 pathway regulation (Bai et al., 2014). Here, we present the first evidence of its involvement in primary sex determination. In *A. sagrei* and other Pleurodonts, we propose that *rpl6y* initiates sex determination through a translation-based mechanism involving ribosomal heterogeneity.

Ribosomes can exhibit heterogeneity, differing in composition or function within cells, across tissues, and even between sexes (Genuth & Barna, 2018b, 2018a; D. Li & Wang, 2020). Emerging evidence suggests ribosomal heterogeneity is more prevalent than previously thought (D. Li & Wang, 2020). Tissue-specific ribosomal protein isoforms may modify ribosomes in a cell-type-specific manner, potentially influencing transcript-specific translation (Genuth & Barna, 2018b, 2018a). Ribosomal heterogeneity can be driven by differences in ribosomal protein composition, resulting in specialized ribosomes that influence gene expression through the preferential translation of specific mRNAs (Xue & Barna, 2012). The discovery of sex-specific ribosome heterogeneity adds complexity to our understanding of gene expression regulation and highlights its potential role in driving sex-specific differences and contributing to sex determination. Sex-specific ribosomal heterogeneity has been documented in several species, including zebra finch (Tang & Wade, 2010) , mice (H. Li et al., 2022), zebrafish (Moser et al., 2025; Shah et al., 2024), and *Drosophila melanogaster* (Hopes et al., 2022). Our discovery of gonad-specific *rpl6x* downregulation and male-specific *rpl6y* upregulation provides evidence of sex-

specific ribosome heterogeneity in *Anolis.* In addition to our findings, we observed that at stages 7, 8, and 9, approximately 6% of XY-biased gonad genes encode ribosomal proteins compared to approximately 0.04% of XX-biased gonad genes. This stark difference further highlights the presence of abundant ribosomal heterogeneity during embryonic gonad development and warrants further investigation. Additionally, we plan to investigate the role of *astra* in *rpl6x* downregulation through CRISPR-mediated approaches, aiming to further elucidate this novel genetic sex determination mechanism.

CONCLUSION

With over 12,000 squamate species, including nearly 8,000 lizards in the Sauria clade (Uetz et al., 2025; reptile-database.org), reptiles represent a significant gap in our understanding of sex determination and gonad differentiation mechanisms. Our discovery of a novel sex determination mechanism driven by a Y-linked ribosomal gene challenges the classical definition of a sex determination gene. Our findings fundamentally reshape our understanding of the molecular mechanisms that drive sex determination initiation. In sex determination biology, we often ask: what makes a good sex determination gene, and what lends such a gene the ability to persist for millions of years? The longevity of *rpl6y* as a conserved primary sex determination gene is comparable to that of *Sry* in mammals and *DMRT1* in birds. Due to evolutionary constraints, a sex determination gene tied to one of the cell's most fundamental processes is unlikely to be lost. Therefore, the persistence of *rpl6y* is likely driven by its essential role in protein synthesis, alongside its function in

male sex determination. While *rpl6y* may seem like an “unusual suspect”, we believe it is one of many waiting to be discovered (Bertho et al., 2021). To better understand sex determination mechanisms across vertebrates, we must remain open to unconventional possibilities and answers. In short, key regulators of sex determination likely remain undiscovered due to our limited knowledge of how these mechanisms work in more diverse species. Our study lays the groundwork for exploring the complex nuances of vertebrate sex determination, with a focus on identifying other ribosomal proteins that may play a role.

MATERIALS AND METHODS

Lizard breeding colony and surgical animals

For this work, adult lizards were obtained from Orlando and Miami, Florida. Animals were housed at our UGA facility (Athens, GA) in harem breeding cages of 5-7 females and 1 male. Eggs were collected weekly and kept at room temperature (~26°C) until dissection. Animal care, handling, and use strictly adhered to IACUC Animal Use Protocol #A2023-11-007-A9.

Tissue collection for RNA-sequencing

To collect tissue for sex genotyping and RNA sequencing, eggs were dissected in 1X Phosphate-Buffered Saline (PBS) solution (137mM NaCl, 10mM Na_2PO_4, 2.7mM KCl, 2mM KH_2PO_4). Embryos were staged using the *Anolis* Staging Series (Sanger et al., 2008). For our analyses, stage 5, 7, 8, and 9 embryos were collected. The head of each embryo was collected for DNA extraction and sex genotyping by PCR (see DNA extraction). Embryos were

opened, and the mesonephroi and attached gonadal ridges were dissected out. Stage 8 and 9 samples were then sex phenotyped visually based on gonad morphology before further dissection. Due to the small size of the stage 5 gonadal ridge, the gonadal ridge and a portion of the attached mesonephros tissue were collected (M+GR samples) for RNA-sequencing. Cuts were made across the mesonephroi above and below the gonadal ridges (Fig. 3.1). Tissue was placed in 200µL of Ambion RNAqueous® Micro Kit lysis buffer (Invitrogen; Waltham, MA), disrupted with a motorized homogenizer, and stored at -80°C until RNA extraction. Identical samples of mesonephroi tissue with the gonadal ridges dissected off were also collected for stage 5 (M samples; figure 3.1) and prepared for RNA extraction with the above protocol. For stages 7, 8, and 9, gonadal ridges were carefully removed from the mesonephroi (Fig. 3.1), placed in 30µL of Ambion RNAqueous® Micro Kit lysis buffer (Invitrogen; Waltham, MA), and stored at -80°C until RNA extraction and library preparation. For stage 5, 20 pairs of mesonephros with or without gonadal ridges were separately collected from individual embryos to make 20 RNA libraries (5 libraries per sex per sample type, M or M+GR). For stages 7-9, 90 pairs of gonads were collected to make 30 pooled RNA libraries (5 libraries per sex per stage, with 3 pairs of stage and sex-matched gonads per pooled per library).

DNA extraction

For DNA extraction, samples were placed in 500µL of DNA lysis buffer (100mM Tris, 5mM EDTA, 0.2% SDS, 200mM NaCl, pH 8.5) and 2.5µL of Proteinase K (ThermoFisher; Waltham, MA) and incubated at 55°C for 24 hours to digest

tissue for DNA extraction. Next, samples were centrifuged at 15,000rpm for 10 minutes, then 300-500μL of isopropanol was added to precipitate out DNA. To pellet the DNA, samples were centrifuged at 15,0000rpm for 10 minutes. Supernatant was removed, 200μL of 70% EtOH was added, and samples were spun at 15,000rpm for 5 minutes. EtOH was removed, and DNA pellets were dried for 5-10 minutes. Next, 500μL of TE buffer (10mM Tris-HCl, 1mM EDTA, pH 8.0) was added, and samples were incubated at 55°C for 1 hour. Samples were vigorously vortexed, and DNA concentration was checked via Nanodrop (ThermoFisher; Waltham, MA). DNA was stored at -20°C until sex genotyping by PCR.

Sex genotyping by PCR

To determine the sex of embryonic samples, PCR sex genotyping was performed using *Anolis*-specific primers, *kank1* and *gnaz* (Geneva, Gamble and Zarkower 2014; Table 3.1). *kank1,* an autosomal marker, is present in both XX and XY animals. *gnaz,* a Y chromosome-specific marker, is present only in XY lizards. In this PCR assay, XX samples have 1 band present, and XY samples have 2 bands present. PCR solution contained DreamTaq PCR Master Mix (Thermo Scientific; Waltham, MA), nuclease-free water, and primers. PCR conditions were as follows: 95°C for 2 mins, 35 cycles of 95°C for 30 secs/ 58°C for 30 secs/ 72°C for 30 secs, and 72°C for 2 mins. Due to a lack of sex-specific morphology at stages 5 and 7, visual phenotyping of gonads cannot be performed, and these samples were only sex genotyped by PCR. For stages 8 and 9 samples, if there

was a mismatch between visual phenotype and PCR genotype, the samples were not used for RNA-sequencing.

RNA extraction for library preparation

In preparation for RNA-sequencing, total RNA was extracted from each sample using the Ambion RNAqueous® Micro Kit (Invitrogen; Waltham, MA) as instructed by the manufacturer. Samples were eluted two times in 10μL of 75°C nuclease-free water. For stage 5, mesonephroi with and without gonads from single embryos were extracted. For stages 7-9, three pairs of stage and sex matched gonads were pooled together before RNA extraction to ensure adequate amounts of total RNA for sequencing. RNA quantification was done using the High Sensitivity RNA Qubit kit (Invitrogen; Waltham, MA). Extracted RNA was kept on ice until quantification was complete. Library preparation immediately followed.

RNA-Sequencing

RNA-seq libraries were constructed in-house using the Illumina® Stranded mRNA Prep kit (San Diego, CA) according to the manufacturer's protocol with minor changes. For stage 5 libraries, a starting total RNA concentration of 150ng was used, and libraries were amplified using 17 PCR cycles. A total of 20 stage 5 libraries were made: 5 XX M+GR, 5 XX M, 5 XY M+GR, 5 XY M. For stages 7-9, a starting total RNA concentration of 50ng was used, and libraries were amplified using 18 PCR cycles. A total of 30 libraries were made for stages 7, 8, and 9: 5 XX and 5 XY pooled libraries per stage.

NEBNext® Purification Beads (New England Biolabs; Ipswich, MA) were used for bead cleanup throughout the protocol. Finally, indexed libraries were pooled and underwent 50 bp paired-end sequencing at the Georgia Genomics and Bioinformatics Core (GGBC). Libraries were sequenced on either a P2 or P3 flow cell on the NextSeq2000 (Illumina; San Diego, CA).

Differential gene expression analysis

All RNA-seq raw reads were assessed for quality using FastQC (v.0.11.5; Andrews, 2010) and then mapped to the AnoSag2.1_PGA_Y genome assembly (Chapter 2) using HISAT2 (v. 2.2.1-gompi-2022a; Kim et al., 2019) and SAMtools (v. 0.1.20-GCC-11.2.0; H. Li et al., 2009). Read summarization was performed with featureCounts (v. 2.16.1; Liao et al., 2014), and differential gene expression analyses were performed using DESeq2 (v. 1.42.1; Love et al., 2014). Normalized read counts were converted into transcripts per million (TPM). To refine our results, DEGs were filtered for p-adjusted value of < 0.01, baseMean > 30, and a fold change of > 1.5. Due to genotyping or staging pooling errors, libraries 7-2 XY, 7-3 XX, and 8-3 XX were excluded from further analyses based on gene expression patterns of known sex determination genes.

To identify a candidate for sex determination, we examined the mRNA expression profiles of known sex determining genes and ancient Y chromosome genes (Marin et al., 2017; Chapter 2). To examine the expression patterns of known male (*amh, dmrt1,* and *sox9*) or female-biased (*foxl2, cyp19a1,* and *wnt4*) sex determination genes across developmental stages, transcripts per million were plotted using GGPlot2 (v.3.5.2; Wickham, 2016; data not shown). A similar

approach was used for ancient Y chromosome genes (*rpl6y, ube2l3y, ccdc74by, gnazy,* and *rsph14y*) and their X paralogs (Table 3.2; data not shown). Once *rpl6y*, *rpl6x*, and *astra* were identified, expression was analyzed as above.

X/Y protein sequence identity analysis of ancient Y genes

X/Y protein sequence identity analysis was performed for ancient Y genes with X paralogs (*rpl6y, ube2l3y, ccdc74by,* and *gnazy*). The protein sequences were aligned and compared in Geneious Prime 2025.2.1 (https://www.geneious.com).

Comparative analyses of *rpl6y* in pleurodont lizards

To analyze *rpl6y* protein evolution across pleurodont lizards, we used BLAST to identify *rpl6x* and *rpl6y* orthologs in 11 other pleurodont lizard XY genomes. To further examine divergence patterns of *rpl6x* and *rpl6y* in related species, protein evolution analyses were conducted in MEGA12 (version 12.0.11; Kumar et al., 2024; Stecher et al., 2020). The phylogeny was inferred using the Maximum Likelihood method and Jones-Taylor-Thornton (1992) model (Jones et al., 1992) of amino acid substitutions and the tree with the highest log likelihood is shown. The percentage of replicate trees in which the associated taxa clustered together (1,000 replicates) is shown next to the branches (Felsenstein, 1985). The initial tree for the heuristic search was selected by choosing the tree with the superior log-likelihood between a Neighbor-Joining (NJ) tree (Saitou & Nei, 1987) and a Maximum Parsimony (MP) tree. The NJ tree was generated using a matrix of pairwise distances computed using the p-distance (Nei &

Kumar, 2000). The MP tree had the shortest length among 10 MP tree searches; each performed with a randomly generated starting tree. The analytical procedure encompassed 23 protein sequences with 259 positions in the final dataset.

CRISPR gene editing surgeries

To assess the *rpl6y* gene function in *Anolis*, CRISPR-Cas9-mediated gene editing surgeries were performed on 78 adult female lizards. Animal handling, surgeries, solution preparation, and screening were done per the Lizard Gene-Editing Handbook (Public Version 1.0, 2021; adapted from Rasys et al., 2019 published protocol) and IACUC Animal Use Protocol #A2023-11-007-A9. Three CRISPR sgRNA guides were used (Table 3.1) to make a 10μM RNP solution for oocyte injection. CRISPR guides were designed using CRISPOR (Concordet & Haeussler, 2018; UCSC). Per animal, 1-6 follicles were injected with ~1-3 μL per follicle. Before use in surgery, RNPs were tested for cutting efficiency in vitro (Lizard Gene Editing Handbook, Public Version 1.0, 2021; IDT Alt-R™ CRISPR_Cas9 System Protocol, 2017). At room temperature, we combined 1μL 10X nuclease reaction buffer (IDT; Coralville, IA), 1μL of 10μM RNP, 1μL of 250nM XY DNA substrate (PCR amplified for *rpl6y* target region and purified using GeneJET PCR Purification Kit; Thermo Scientific; Waltham, MA), and 7μL of nuclease free water, and incubated at 37°C for 1 hour. Next, 1μL of 20mg/mL Proteinase K (ThermoFisher; Waltham, MA) was added to the reaction and incubated at 56°C for 10 minutes. The digested product was visualized by

agarose gel electrophoresis. From surgeries, 148 eggs were collected and incubated at 28°C until hatching.

Sanger sequencing and confirmation of mutants

Upon hatching, tail clips were taken, DNA was extracted (see DNA extraction above), and sex genotyping PCR was performed (see Sex genotyping by PCR above). XX hatchlings were humanely euthanized via Tricaine injection (IACUC Animal Use Protocol #A2023-11-007-A9) or kept as wildtype controls. *rpl6y* genotyping PCR was performed for XY hatchlings using different combinations of *rpl6y* primers (Table 3.1) and the above protocol. The remaining PCR product was purified with the GeneJET PCR Purification Kit (Thermo Scientific; Waltham, MA) and sent for Sanger sequencing (GENEWIZ, South Plainfield, NJ). Sequencing data was aligned and viewed using Geneious Prime 2025.2.1 (https://www.geneious.com). Wildtype XY hatchlings were euthanized or kept as controls. *rpl6y* XY mutants were raised to adulthood for further analyses.

Phenotypic analysis of the rpl6y XY mutant female

External phenotypes of the *rpl6y* XY mutant female and 3 wildtype males and females were examined. Animals were lightly anesthetized (Lizard Gene Editing Handbook, Public Version 1.0, 2021), and photographs were taken using a Canon EOS RP camera and a Canon 35mm lens (Canon; Ota City, Tokyo, Japan). First, lizards were weighed in grams. Next, body length was measured from the nose tip to the base of the tail. Lastly, we measured dewlap length at the attachment points and width at the widest part during full extension. Dorsal and

ventral photos of each lizard were taken in addition to pictures of their back pattern phenotype and dewlap size. Post anal scale morphology was photographed on a Zeiss steREO Discovery.V12 microscope with a Zeiss Axiocam MRc5 (Oberkochen, Germany) camera attachment using a 1.0x lens. Lizards were subsequently euthanized to examine internal reproductive anatomy. Lizards were opened, and reproductive tracts were dissected out and placed in 1X PBS (137mM NaCl, 10mM Na_2PO_4, 2.7mM KCl, 2mM KH_2PO_4) for imaging. Reproductive tracts were imaged on a Zeiss steREO Discovery.V12 microscope with a Zeiss Axiocam MRc5 (Oberkochen, Germany) camera attachment using a 0.63x lens. After imaging, the paired reproductive tracts were separated and fixed overnight in Bouin's fixative (Poly Sciences; Warrington, PA). Samples were washed 3x in 1X PBS (137mM NaCl, 10mM Na_2PO_4, 2.7mM KCl, 2mM KH_2PO_4) for 5 mins, and dehydrated in EtOH (1x in 20%, 1x in 50%, 1x in 80%, and 2x in 100%) for 10 mins each. Samples were stored at room temperature until paraffin sectioning.

Histological analysis of the *rpl6y* XY mutant female

Reproductive tract samples were prepped for paraffin sectioning and histology to examine reproductive anatomy at a cellular level. Samples were washed 2x with 100% EtOH for 10 mins each and then transitioned into 100% Xylene (Fisher Chemical; Waltham, MA). The Xylene was replaced with fresh paraffin wax, and samples were incubated at 65°C for 1 hour. The paraffin wax was removed, replaced with fresh wax, and incubated overnight at 65°C. The next day, the paraffin wax was changed once more, and samples were incubated

at 65°C for 1 hour. Samples were embedded in sectioning molds with fresh paraffin wax and allowed to set overnight. Embedded samples were carved and mounted for sectioning. Samples were sectioned at 10μm on a Leica RM2155 microtome. Sections were placed into a preheated water bath and affixed onto slides. A subset of slides was chosen for Hematoxylin and Eosin staining. The chosen slides were placed in Xylene (#1) for 10 minutes, followed by Xylene (#2) for 5 minutes to remove paraffin wax. Slides were rehydrated in EtOH (100%, 95%, 90%, and 70%) and washed with water. All steps for 5 minutes each. Slides were placed in Hematoxylin stain (Ricca; Arlington, TX) for 10 seconds and washed with water until clear. Next, slides were placed in Eosin stain (Sigma-Aldrich; St. Louis, MO) for 1 minute and washed quickly with water 3x until clear. Slides were dehydrated quickly into EtOH (70%, 90%, 95%, and 100%) for 1 minute each. Lastly, slides were placed in fresh 100% Xylene (#3) for 10 minutes. Slides were cover slipped using Cytoseal (Electron Microscopy Sciences; Hatfield, PA) and allowed to dry in the chemical hood overnight. Stained slides were imaged on a Keyence BZ-X800 microscope (Osaka, Japan).

HCR™ RNA-FISH

To investigate cellular expression patterns, HCR™ RNA-FISH (Molecular Instruments; Los Angeles, CA) was performed on XX and XY embryonic gonad sections. Eggs were collected and dissected open as above (see Tissue collection for RNA-sequencing). Tail clips were taken for DNA extraction and sex genotyping (prepared as above; see DNA extraction). Internal organs were removed from embryos, leaving the spine, some dorsal tissue, the mesonephroi,

and attached gonadal ridges. The “torso” samples were fixed overnight in 4% PFA at 4°C. Samples were washed 3x in 1X Phosphate-Buffered Saline solution + 10% tween-20 for 5 minutes each and then dehydrated into 100% MeOH using increasing concentrations of MeOH and 1X PBST (20%, 40%, 60%, 80%, 100%) for 10 minutes each. Samples were placed into fresh 100% MeOH and stored at -20℃ until embedded for cryo-sectioning. For cryo-sectioning, samples were placed in sucrose overnight and then transitioned into new sucrose until embedding. Samples were embedded in cryostat molds using O.C.T. Compound (Tissue-Tek®; Torrance, CA) and sectioned at 5µm on a Leica CM1850 cryostat microtome (Wetzlar, Germany). HCR™ RNA-FISH was performed according to the Molecular Instruments “HCR™ RNA-FISH protocol for sample on slide” protocol (cite). Probes for the gene *amh* and the mRNA transcript *astra* were used. Slides were imaged on a Zeiss LSM 880 confocal microscope (Oberkochen, Germany). Fiji was used for analysis (Schindelin et al., 2012).

FIGURES

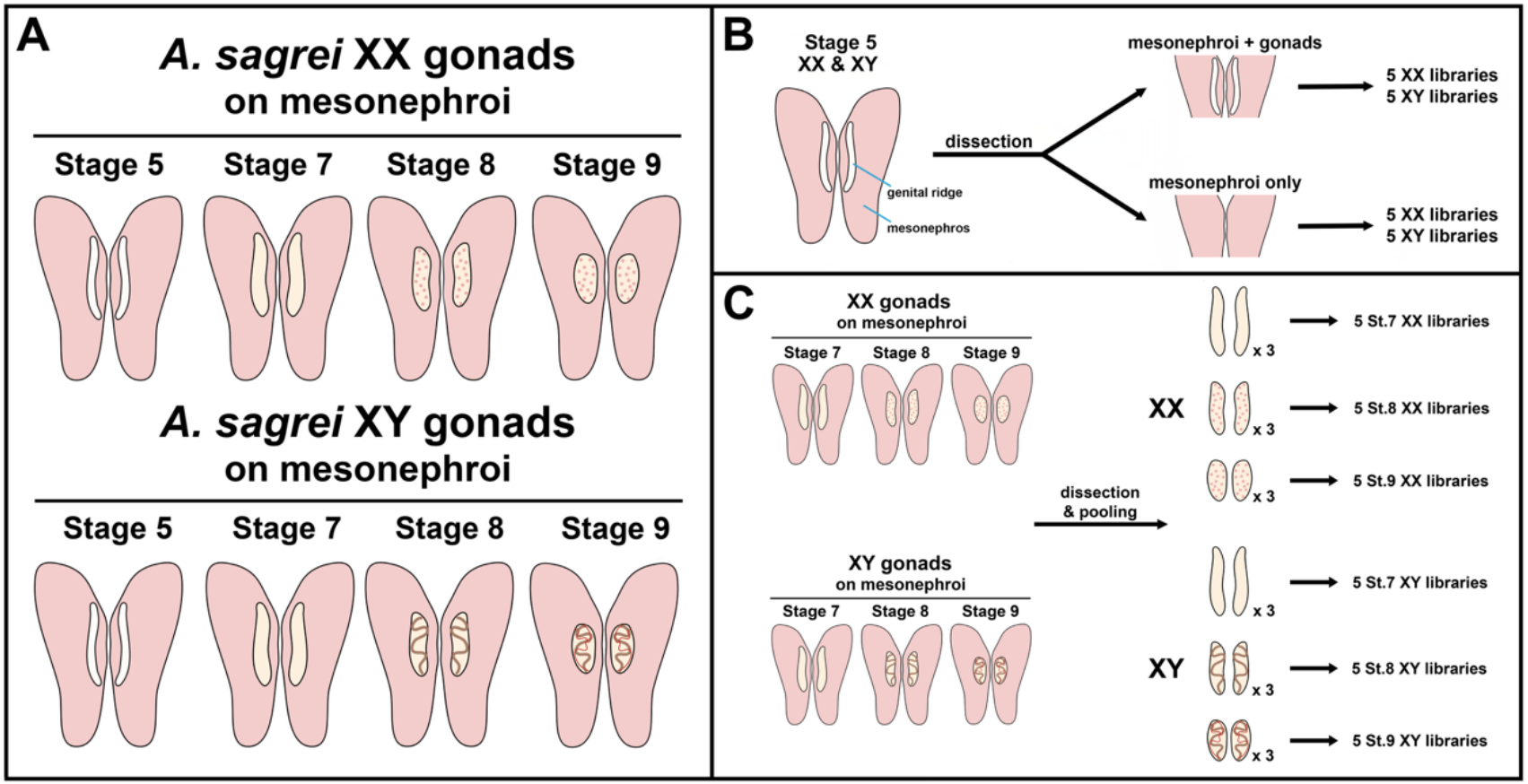
A
A. sagrei XX gonads
on mesonephroi
Stage 5
Stage 7
Stage 8
Stage 9
A. sagrei XY gonads
on mesonephroi
Stage 5
Stage 7
Stage 8
Stage 9
B
Stage 5
XX & XY
genital ridge
mesonephros
dissection
mesonephroi + gonads
5 XX libraries
5 XY libraries
mesonephroi only
5 XX libraries
5 XY libraries
C
XX gonads
on mesonephroi
Stage 7
Stage 8
Stage 9
dissection
& pooling
XX
x 3
5 St.7 XX libraries
x 3
5 St.8 XX libraries
x 3
5 St.9 XX libraries
XY gonads
on mesonephroi
Stage 7
Stage 8
Stage 9
XY
x 3
5 St.7 XY libraries
x 3
5 St.8 XY libraries
x 3
5 St.9 XY libraries

Figure 3.1. *A. sagrei* embryonic gonad morphology and RNA-seq tissue sample collection. (A) XX embryonic gonads (top) and XY embryonic gonads (bottom) attached to mesonephroi. Gonads are depicted in white (stage 5) or cream (stages 7, 8, 9) and mesonephroi are depicted in pink. As the XX gonadal ridge develops it condenses into a round gonad with scattered puncta visible in stages 8 and 9 (light pink). As the XY gonadal ridge develops it condenses into a round gonad with the testicular cords visible at stage 8 (light brown lines) and testicular vasculature visible at stage 9 (red lines). (B) Stage 5 tissue collection for RNA-seq. For mesonephroi and gonad libraries (M+GR), mesonephros was cut above and below the gonadal ridges. For mesonephroi only libraries (M), the same cuts were made, and then the gonads were removed. Each library contained one sample. (C) Stages 7, 8, and 9 tissue collection for RNA-seq. Paired gonadal ridges were dissected off mesonephroi. Three samples were pooled for each library. Figured generated with BioRender.

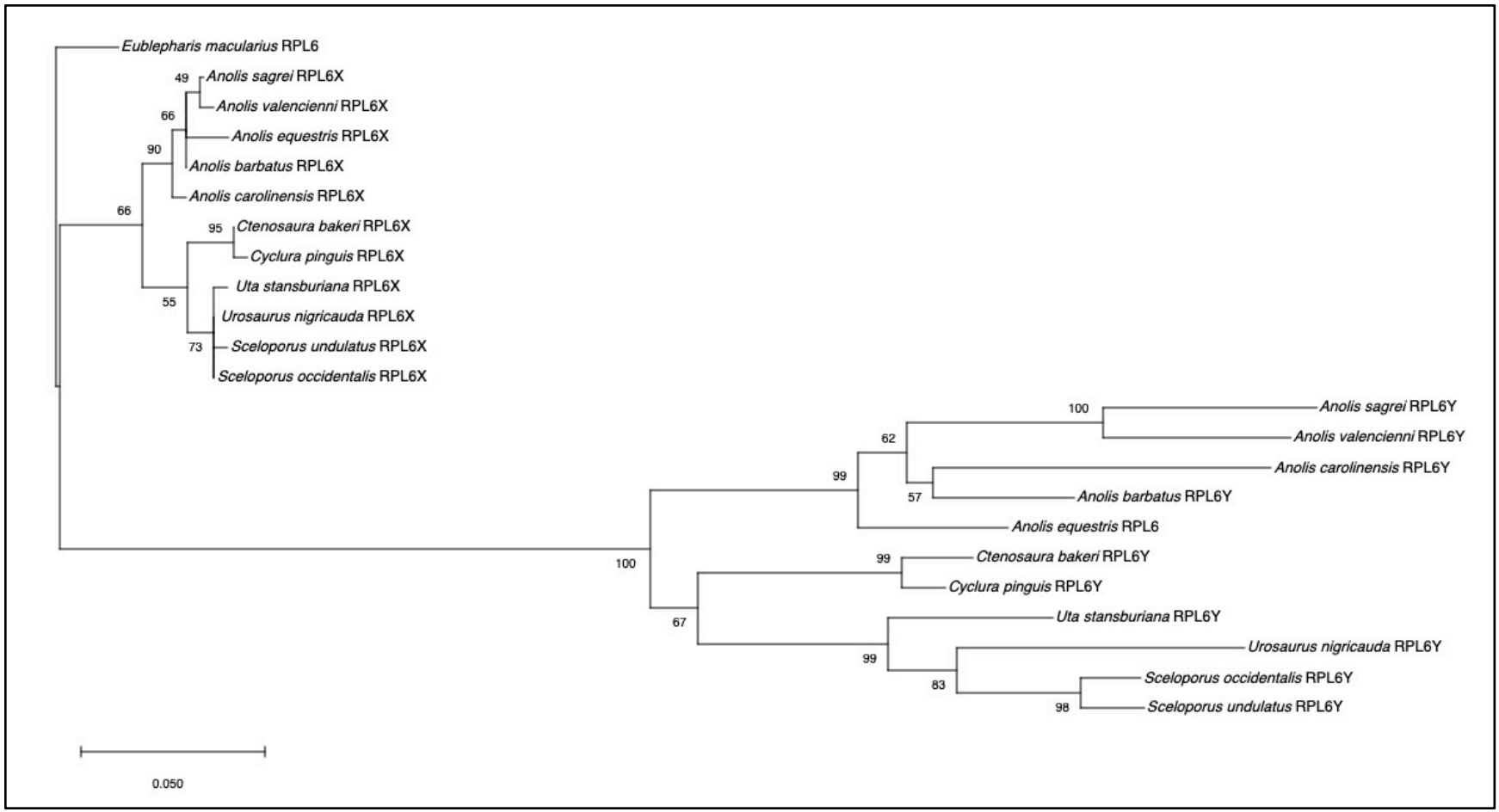
Eublepharis macularius RPL6
Anolis sagrei RPL6X
Anolis valencienni RPL6X
Anolis equestris RPL6X
Anolis barbatus RPL6X
Anolis carolinensis RPL6X
Ctenosaura bakeri RPL6X
Cyclura pinguis RPL6X
Uta stansburiana RPL6X
Urosaurus nigricauda RPL6X
Sceloporus undulatus RPL6X
Sceloporus occidentalis RPL6X
Anolis sagrei RPL6Y
Anolis valencienni RPL6Y
Anolis carolinensis RPL6Y
Anolis barbatus RPL6Y
Anolis equestris RPL6
Ctenosaura bakeri RPL6Y
Cyclura pinguis RPL6Y
Uta stansburiana RPL6Y
Urosaurus nigricauda RPL6Y
Sceloporus occidentalis RPL6Y
Sceloporus undulatus RPL6Y
49
66
90
66
95
55
73
100
62
99
57
100
99
67
99
83
98
0.050

Figure 3.2. RPL6X and RPL6Y protein-based tree. RPL6 protein sequence evolution was analyzed in 11 Pleurodont species from the families, *Phrynosomatidae, Iguanidae,* and *Dactyloidae.* RPL6Y is diverging at a much higher rate than RPL6X in Pleurodont lizards. Longer branch lengths = greater amino acid sequence divergence. Scale bar = 0.050

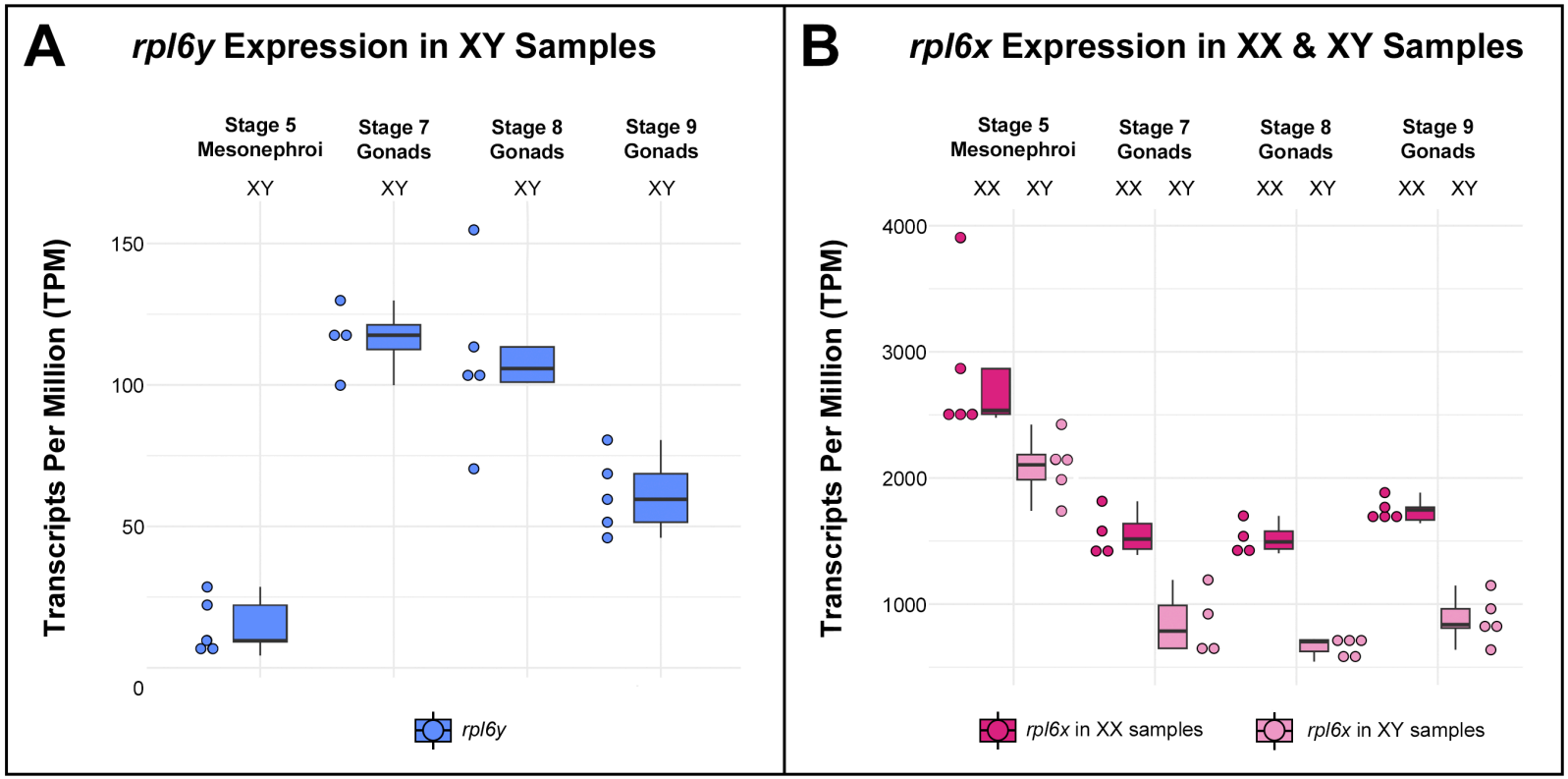

Figure 3.3. *rpl6y and rpl6x* expression in embryonic mesonephroi and gonads. (A) *rpl6y* expression in XY embryonic mesonephroi or gonads. (B) *rpl6x* expression in XX and XY embryonic mesonephroi or gonads (XX-dark pink, XY-light pink). *rpl6x* is differentially expressed between XX and XY gonads at all these stages shown. Expression is shown in Transcripts Per Million (TPM). Each point represents a single RNA-sequencing library and biological replicate (n=4 or 5).

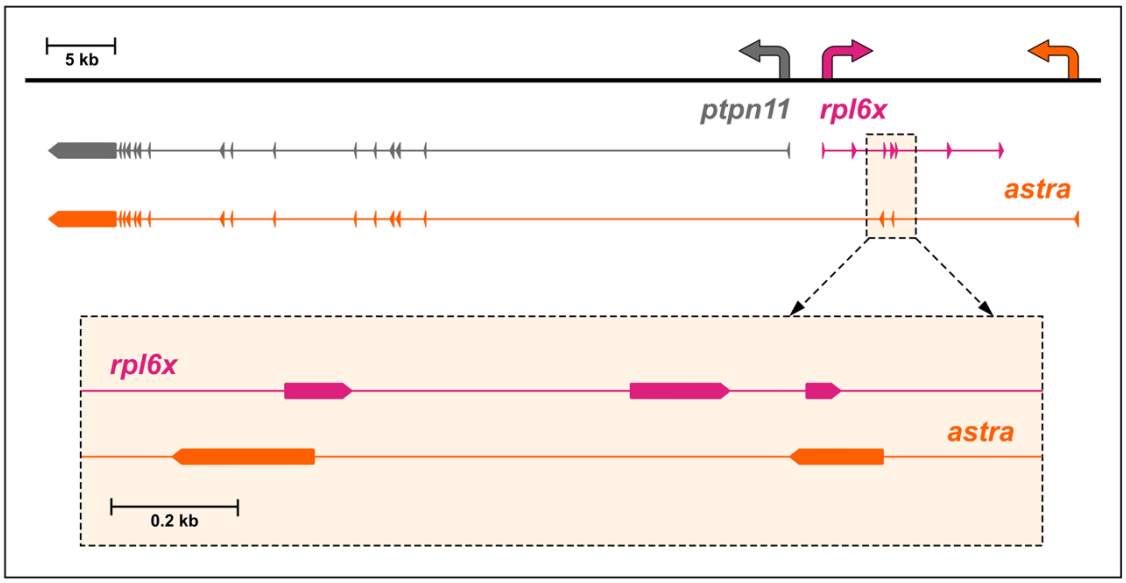

Figure 3.4. Exon structure of *astra, rpl6x,* and *ptpn11*. The genes, *rpl6x* and *ptpn11*, sit in a head-to-head orientation and are transcribed in opposite directions (top)**.** During early embryogenesis, a gonad-specific promotor generates *astra* in XX and XY gonads (middle). *astra* is a distinct mRNA isoform of *ptpn11* that is initiated 3' of *rpl6x*. The two 5' UTR exons of *astra* overlap with *rpl6x* exons 3 and 5. Curved arrows represent the promoters and direction of transcription for *ptpn11* (grey), *rpl6x* (pink), and *astra* (orange). The dashed inset shows the *rpl6x* and *astra* overlapping exons (bottom).

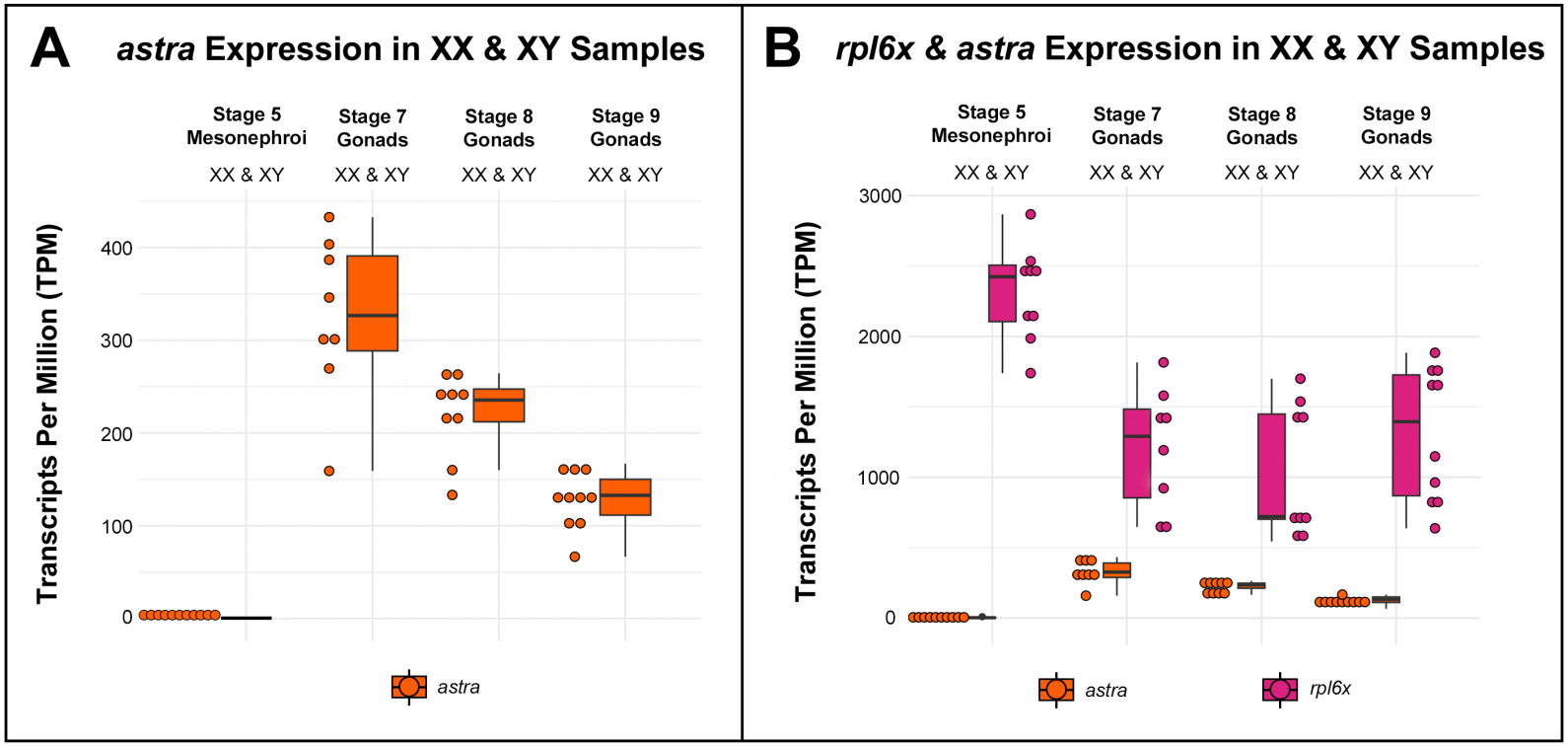

Figure 3.5. *astra and rpl6x* expression in embryonic mesonephroi and gonads. (A) *astra* expression in XX & XY embryonic mesonephroi or gonads. (B) *astra* and *rpl6x* expression in XX and XY embryonic mesonephroi or gonads. Expression is shown in Transcripts Per Million (TPM). Each point represents a single RNA-sequencing library and biological replicate (n= 8-10).

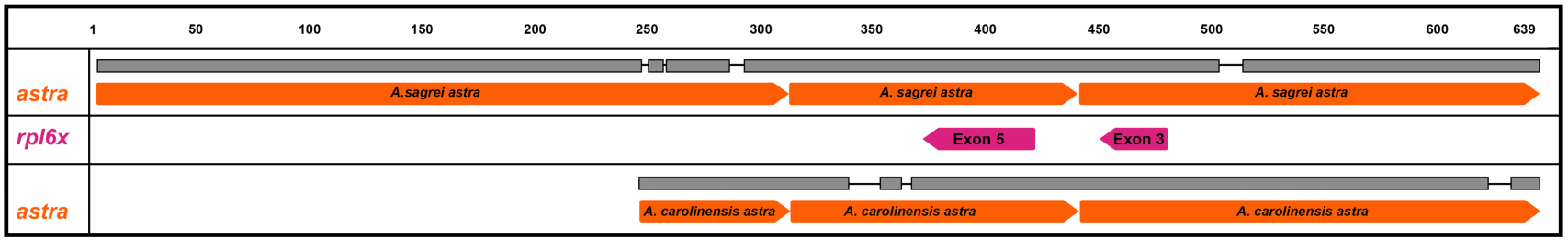

Figure 3.6. The anti-*rpl6x* mRNA transcript, *astra,* is conserved in *Anolis carolinensis*. The 5' UTR splice sites of *A. sagrei* (top, orange) and *A. Carolinensis* (bottom, orange) are perfectly conserved. The overlapping exons of *rpl6x* are shown in pink (middle).

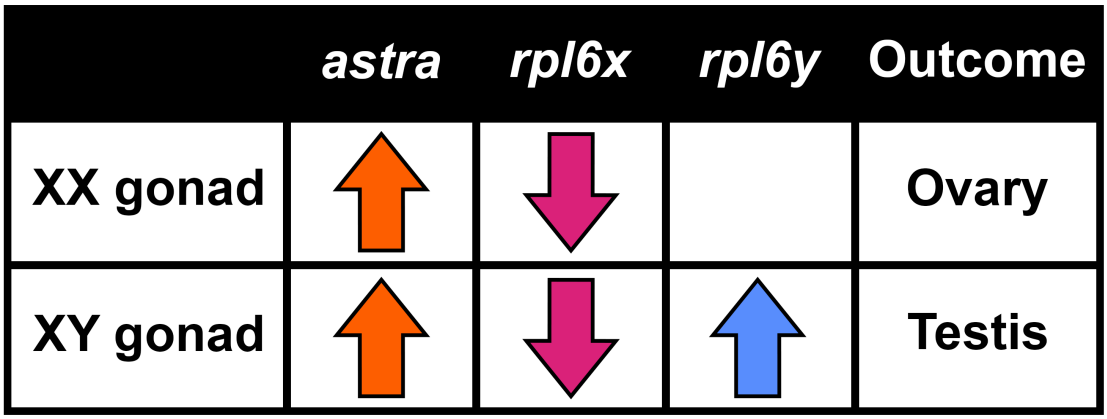

Figure 3.7. *Anolis* sex determination model. In XX and XY gonads, expression of the mRNA transcript, *astra,* results in decreased *rpl6x* expression prior to sex determination initiation. In XY gonads, *rpl6y* is subsequently upregulated, initiating sex determination and inducing testis differentiation.

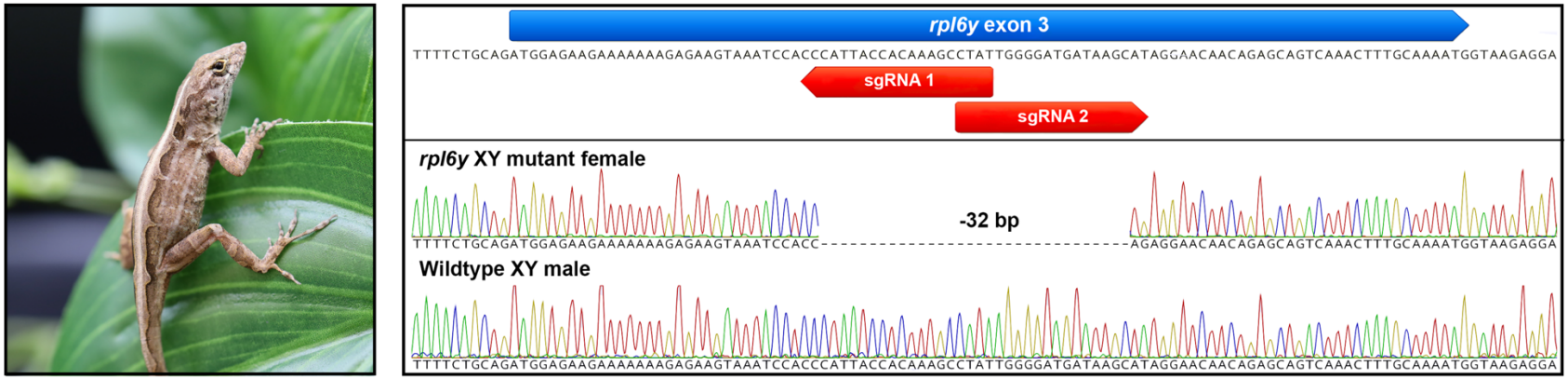

Figure 3.8. Identification of *rpl6y* XY mutant by Sanger sequencing. Adult *rpl6y* XY mutant female lizard that has undergone complete male-to-female sex reversal (left). Sanger sequencing chromatogram for *rpl6y* XY mutant female and wildtype XY male (right). *rpl6y* exon 3 (blue) was targeted for CRISPR-gene editing with 3 guide RNAs. Guide RNAs 1 and 2 are shown above (red). Guide 3 contains a common SNP variant of sgRNA 2 and is therefore not shown. A -32bp frameshift mutation in *rpl6y* exon 3 was identified, resulting in a *rpl6y* mutant XY female.

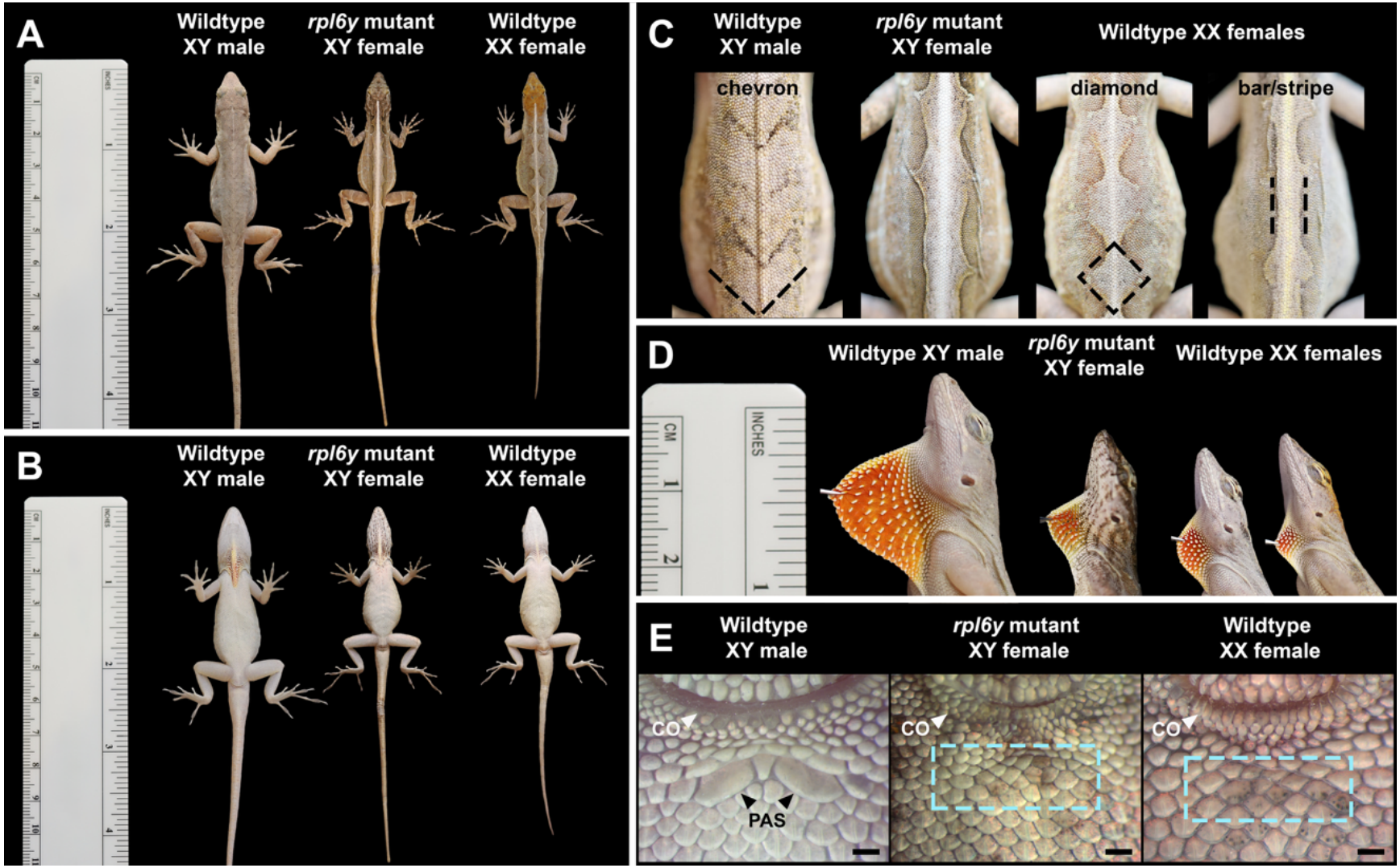
A
Wildtype XY male
rpl6y mutant XY female
Wildtype XX female
B
Wildtype XY male
rpl6y mutant XY female
Wildtype XX female
C
Wildtype XY male
rpl6y mutant XY female
Wildtype XX females
chevron
diamond
bar/stripe
D
Wildtype XY male
rpl6y mutant XY female
Wildtype XX females
CM
INCHES
E
Wildtype XY male
rpl6y mutant XY female
Wildtype XX female
CO
PAS

Figure 3.9. External phenotype of *rpl6y* mutant XY female. (A) Dorsal and (B) ventral view of body size. The *rpl6y* mutant XY female's body size is consistent with that of wildtype females. (C) Dorsal back patterns of wildtype and mutant animals. Black dashed lines represent wildtype patterns and their commonly used names in the literature. *rpl6y* mutant XY female displays the female-limited diamond/bar back pattern. (D) Dewlap size and morphology. *rpl6y* mutant XY female has a small female-like dewlap. (E) Post anal scale morphology of wildtype and mutant animals. Post anal scales are a sexually dimorphic trait present in males. The rpl6y mutant XY female lacks post anal scales. Light blue dashed boxes highlight lack of post anal scales in wildtype and mutant females. PAS = post anal scales, CO = cloacal opening, Scale bars = 500μm.

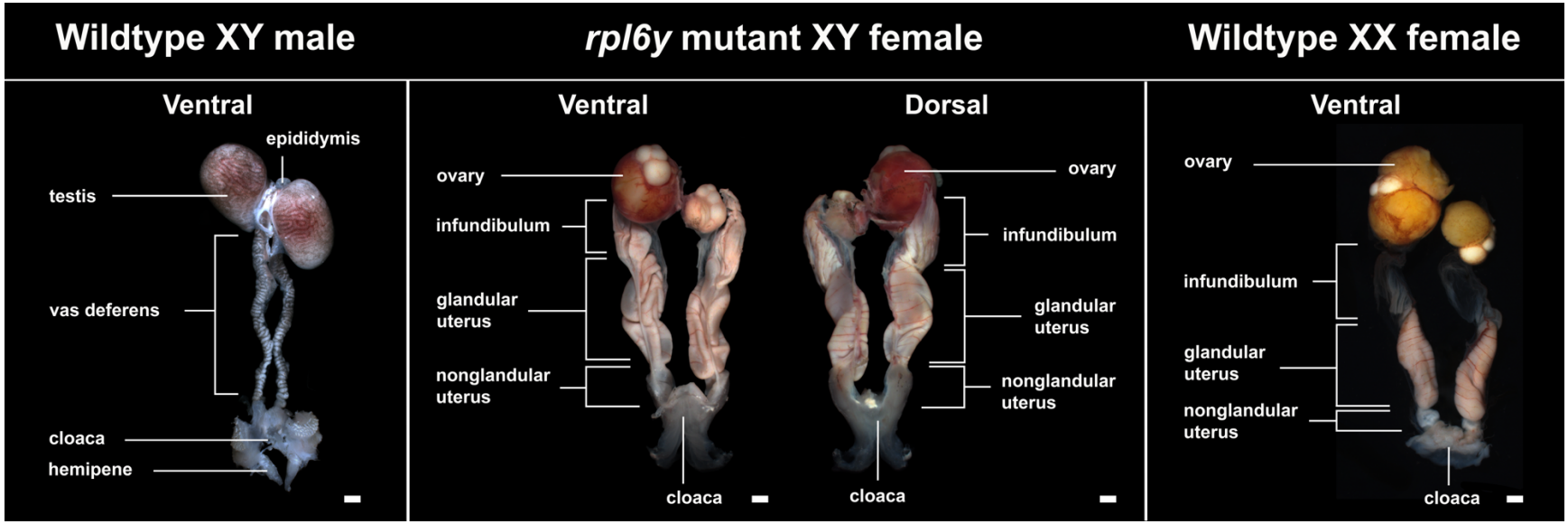

Figure 3.10. Reproductive anatomy of *rpl6y* mutant XY female. Wildtype XY male reproductive anatomy includes testes, epididymides, vasa deferentia, hemipenes, and a cloaca (left). Wildtype XX female reproductive anatomy includes ovaries, infundibula, glandular uteri, non-glandular uteri, hemiclitores (not pictured), and a cloaca (right). *rpl6y* mutant XY female displayed wildtype female-like anatomy (center). Scale bars = 1000μm

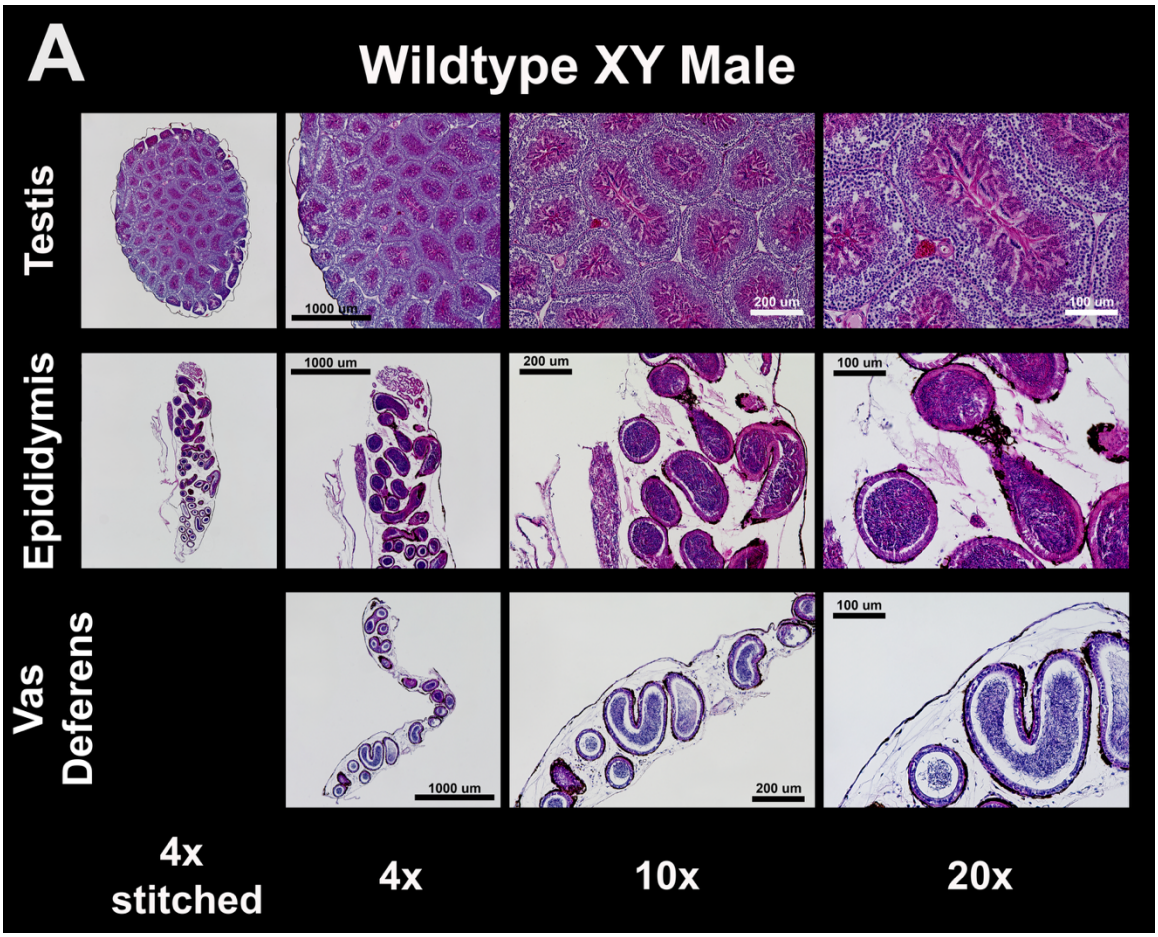
A
Wildtype XY Male
Testis
Epididymis
Vas Deferens
1000 um
200 um
100 um
4x stitched
4x
10x
20x

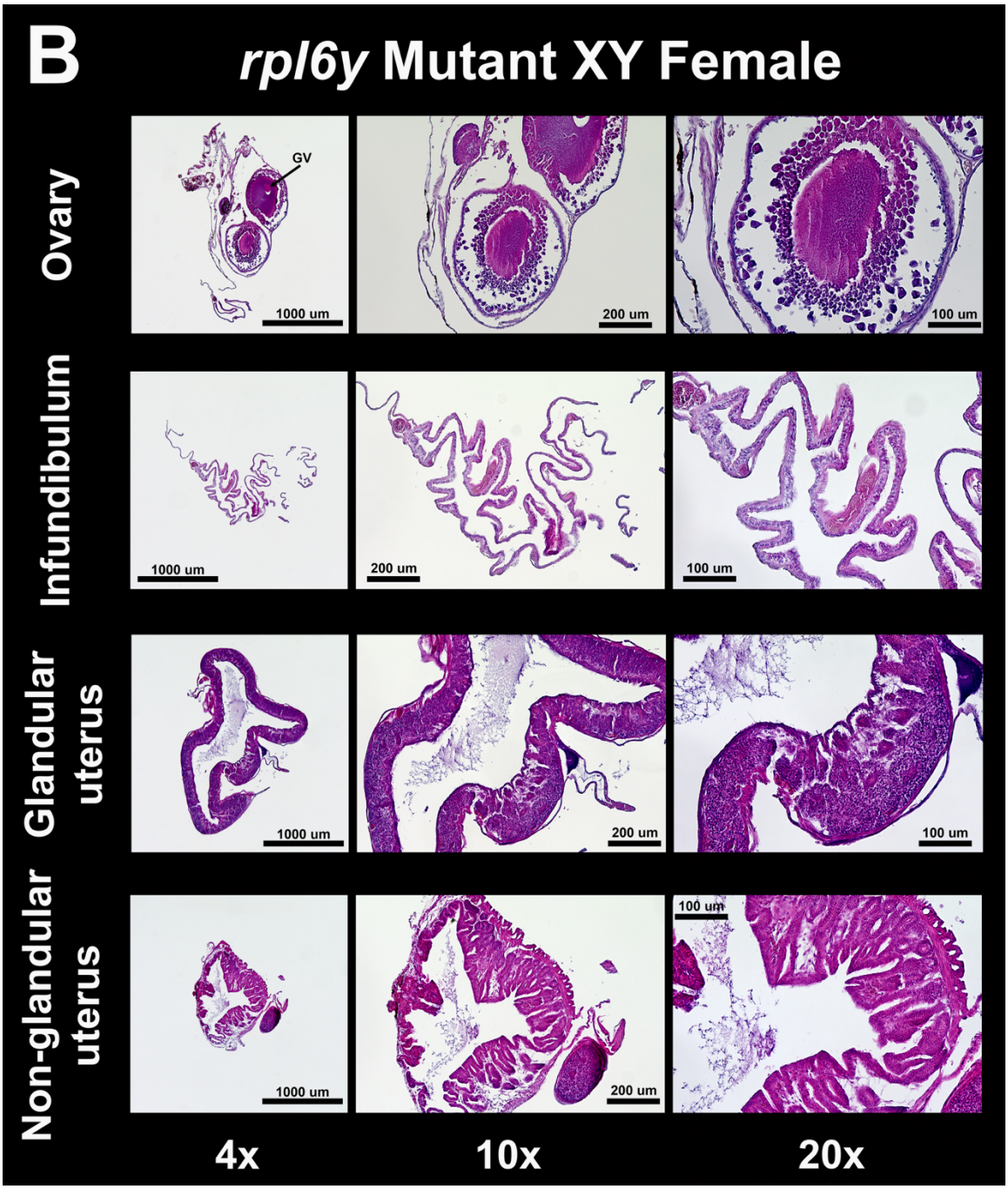
B
rpl6y Mutant XY Female
Ovary
Infundibulum
Glandular uterus
Non-glandular uterus
GV
1000 um
200 um
100 um
4x
10x
20x

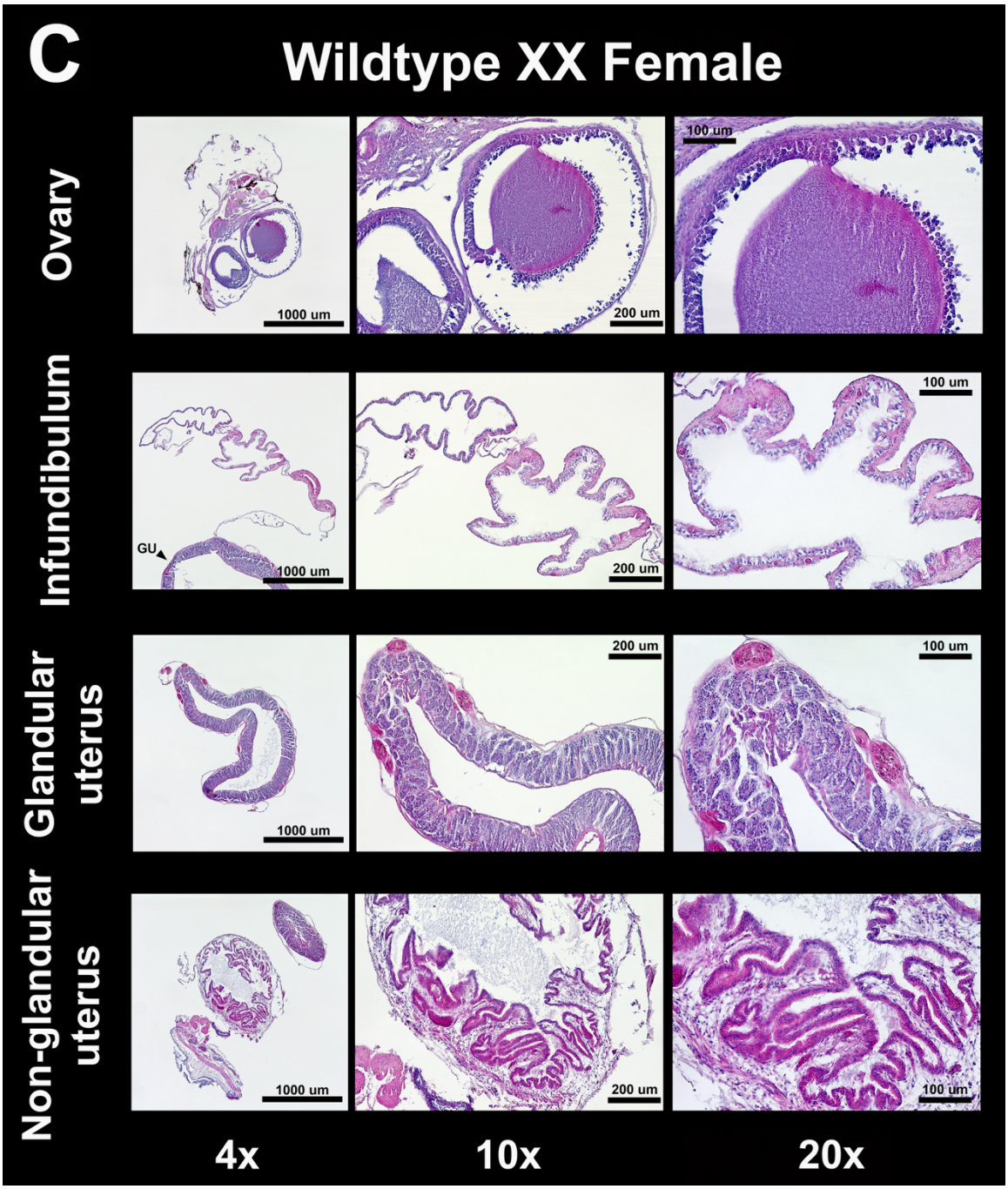
C
Wildtype XX Female
Ovary
Infundibulum
Glandular uterus
Non-glandular uterus
4x
10x
20x
1000 um
200 um
100 um
GU

Figure 3.11. Hematoxylin and Eosin histological analysis of *rpl6y* mutant XY female. (A) Wildtype XY male histology of testis, epididymis, and vas deferens. (B) *rpl6y* mutant XY female histology of ovary, infundibulum, glandular uterus, and non-glandular uterus. (C) Wildtype XX female histology of ovary, infundibulum, glandular uterus, and non-glandular uterus. Hematoxylin was used to stain cell nuclei (dark purple or blue) and Eosin was used as a counterstain for cytoplasm (pink) on 10µm paraffin sections. GV = germinal vesicle, 4x scale bars = 1000µm, 10x scale bars = 200µm, 20x scale bars = 100µm

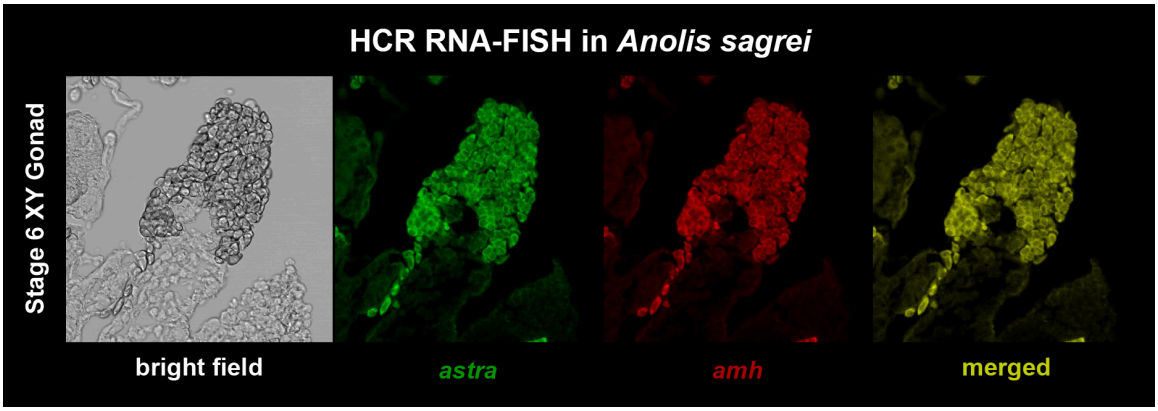

Figure 3.12. Preliminary HCR RNA-FISH in stage 6 XY *A. sagrei* gonad. *astra* expression is shown in green, *amh* expression is shown in red, and merged expression is shown in yellow. *amh* and *astra* appear to be co-expressed in the somatic cells of the XY gonad.

TABLES

Table 3.1. DNA primers and sgRNAs used.

***rpl6y* Genotyping Primers**		
Gene	**Primer**	**Sequence**
rpl6y	forward 1	5’-CACCCTGCTTCTGGATAGCTG-3’
rpl6y	forward 2	5’-CCACACATTTAGAACTCTGAGTTGA-3’
rpl6y	forward 3	5’-CAAAGCTGTCTCAGTTTCATATTAGAC-3’
rpl6y	forward 4	5’-AAATGCCCAGTGTCAGAGGAAC-3’
rpl6y	forward 5	5’-CTATCAGTTCATAAATGCCCAGTGTC-3’
rpl6y	reverse 1	5’-GATCGATATCCATTGTCATCCCAG-3’
rpl6y	reverse 2	5’-GTATTCAATGCCCCATATCAACTTG-3’
rpl6y	reverse 3	5’-CATTCAGCTGTGGACTTCTCATT-3’
rpl6y	reverse 4	5’-GGTGAGGTGTAACTAATGCAAAAGTG-3’
rpl6y	reverse 5	5’-GCTCTGGACCTGCTTGAAGTAG-3’
rpl6y	reverse 6	5’-TTTTGGCACTCCGTCTTAGCTTC-3’
Sex Genotyping Primers		
Gene	**Primer**	**Sequence**
kank1	forward	5’-CCTTCCTTTGTAGGATCCAGTG-3'
kank1	reverse	5’-GGAGCACAGGGATAGTTTTGAC-3'
gnaz	forward	5’-GTGGTGGGTTCAACCTAGAGG-3'
gnaz	reverse	5’-CGTAGGATGTCCTCCACTGTG-3’
CRISPR guide RNAs for rpl6y		
Gene	**Guide**	**Sequence**
rpl6y	sgRNA1	5'-CCCATTACCACAAAGCCTAT-3'
rpl6y	sgRNA2	5'-CTATTGGGGATGATAAGCAT-3'
rpl6y	sgRNA3	5'-CTATTGGGGATGATAAACAT-3'

Table 3.2. Differentially expressed genes (DEGs) in XX and XY gonads from RNA-sequencing. DEGs were filtered based on padj, baseMean, and fold change. padj= adjusted p value.

Differentially Expressed Genes* in XX and XY Gonads

*padj ≤ 0.01, baseMean ≥ 30, and fold change ≥ 1.5

	Developmental Stage		
	Stage 7	Stage 8	Stage 9
XX-biased DEGs	704	1422	1481
XY-biased DEGs	802	1916	1272
Total DEGs	1506	3338	2753

Table 3.3. Genes previously implicated in sex determination or gonad differentiation that were found to be differentially expressed in XX or XY gonads in *A. sagrei.* Genes shaded in blue are XY-biased and more strongly expressed in males. Genes shaded in pink are XX-biased and more strongly expressed in females.

Differentially Expressed Gonad Differentiation Genes in XX and XY Gonads:

Stage 7

Gene	baseMean	pvalue	padj	log2FoldChange	Fold Change	
col9a1	930.4	1.24E-19	1.50E-17	5.07	33.5	XY-biased
col9a2	2063.4	5.56E-57	3.27E-54	4.36	20.5	
col9a3	5618.4	1.93E-28	4.34E-26	3.95	15.5	
dhh	480.0	4.96E-21	6.84E-19	3.64	12.5	
sox9	10182.5	5.98E-32	1.58E-29	2.52	5.7	
mayex	254.2	2.39E-19	2.80E-17	2.46	5.5	
sox10	70.8	4.33E-05	5.92E-04	1.73	3.3	
amh	64339.1	3.45E-13	2.37E-11	1.67	3.2	
wnt5a	4965.0	7.52E-11	3.55E-09	1.43	2.7	
sox13	1541.1	9.60E-13	6.11E-11	1.18	2.3	
dmrt1	1598.5	3.18E-22	4.82E-20	1.12	2.2	
foxl2	285.3	1.37E-04	1.58E-03	3.30	9.9	XX-biased
wnt4	467.4	6.86E-08	1.80E-06	2.40	5.3	
amhr2	10613.6	5.93E-09	1.92E-07	1.88	3.7	
lef1	1716.6	5.32E-07	1.18E-05	1.12	2.2	

Stage 8

Gene	baseMean	pvalue	padj	log2FoldChange	Fold Change	
col9a1	1478.2	4.29E-120	4.19E-117	6.67	101.6	XY-biased
col9a3	9053.4	1.23E-155	3.81E-152	5.38	41.6	
col9a2	3216.2	1.62E-193	1.00E-189	5.24	37.8	
dhh	583.6	2.47E-81	7.77E-79	4.86	29.0	
sox9	10025.5	3.22E-134	5.43E-131	3.68	12.9	
mayex	220.0	7.59E-25	4.53E-23	2.84	7.2	
amh	76631.0	2.50E-53	4.14E-51	2.71	6.5	
wnt5a	4910.1	4.75E-90	2.00E-87	2.19	4.6	
dmrt1	1239.3	2.30E-16	8.03E-15	1.46	2.7	
sox13	1161.9	3.31E-08	4.59E-07	0.91	1.9	
fgf2	391.3	2.52E-10	4.76E-09	0.87	1.8	
cyp19a1	21073.9	1.94E-101	1.09E-98	10.63	1589.9	XX-biased
foxl2	298.2	5.93E-82	1.93E-79	6.73	106.2	
wnt4	402.4	8.53E-51	1.32E-48	3.56	11.8	
amhr2	9272.2	1.91E-48	2.68E-46	2.74	6.7	
lef1	1275.6	2.74E-21	1.35E-19	1.60	3.0	
fgf9	2178.4	7.08E-09	1.08E-07	0.83	1.8	
fgfr2	5956.0	2.00E-09	3.29E-08	0.67	1.6	

Stage 9

Gene	baseMean	pvalue	padj	log2FoldChange	Fold Change	
col9a1	1592.0	4.87E-69	1.45E-66	5.51	45.6	XY-biased
dhh	569.8	5.19E-105	3.29E-102	4.74	26.8	
col9a3	7093.5	3.10E-131	3.69E-128	4.61	24.4	
col9a2	2566.0	3.39E-178	1.61E-174	4.44	21.6	
sox9	9188.3	2.37E-147	5.01E-144	4.06	16.7	
amh	80440.4	8.32E-60	1.91E-57	2.64	6.2	
mayex	177.7	1.41E-19	6.52E-18	2.55	5.9	
wnt5a	4554.2	3.13E-34	3.05E-32	2.20	4.6	
dmrt1	1432.9	1.55E-11	3.66E-10	1.35	2.6	
sox13	1275.6	7.41E-11	1.64E-09	1.05	2.1	
fgf2	458.1	9.40E-06	9.88E-05	0.92	1.9	
sox8	219.1	6.40E-05	5.48E-04	0.79	1.7	
cyp19a1	25764.4	4.37E-76	1.57E-73	11.2	2363.4	XX-biased
foxl2	457.7	8.34E-68	2.37E-65	8.1	270.7	
amhr2	10219.8	6.13E-56	1.24E-53	3.0	8.1	
wnt4	392.2	8.96E-24	5.33E-22	2.8	6.8	
lef1	1399.1	2.82E-19	1.27E-17	1.6	3.1	
rspo1	66.6	9.33E-04	5.79E-03	1.0	2.0	
fgf9	2241.3	1.36E-05	1.37E-04	0.8	1.7	
fgfr2	6352.4	7.02E-10	1.38E-08	0.8	1.7	
sox4	17013.6	2.55E-09	4.70E-08	0.7	1.7	

Table 3.4. Previously identified ancient Y-chromosome genes of *Anolis sagrei.* Gene expression is reported in Transcripts Per Million (TPM) from Stage 7 XY gonad RNA-sequencing libraries. X chromosome paralogs, protein sequence identity, and conservation among Pleurodont lizards were identified by BLAST analysis.

Ancient Y Genes* Present on *Anolis sagrei* Y chromosome

Gene	XY Gonad Expression (TPM at Stage 7)	X Chromosome Paralog?	X/Y Protein Identity (%)	Conserved in Pleurodont lizards?
rpl6y	114	Yes	70%	Yes
ube2l3y	16	Yes	100%	Yes
ccdc74by	0.2	Yes	76%	No
gnazy	0.04	Yes	96%	Yes
rsph14y	0.1	No	--	Yes

*Motley & Park, unpublished; Marin et al.; 2017

REFERENCES

Alföldi, J., Di Palma, F., Grabherr, M., Williams, C., Kong, L., Mauceli, E., Russell, P., Lowe, C. B., Glor, R. E., Jaffe, J. D., Ray, D. A., Boissinot, S., Shedlock, A. M., Botka, C., Castoe, T. A., Colbourne, J. K., Fujita, M. K., Moreno, R. G., ten Hallers, B. F., … Lindblad-Toh, K. (2011). The genome of the green anole lizard and a comparative analysis with birds and mammals. *Nature*, *477*(7366), 587–591. https://doi.org/10.1038/nature10390

Andrews, S. (2010). FastQC: A Quality Control Tool for High Throughput Sequence Data. (http://www.bioinformatics.babraham.ac.uk/projects/fastqc/)

Anirudhan, A., Angulo-Bejarano, P. I., Paramasivam, P., Manokaran, K., Kamath, S. M., Murugesan, R., Sharma, A., & Ahmed, S. S. S. J. (2021). RPL6: A Key Molecule Regulating Zinc- and Magnesium-Bound Metalloproteins of Parkinson's Disease. *Frontiers in Neuroscience*, *15*, 631892. https://doi.org/10.3389/fnins.2021.631892

Arbuckle, K., Bennett, C. M., & Speed, M. P. (2014). A simple measure of the strength of convergent evolution. *Methods in Ecology and Evolution*, *5*(7), 685–693. https://doi.org/10.1111/2041-210X.12195

Bachtrog, D., Mank, J. E., Peichel, C. L., Kirkpatrick, M., Otto, S. P., Ashman, T. L., Hahn, M. W., Kitano, J., Mayrose, I., Ming, R., Perrin, N., Ross, L., Valenzuela, N., & Vamosi, J. C. (2014). Sex determination: Why so many ways of doing it? *PLoS Biol*, *12*(7), e1001899. https://doi.org/10.1371/journal.pbio.1001899

Baeckens, S., Driessens, T., Huyghe, K., Vanhooydonck, B., & Van Damme, R. (2018). Intraspecific Variation in the Information Content of an Ornament: Why Relative Dewlap Size Signals Bite Force in Some, But Not All Island Populations of Anolis

sagrei. *Integrative and Comparative Biology*, *58*(1), 25–37. https://doi.org/10.1093/icb/icy012

Bai, D., Zhang, J., Xiao, W., & Zheng, X. (2014). Regulation of the HDM2-p53 pathway by ribosomal protein L6 in response to ribosomal stress. *Nucleic Acids Research*, *42*(3), 1799–1811. https://doi.org/10.1093/nar/gkt971

Bertho, S., Herpin A, Schartl M, & Guiguen Y. (2021). Lessons from an unusual vertebrate sex-determining gene—PubMed. *Philosophical Transactions of the Royal Society of London. Series B, Biological Sciences*, *376*(1832). https://doi.org/10.1098/rstb.2020.0092

Bitgood, M. J., Shen, L., & McMahon, A. P. (1996). Sertoli cell signaling by Desert hedgehog regulates the male germline. *Current Biology: CB*, *6*(3), 298–304. https://doi.org/10.1016/s0960-9822(02)00480-3

Bock, D. G., Baeckens, S., Pita-Aquino, J. N., Chejanovski, Z. A., Michaelides, S. N., Muralidhar, P., Lapiedra, O., Park, S., Menke, D. B., Geneva, A. J., Losos, J. B., & Kolbe, J. J. (2021). Changes in selection pressure can facilitate hybridization during biological invasion in a Cuban lizard. *Proceedings of the National Academy of Sciences of the United States of America*, *118*(42), e2108638118. https://doi.org/10.1073/pnas.2108638118

Bull, J. (1983). *Evolution of Sex Determining Mechanisms*. Benjamin/Cummings Pub. Co.

Burgoyne, Buehr, & McLaren. (1988). XY follicle cells in ovaries of XX----XY female mouse chimaeras—PubMed. *Development (Cambridge, England)*, *104*(4). https://doi.org/10.1242/dev.104.4.683

Capel, B. (2017). Vertebrate sex determination: Evolutionary plasticity of a fundamental switch. *Nature Reviews. Genetics*, *18*(11), 675–689. https://doi.org/10.1038/nrg.2017.60

Capel, B. (2019). WOMEN IN REPRODUCTIVE SCIENCE: To be or not to be a testis. *Reproduction*, *158*(6), F101-f111. https://doi.org/10.1530/rep-19-0151

Charlesworth, B. (1996). The evolution of chromosomal sex determination and dosage compensation—PubMed. *Current Biology : CB*, *6*(2). https://doi.org/10.1016/s0960-9822(02)00448-7

Concordet, J.-P., & Haeussler, M. (2018). CRISPOR: Intuitive guide selection for CRISPR/Cas9 genome editing experiments and screens. *Nucleic Acids Research*, *46*(W1), W242–W245. https://doi.org/10.1093/nar/gky354

Cortez, D., Marin, R., Toledo-Flores, D., Froidevaux, L., Liechti, A., Waters, P. D., Grützner, F., & Kaessmann, H. (2014). Origins and functional evolution of Y chromosomes across mammals. *Nature*, *508*(7497), 488–493. https://doi.org/10.1038/nature13151

Ezaz, T., Sarre, S. D., O'Meally, D., Graves, J. A. M., & Georges, A. (2009). Sex chromosome evolution in lizards: Independent origins and rapid transitions. *Cytogenetic and Genome Research*, *127*(2–4), 249–260. https://doi.org/10.1159/000300507

Feiner, N., Brun-Usan M, Andrade P, Pranter R, Park S, Menke DB, Geneva AJ, & Uller T. (2022). A single locus regulates a female-limited color pattern polymorphism in a reptile—PubMed. *Science Advances*, *8*(10). https://doi.org/10.1126/sciadv.abm2387

Felsenstein, J. (1985). CONFIDENCE LIMITS ON PHYLOGENIES: AN APPROACH USING THE BOOTSTRAP. *Evolution; International Journal of Organic Evolution*, *39*(4), 783–791. https://doi.org/10.1111/j.1558-5646.1985.tb00420.x

Ford, Jones, Polani, De Almeida, & Briggs. (1959). A sex-chromosome anomaly in a case of gonadal dysgenesis (Turner's syndrome)—PubMed. *Lancet (London, England)*, *1*(7075). https://doi.org/10.1016/s0140-6736(59)91893-8

Gamble, T., Geneva, A. J., Glor, R. E., & Zarkower, D. (2014). Anolis sex chromosomes are derived from a single ancestral pair. *Evolution*, *68*(4), 1027–1041. https://doi.org/10.1111/evo.12328

Gao, Y., Wang, Z., Long, Y., Yang, L., Jiang, Y., Ding, D., Teng, B., Chen, M., Yuan, J., & Gao, F. (2024). Unveiling the roles of Sertoli cells lineage differentiation in reproductive development and disorders: A review. *Frontiers in Endocrinology*, *15*, 1357594. https://doi.org/10.3389/fendo.2024.1357594

Geneva, A. J., Park S, Bock DG, de Mello PLH, Sarigol F, Tollis M, Donihue CM, Reynolds RG, Feiner N, Rasys AM, Lauderdale JD, Minchey SG, Alcala AJ, Infante CR, Kolbe JJ, Schluter D, Menke DB, & Losos JB. (2022). Chromosome-scale genome assembly of the brown anole (Anolis sagrei), an emerging model species—PubMed. *Communications Biology*, *5*(1). https://doi.org/10.1038/s42003-022-04074-5

Genuth, N. R., & Barna, M. (2018a). Heterogeneity and specialized functions of translation machinery: From genes to organisms. *Nature Reviews. Genetics*, *19*(7), 431–452. https://doi.org/10.1038/s41576-018-0008-z

Genuth, N. R., & Barna, M. (2018b). The Discovery of Ribosome Heterogeneity and Its Implications for Gene Regulation and Organismal Life. *Molecular Cell*, *71*(3), 364–374. https://doi.org/10.1016/j.molcel.2018.07.018

Giovannotti, M., Trifonov, V. A., Paoletti, A., Kichigin, I. G., O'Brien, P. C., Kasai, F., Giovagnoli, G., Ng, B. L., Ruggeri, P., Cerioni, P. N., Splendiani, A., Pereira, J. C., Olmo, E., Rens, W., Caputo Barucchi, V., & Ferguson-Smith, M. A. (2017). New insights into sex chromosome evolution in anole lizards (Reptilia, Dactyloidae). *Chromosoma*, *126*(2), 245–260. https://doi.org/10.1007/s00412-016-0585-6

Hopes, T., Norris, K., Agapiou, M., McCarthy, C. G. P., Lewis, P. A., O'Connell, M. J., Fontana, J., & Aspden, J. L. (2022). Ribosome heterogeneity in Drosophila melanogaster gonads through paralog-switching. *Nucleic Acids Research*, *50*(4), 2240–2257. https://doi.org/10.1093/nar/gkab606

Huie, J. M., Prates, I., Bell, R. C., & de Queiroz, K. (2021). Convergent patterns of adaptive radiation between island and mainland Anolis lizards. *Biological Journal of the Linnean Society*, *134*(1). https://doi.org/10.1093/biolinnean/blab072

Jones, D. T., Taylor, W. R., & Thornton, J. M. (1992). The rapid generation of mutation data matrices from protein sequences. *Computer Applications in the Biosciences: CABIOS*, *8*(3), 275–282. https://doi.org/10.1093/bioinformatics/8.3.275

Kamiya, Kai W, Tasumi S, Oka A, Matsunaga T, Mizuno N, Fujita M, Suetake H, Suzuki S, Hosoya S, Tohari S, Brenner S, Miyadai T, Venkatesh B, Suzuki Y, & Kikuchi K. (2012). A trans-species missense SNP in Amhr2 is associated with sex determination in the tiger pufferfish, Takifugu rubripes (fugu)—PubMed. *PLoS Genetics*, *8*(7). https://doi.org/10.1371/journal.pgen.1002798

Keating, S. E., Blumer, M., Grismer, L. L., Lin, A., Nielsen, S. V., Thura, M. K., Wood, P. L., Quah, E. S. H., & Gamble, T. (2021). Sex Chromosome Turnover in Bent-Toed Geckos (Cyrtodactylus). *Genes (Basel)*, *12*(1). https://doi.org/10.3390/genes12010116

Kichigin, I. G., Giovannotti, M., Makunin, A. I., Ng, B. L., Kabilov, M. R., Tupikin, A. E., Barucchi, V. C., Splendiani, A., Ruggeri, P., Rens, W., O'Brien, P. C., Ferguson-Smith, M. A., Graphodatsky, A. S., & Trifonov, V. A. (2016). Evolutionary dynamics of Anolis sex chromosomes revealed by sequencing of flow sorting-derived microchromosome-specific DNA. *Mol Genet Genomics*, *291*(5), 1955–1966. https://doi.org/10.1007/s00438-016-1230-z

Kim, D., Paggi, J. M., Park, C., Bennett, C., & Salzberg, S. L. (2019). Graph-based genome alignment and genotyping with HISAT2 and HISAT-genotype. *Nature Biotechnology*, *37*(8), 907–915. https://doi.org/10.1038/s41587-019-0201-4

Kircher, B. K., Liu, B., Bramble, M. D., Moses, M. M., & Behringer, R. R. (2024). Gene expression profile analysis of subregions of the adult female reproductive tract in the brown anole, Anolis sagrei. *Reproduction (Cambridge, England)*, *169*(2), e240062. https://doi.org/10.1530/REP-24-0062

Kircher, B. K., McCown MA, Scully DM, Behringer RR, & Larina IV. (2024). Structural analysis of the female reptile reproductive system by micro-computed tomography and optical coherence tomography†—PubMed. *Biology of Reproduction*, *110*(6). https://doi.org/10.1093/biolre/ioae039

Kircher, B. K., Stanley EL, & Behringer RR. (2024). Anatomy of the female reproductive tract organs of the brown anole (Anolis sagrei)—PubMed. *Anatomical Record (Hoboken, N.J. : 2007)*, *307*(2). https://doi.org/10.1002/ar.25293

Koopman, Sinclair, & Lovell-Badge. (2016). Of sex and determination: Marking 25 years of Randy, the sex-reversed mouse—PubMed. *Development (Cambridge, England)*, *143*(10). https://doi.org/10.1242/dev.137372

Kumar, S., Stecher, G., Suleski, M., Sanderford, M., Sharma, S., & Tamura, K. (2024). MEGA12: Molecular Evolutionary Genetic Analysis Version 12 for Adaptive and Green Computing. *Molecular Biology and Evolution*, *41*(12), msae263. https://doi.org/10.1093/molbev/msae263

Lahn, & Page. (1999). Four evolutionary strata on the human X chromosome—PubMed. *Science (New York, N.Y.)*, *286*(5441). https://doi.org/10.1126/science.286.5441.964

Lapiedra, O., Chejanovski, Z., & Kolbe, J. J. (2017). Urbanization and biological invasion shape animal personalities. *Global Change Biology*, *23*(2), 592–603. https://doi.org/10.1111/gcb.13395

Lapiedra, O., Schoener, T. W., Leal, M., Losos, J. B., & Kolbe, J. J. (2018). Predator-driven natural selection on risk-taking behavior in anole lizards. *Science (New York, N.Y.)*, *360*(6392), 1017–1020. https://doi.org/10.1126/science.aap9289

Li, D., & Wang, J. (2020). Ribosome heterogeneity in stem cells and development. *The Journal of Cell Biology*, *219*(6), e202001108. https://doi.org/10.1083/jcb.202001108

Li, H., Handsaker, B., Wysoker, A., Fennell, T., Ruan, J., Homer, N., Marth, G., Abecasis, G., Durbin, R., & 1000 Genome Project Data Processing Subgroup. (2009). The Sequence Alignment/Map format and SAMtools. *Bioinformatics (Oxford, England)*, *25*(16), 2078–2079. https://doi.org/10.1093/bioinformatics/btp352

Li, H., Huo, Y., He, X., Yao, L., Zhang, H., Cui, Y., Xiao, H., Xie, W., Zhang, D., Wang, Y., Zhang, S., Tu, H., Cheng, Y., Guo, Y., Cao, X., Zhu, Y., Jiang, T., Guo, X., Qin, Y., & Sha, J. (2022). A male germ-cell-specific ribosome controls male fertility. *Nature*, *612*(7941), 725–731. https://doi.org/10.1038/s41586-022-05508-0

Liao, Y., Smyth, G. K., & Shi, W. (2014). featureCounts: An efficient general purpose program for assigning sequence reads to genomic features. *Bioinformatics (Oxford, England)*, *30*(7), 923–930. https://doi.org/10.1093/bioinformatics/btt656

Lisachov, A. P., Trifonov VA, Giovannotti M, Ferguson-Smith MA, & Borodin PM. (2017). Heteromorphism of “Homomorphic” Sex Chromosomes in Two Anole Species (Squamata, Dactyloidae) Revealed by Synaptonemal Complex Analysis—PubMed. *Cytogenetic and Genome Research*, *151*(2). https://doi.org/10.1159/000460829

Losos, J. B., & Pringle, R. M. (2011). Competition, predation and natural selection in island lizards. *Nature*, *475*(7355), E1-2; discussion E3. https://doi.org/10.1038/nature10140

Love, M. I., Huber, W., & Anders, S. (2014). Moderated estimation of fold change and dispersion for RNA-seq data with DESeq2. *Genome Biology*, *15*(12), 550. https://doi.org/10.1186/s13059-014-0550-8

Marin, R., Cortez, D., Lamanna, F., Pradeepa, M. M., Leushkin, E., Julien, P., Liechti, A., Halbert, J., Brüning, T., Mössinger, K., Trefzer, T., Conrad, C., Kerver, H. N., Wade, J., Tschopp, P., & Kaessmann, H. (2017). Convergent origination of a Drosophila-like dosage compensation mechanism in a reptile lineage. *Genome Res*, *27*(12), 1974–1987. https://doi.org/10.1101/gr.223727.117

McClive, P. J., & Sinclair, A. H. (2003). Type II and type IX collagen transcript isoforms are expressed during mouse testis development. *Biology of Reproduction*, *68*(5), 1742–1747. https://doi.org/10.1095/biolreprod.102.008235

Moser, T. V., Bond, D. M., & Hore, T. A. (2025). Variant ribosomal DNA is essential for female differentiation in zebrafish. *Philosophical Transactions of the Royal Society of London. Series B, Biological Sciences*, *380*(1921), 20240107. https://doi.org/10.1098/rstb.2024.0107

Nei M. and Kumar S. (2000). Molecular Evolution and Phylogenetics. Oxford University Press, New York.

Nicholson, K. E., Crother, B. I., Guyer, C., & Savage, J. M. (2012). It is time for a new classification of anoles (Squamata: Dactyloidae). *Zootaxa*, *3477*(1). https://doi.org/10.11646/zootaxa.3477.1.1

Ord, T. J., Stamps, J. A., & Losos, J. B. (2013). Convergent evolution in the territorial communication of a classic adaptive radiation: Caribbean *Anolis* lizards. *Animal Behaviour*, *85*(6), 1415–1426. https://doi.org/10.1016/j.anbehav.2013.03.037

Pierucci-Alves, F., Clark, A. M., & Russell, L. D. (2001). A developmental study of the Desert hedgehog-null mouse testis. *Biology of Reproduction*, *65*(5), 1392–1402. https://doi.org/10.1095/biolreprod65.5.1392

Pinto, B. J., Keating, S. E., Nielsen, S. V., Scantlebury, D. P., Daza, J. D., & Gamble, T. (2022). Chromosome-Level Genome Assembly Reveals Dynamic Sex Chromosomes in Neotropical Leaf-Litter Geckos (Sphaerodactylidae: Sphaerodactylus). *The Journal of Heredity*, *113*(3), 272–287. https://doi.org/10.1093/jhered/esac016

Pringle, R. M., Kartzinel, T. R., Palmer, T. M., Thurman, T. J., Fox-Dobbs, K., Xu, C. C. Y., Hutchinson, M. C., Coverdale, T. C., Daskin, J. H., Evangelista, D. A., Gotanda, K. M., A. Man in ’t Veld, N., Wegener, J. E., Kolbe, J. J., Schoener, T. W., Spiller, D. A., Losos, J. B., & Barrett, R. D. H. (2019). Predator-induced collapse of niche structure and species coexistence. *Nature*, *570*(7759), 58–64. https://doi.org/10.1038/s41586-019-1264-6

Rasys, A. M., Park, S., Ball, R. E., Alcala, A. J., Lauderdale, J. D., & Menke, D. B. (2019). CRISPR-Cas9 Gene Editing in Lizards through Microinjection of Unfertilized Oocytes. *Cell Rep*, *28*(9), 2288-2292.e3. https://doi.org/10.1016/j.celrep.2019.07.089

Rovatsos, M., Altmanová, M., Pokorná, M., & Kratochvíl, L. (2014). Conserved sex chromosomes across adaptively radiated Anolis lizards. *Evolution*, *68*(7), 2079–2085. https://doi.org/10.1111/evo.12357

Rovatsos, M., Pokorná, M., Altmanová, M., & Kratochvíl, L. (2014). Cretaceous park of sex determination: Sex chromosomes are conserved across iguanas. *Biol Lett*, *10*(3), 20131093. https://doi.org/10.1098/rsbl.2013.1093

Saitou, N., & Nei, M. (1987). The neighbor-joining method: A new method for reconstructing phylogenetic trees. *Molecular Biology and Evolution*, *4*(4), 406–425. https://doi.org/10.1093/oxfordjournals.molbev.a040454

Sanger, T. J., Losos, J. B., & Gibson-Brown, J. J. (2008). A developmental staging series for the lizard genus Anolis: A new system for the integration of evolution, development, and ecology. *Journal of Morphology*, *269*(2), 129–137. https://doi.org/10.1002/jmor.10563

Schindelin, J., Arganda-Carreras, I., Frise, E., Kaynig, V., Longair, M., Pietzsch, T., Preibisch, S., Rueden, C., Saalfeld, S., Schmid, B., Tinevez, J.-Y., White, D. J., Hartenstein, V., Eliceiri, K., Tomancak, P., & Cardona, A. (2012). Fiji: An open-source platform for biological-image analysis. *Nature Methods*, *9*(7), 676–682. https://doi.org/10.1038/nmeth.2019

Schoener, T. W., & Schoener, A. (1980). Densities, Sex Ratios, and Population Structure in Four Species of Bahamian Anolis Lizards. *Journal of Animal Ecology*, *49*(1), 19–53. https://doi.org/10.2307/4276

Shah, A. N., Leesch, F., Lorenzo-Orts, L., Grundmann, L., Novatchkova, M., Haselbach, D., Calo, E., & Pauli, A. (2024). A dual ribosomal system in the zebrafish soma and germline. *bioRxiv: The Preprint Server for Biology*, 2024.08.29.610041. https://doi.org/10.1101/2024.08.29.610041

Stecher, G., Tamura, K., & Kumar, S. (2020). Molecular Evolutionary Genetics Analysis (MEGA) for macOS. *Molecular Biology and Evolution*, *37*(4), 1237–1239. https://doi.org/10.1093/molbev/msz312

Stöck M, Kratochvíl L, Kuhl H, Rovatsos M, Evans BJ, Suh A, Valenzuela N, Veyrunes F, Zhou Q, Gamble T, Capel B, Schartl M, & Guiguen Y. (2021). A brief review of vertebrate sex evolution with a pledge for integrative research: Towards ' sexomics'—PubMed. *Philosophical Transactions of the Royal Society of London. Series B, Biological Sciences*, *376*(1832). https://doi.org/10.1098/rstb.2020.0426

Tang, Y. P., & Wade, J. (2010). Sex- and age-related differences in ribosomal proteins L17 and L37, as well as androgen receptor protein, in the song control system of zebra finches. *Neuroscience*, *171*(4), 1131–1140. https://doi.org/10.1016/j.neuroscience.2010.10.014

Uetz, P., Freed, P, Aguilar, R., Reyes, F., Kudera, J. & Hošek, J. (eds.) (2025) The Reptile Database, http://www.reptile-database.org, accessed August 2025.

Wagner, S., Whiteley, S. L., Castelli, M., Patel, H. R., Deveson, I. W., Blackburn, J., Holleley, C. E., Marshall Graves, J. A., & Georges, A. (2023). Gene expression of male pathway genes sox9 and amh during early sex differentiation in a reptile departs from the classical amniote model. *BMC Genomics*, *24*(1), 243. https://doi.org/10.1186/s12864-023-09334-0

Weberling, A., Shylo NA, Kircher BK, Wilson H, McClain M, Marchini M, Starr KB, Sanger TJ, Hollfelder F, & Trainor PA. (2025). Pre-oviposition development of the brown anole (Anolis sagrei)—PubMed. *Developmental Dynamics : An Official Publication of the American Association of Anatomists*. https://doi.org/10.1002/dvdy.70027

Wickham H (2016). *ggplot2: Elegant Graphics for Data Analysis*. Springer-Verlag New York. ISBN 978-3-319-24277-4, https://ggplot2.tidyverse.org.

Xue, S., & Barna, M. (2012). Specialized ribosomes: A new frontier in gene regulation and organismal biology. *Nature Reviews. Molecular Cell Biology*, *13*(6), 355–369. https://doi.org/10.1038/nrm3359

Yang, C., Zang, W., Ji, Y., Li, T., Yang, Y., & Zheng, X. (2019). Ribosomal protein L6 (RPL6) is recruited to DNA damage sites in a poly(ADP-ribose) polymerase-dependent manner and regulates the DNA damage response. *The Journal of Biological Chemistry*, *294*(8), 2827–2838. https://doi.org/10.1074/jbc.RA118.007009

Zhang, J., Ma, Q., Han, Y., Wen, H., Zhang, Z., Hao, Y., Xiao, F., & Liang, C. (2022). Downregulated RPL6 inhibits lung cancer cell proliferation and migration and promotes cell apoptosis by regulating the AKT signaling pathway. *Journal of Thoracic Disease*, *14*(2), 507–514. https://doi.org/10.21037/jtd-22-116

Zhu, Z., Younas, L., & Zhou, Q. (2025). Evolution and regulation of animal sex chromosomes. *Nat Rev Genet*, *26*(1), 59–74. https://doi.org/10.1038/s41576-024-00757-3

AUTHOR CONTRIBUTIONS

Megan Motley contributed to conceptualization, molecular work, data analysis, figure generation, funding acquisition, and writing. Sungdae Park contributed to molecular work, data analysis, and figure generation. Briana Roman contributed histological sectioning and staining. Sneha Mohan contributed confocal imaging. Rida Osman contributed to surgeries, molecular work, and animal care. Winston Bellot contributed to data analysis. Makenna Burslie contributed to surgeries and animal care. Nareem Al-Shurafa contributed to cryosectioning and embryo

collection. David Page and Jim Lauderdale contributed resources and lab personnel. Douglas Menke contributed to conceptualization, funding acquisition, data analysis, writing, editing, supervision, and figure generation.

All Co-authors agree that the work may be included in this thesis or dissertation.

CHAPTER 4

CONCLUSIONS AND FUTURE DIRECTIONS

Introduction

Our understanding of vertebrate sex chromosome evolution and sex determination mechanisms has largely been shaped by studies in a few traditional model organisms, such as mammals and birds (Bachtrog et al., 2014; Charlesworth, 1991; Muller, 1914; Ohno, 1967; Rovatsos & Kratochvíl, 2021). However, despite being one of the largest and most species-rich vertebrate classes, reptiles remain underrepresented in this research. As a group that exhibits nearly every known mechanism of sex determination, including environmental and genetic systems, reptile lineages offer a unique and valuable opportunity to explore the full diversity of sex determination pathways and the evolutionary dynamics of sex chromosomes. Yet, our knowledge of the molecular mechanisms driving these biological processes in reptiles remains highly limited. I hope that the work presented in this thesis will serve as a foundation for future comparative studies in other pleurodont lizards, as well as broader investigations into the diversity of sex chromosome systems across reptiles.

Using the brown anole, *Anolis sagrei,* I have addressed key gaps in our understanding of reptilian sex determination and sex chromosome biology by investigating the ancient XX/XY sex chromosome system conserved across most pleurodont lizards (Gamble et al., 2014). This system provided a valuable opportunity to explore the dynamics of vertebrate sex chromosome evolution and

the regulation of ancient XX/XY sex determination outside of mammals. The research presented here advances our knowledge of sex chromosome evolution in vertebrates and significantly expands our understanding of this process within pleurodont lizards.

Major findings of Chapter 2

A major outcome of this work is the generation of a highly complete and contiguous assembly of the *A. sagrei* Y chromosome, which enabled the characterization of Y-linked gene loss across both ancient and more recently evolved regions of the neo-Y chromosome. The *A. sagrei* Y has undergone multiple chromosomal inversions and shows substantial Y-linked gene loss relative to its X chromosome counterpart. These findings support and extend the canonical model of sex chromosome evolution, providing another compelling example of Y chromosome degeneration in vertebrates.

In addition, analysis of synonymous divergence (dS) revealed differences in median dS values between ancient and more recently acquired regions of the Y chromosome. However, this analysis did not identify distinct evolutionary strata, suggesting that sex chromosome differentiation in *A. sagrei* may have proceeded more gradually than in other vertebrate species. This pattern likely reflects a more continuous and lineage-specific mode of recombination suppression, contrasting with the canonical model of sex chromosome evolution, which involves the stepwise accumulation of evolutionary strata as seen in mammals and birds (Lahn & Page, 1999; Nam & Ellegren, 2008).

This work presents the first characterization of dosage compensation across the *A. sagrei* X chromosome. My results support chromosome-wide twofold upregulation of the male X, a mechanism reminiscent of that observed in *A. carolinensis,* suggesting the presence of a conserved ancestral dosage compensation system (Marin et al., 2017; Rupp et al., 2017; Tenorio et al., 2024). However, my analyses revealed regional variability in dosage compensation across the X-specific region. I found that gene expression between XX and XY individuals appears to be more balanced in the ancient X region (XSR3) than in the more recently added neo-X regions (XSR1, XSR2, and XSR4).

This pattern suggests that, following sex chromosome-to-autosome fusion events, dosage compensation mechanisms have gradually evolved across the newly added X-linked regions. Older X-linked genes, having diverged over a longer evolutionary timescale, may have had more opportunity to achieve balanced gene expression through regulatory adaptation. These findings are consistent with the theory that ancestral dosage compensation mechanisms are often co-opted or adapted to evolve dosage balance in newly differentiated regions of sex chromosomes (Ellison C & Bachtrog D, 2019; Zhou et al., 2013).

Most notably, differential expression analysis revealed male- and female-biased subsets of genes with interesting patterns of expression. In XX individuals, 278 X-linked genes were significantly upregulated, resulting in approximately 20% higher X-linked gene expression relative to autosomal levels. This suggests a pattern of female-biased overexpression across the X-chromosome. In XY individuals, 32 X-linked genes lacking Y-linked gametologs

were found to be overcompensated, with significant upregulation in males. I hypothesize that these genes may be dosage sensitive or play roles in male development.

These observations also point to the possibility of adaptive regulatory evolution as a response to Y-linked gene loss. As Y gametologs are lost, selective pressure may favor increased expression of their X-linked counterparts. This upregulation may occur through regulatory mechanisms that increase X-linked gene expression in both sexes or through male-specific regulatory changes (Tenorio et al., 2024).

Taken altogether, my findings establish the brown anole as an important model for studying neo-sex chromosome evolution and dosage compensation, providing new insights that broaden our current understanding of these processes in vertebrates.

Major findings of Chapter 3

The work presented in Chapter 3 represents the first functional identification of a primary sex determination gene in a reptile, and the first to implicate a ribosomal protein gene, *rpl6y*, as the initiating determinant of sex in a vertebrate. These findings fundamentally change our current understanding of vertebrate sex determination biology and are likely to influence future research into both sex determination mechanisms and gene expression regulation via ribosomal heterogeneity. Moreover, this work marks the beginning of large-scale

comparative studies in other pleurodont lizards that share a homologous XX/XY sex chromosome system.

Using genomic and transcriptomic approaches, I have identified a novel sex determination mechanism in *A. sagrei* that is likely conserved across more than 1,200 pleurodont lizard species. RNA-seq analysis of XX and XY gonads led to the identification of *astra,* an antisense RNA transcript proposed to downregulate *rpl6x* gonad-specific expression in both sexes. In XY individuals, sex is determined by the upregulation of *rpl6y*, suggesting a regulatory mechanism in which astra reduces *rpl6x* expression before male-specific activation of *rpl6y*.

rpl6y was identified as a strong Y-linked candidate for sex determination based on its early and elevated expression in XY embryos during gonadogenesis, its conservation across related pleurodont species, and its high sequence divergence from its X-linked paralog, *rpl6x*. Functional validation using CRISPR-gene editing revealed that loss of *rpl6y* in XY individuals results in complete male-to-female sex reversal. The *rpl6y* XY mutant female displayed external and internal morphology strikingly similar to wild-type XX females, including small body size and dewlap, and well-developed ovaries and uteri. Histological examination further confirmed female-like cellular morphology of the gonads. Thus, *rpl6y* is required for male sex determination in *A. sagrei*.

rpl6y encodes a highly diverged variant of RPL6, a core protein component of the 60S large ribosomal subunit. While RPL6 is essential for protein synthesis, it also performs a range of extra-ribosomal functions, including

DNA damage repair (Yang et al., 2019) and cell cycle regulation (Zhang et al., 2022). This study provides the first evidence implicating RPL6 in primary sex determination. I hypothesize that *rpl6y* initiates sex determination in *Anolis* through a translation-based mechanism that depends on ribosomal heterogeneity, potentially modulating ribosomal composition or specificity during early gonadal development.

The findings presented here add important complexity to our understanding of gene expression regulation and highlight the potential role of ribosomes in driving sex-specific expression differences and contributing to sex determination. The discovery of gonad-specific *rpl6x* downregulation and male-specific *rpl6y* upregulation provides compelling evidence for sex-specific ribosome heterogeneity in *A. sagrei* and potentially other pleurodont lizards.

Additionally, when this project began in 2019, no well-assembled Y chromosome genomes existed for any pleurodont species. Through collaborative efforts, this work has helped catalyze the generation of multiple XY *Anolis* genome assemblies, some of which were instrumental in identifying *rpl6y* as a candidate primary sex-determining gene.

Questions remaining and future directions

In *Anolis carolinensis*, recent work identified a long non-coding RNA, *MAYEX*, and proposed that it may play a central role in dosage compensation by upregulating X-linked gene expression in XY individuals (Tenorio et al., 2024). However, the underlying mechanism of dosage compensation in *Anolis*, including

the twofold upregulation of the male X, remains poorly understood, and the regulatory control of *MAYEX* is still unknown. Future studies could leverage the recently developed immortalized XX and XY *A. sagrei* cell lines to functionally investigate *MAYEX* (Samudra et al., 2024). Gain- and loss-of-function experiments using CRISPR gene editing may provide critical insight into its role. Now that dosage compensation patterns have been well characterized in *A. sagrei,* targeted manipulation of *MAYEX* could potentially alter these patterns, thereby revealing its functional role in dosage compensation.

The mechanism by which *rpl6y* initiates sex determination in *A. sagrei* remains a central question in fully understanding this novel pathway. A critical next step is to determine whether *rpl6y* functions by directly influencing the translation of key mRNAs involved in gonadal differentiation, or whether its role in sex determination is extra-ribosomal. To address this, proteomic analyses and ribosomal profiling (Ribo-seq) in developing XY gonads will be essential. These approaches will help to determine whether *rpl6y* alters ribosome composition or specificity to promote testis development.

It is also important to determine the functional role of *astra*, particularly whether it plays a regulatory role in the gonad-specific downregulation of *rpl6x* expression. Furthermore, understanding whether *astra* is required for, or contributes to, testis differentiation is essential for clarifying its role in the *Anolis* sex determination pathway. Loss-of-function experiments, both in vitro and in vivo using CRISPR gene editing, could provide critical insights into the function of the *astra* transcript and help uncover its role in regulating early gonad development.

Given that the XX/XY sex determination system is conserved across approximately 1,200 pleurodont lizard species, it is of critical importance to determine whether *rpl6y* serves as the primary sex-determining gene in related taxa. Using publicly available XY genome assemblies, the *rpl6y* coding sequence has been identified in 11 additional pleurodont species. These findings highlight the need to investigate the conservation, expression, and function of *rpl6y* across this diverse group. Comparative gene expression analyses and functional studies using CRISPR gene editing will be essential to assess whether *rpl6y* is a conserved primary regulator of sex determination among pleurodonts.

Perhaps the most critical outstanding question from this thesis is whether *rpl6y* is sufficient to initiate male sex determination. To address this, *rpl6y* would need to be ectopically expressed in XX embryos to determine whether it can induce female-to-male sex reversal. Such gain-of-function experiments would provide essential functional evidence to support *rpl6y's* role as the primary regulator of male development in *Anolis*. Although transgenic knock-in approaches are not yet established for *A. sagrei,* the development of such genomic tools is ongoing and may soon enable these critical experiments.

Many questions remain regarding the molecular mechanisms underlying dosage compensation via male-specific X upregulation in Anolis, as well as the initiation of male sex determination by *rpl6y*. The work presented in this thesis represents important first steps towards elucidating these processes, laying the groundwork for a deeper understanding of sex chromosome biology, dosage compensation, and sex determination in *Anolis* and other pleurodont lizards.

REFERENCES

Bachtrog, D., Mank, J. E., Peichel, C. L., Kirkpatrick, M., Otto, S. P., Ashman, T. L., Hahn, M. W., Kitano, J., Mayrose, I., Ming, R., Perrin, N., Ross, L., Valenzuela, N., & Vamosi, J. C. (2014). Sex determination: Why so many ways of doing it? *PLoS Biol*, *12*(7), e1001899. https://doi.org/10.1371/journal.pbio.1001899

Charlesworth, B. (1991). The evolution of sex chromosomes. *Science*, *251*(4997), 1030–1033. https://doi.org/10.1126/science.1998119

Ellison C, & Bachtrog D. (2019). Contingency in the convergent evolution of a regulatory network: Dosage compensation in Drosophila—PubMed. *PLoS Biology*, *17*(2). https://doi.org/10.1371/journal.pbio.3000094

Gamble, T., Geneva, A. J., Glor, R. E., & Zarkower, D. (2014). Anolis sex chromosomes are derived from a single ancestral pair. *Evolution*, *68*(4), 1027–1041. https://doi.org/10.1111/evo.12328

Lahn, & Page. (1999). Four evolutionary strata on the human X chromosome—PubMed. *Science (New York, N.Y.)*, *286*(5441). https://doi.org/10.1126/science.286.5441.964

Marin, R., Cortez, D., Lamanna, F., Pradeepa, M. M., Leushkin, E., Julien, P., Liechti, A., Halbert, J., Brüning, T., Mössinger, K., Trefzer, T., Conrad, C., Kerver, H. N., Wade, J., Tschopp, P., & Kaessmann, H. (2017). Convergent origination of a Drosophila-like dosage compensation mechanism in a reptile lineage. *Genome Res*, *27*(12), 1974–1987. https://doi.org/10.1101/gr.223727.117

Muller, H. J. (1914). A gene for the fourth chromosome of Drosophila. *Journal of Experimental Zoology*, *17*(3). https://doi.org/10.1002/jez.1400170303

Nam, K., & Ellegren, H. (2008). The chicken (Gallus gallus) Z chromosome contains at least three nonlinear evolutionary strata. *Genetics*, *180*(2), 1131–1136. https://doi.org/10.1534/genetics.108.090324

Ohno, S. (1967). *Sex Chromosomes and Sex-Linked Genes*.

Rovatsos, M., & Kratochvíl, L. (2021). Evolution of dosage compensation does not depend on genomic background. *Molecular Ecology*, *30*(8), 1836–1845. https://doi.org/10.1111/mec.15853

Rupp, S. M., Webster, T. H., Olney, K. C., Hutchins, E. D., Kusumi, K., & Wilson Sayres, M. A. (2017). Evolution of Dosage Compensation in Anolis carolinensis, a Reptile with XX/XY Chromosomal Sex Determination. *Genome Biol Evol*, *9*(1), 231–240. https://doi.org/10.1093/gbe/evw263

Samudra, S. P., Park, S., Esser, E. A., McDonald, T. P., Borges, A. M., Eggenschwiler, J., & Menke, D. B. (2024). A new cell culture resource for investigations of reptilian gene function. *Development (Cambridge, England)*, *151*(22), dev204275. https://doi.org/10.1242/dev.204275

Tenorio M, Cruz-Ruiz S, Encarnación-Guevara S, Hernández M, Corona-Gomez JA, Sheccid-Santiago F, Serwatowska J, López-Perdomo S, Flores-Aguirre CD, Arenas-Moreno DM, Ossiboff RJ, Méndez-de-la-Cruz F, Fernandez-Valverde SL, Zurita M, Oktaba K, & Cortez D. (2024). MAYEX is an old long noncoding RNA recruited for X chromosome dosage

compensation in a reptile—PubMed. *Science (New York, N.Y.)*, *385*(6715). https://doi.org/10.1126/science.adp1932

Yang, C., Zang, W., Ji, Y., Li, T., Yang, Y., & Zheng, X. (2019). Ribosomal protein L6 (RPL6) is recruited to DNA damage sites in a poly(ADP-ribose) polymerase-dependent manner and regulates the DNA damage response. *The Journal of Biological Chemistry*, *294*(8), 2827–2838. https://doi.org/10.1074/jbc.RA118.007009

Zhang, J., Ma, Q., Han, Y., Wen, H., Zhang, Z., Hao, Y., Xiao, F., & Liang, C. (2022). Downregulated RPL6 inhibits lung cancer cell proliferation and migration and promotes cell apoptosis by regulating the AKT signaling pathway. *Journal of Thoracic Disease*, *14*(2), 507–514. https://doi.org/10.21037/jtd-22-116

Zhou, Q., Ellison, C. E., Kaiser, V. B., Alekseyenko, A. A., Gorchakov, A. A., & Bachtrog, D. (2013). The epigenome of evolving Drosophila neo-sex chromosomes: Dosage compensation and heterochromatin formation. *PLoS Biology*, *11*(11), e1001711. https://doi.org/10.1371/journal.pbio.1001711